GE 136A: Fall 2024 Field Guide

Owens Valley and CA-395

Instructor: Joe Kirschvink
TAs: Nick Anderson
Cover Photo: Nick Anderson

Table of Contents

1 Trip Schedule 2

2 Routes 3

2.1 Day 1: November 1, 2024 3
2.2 Day 2: November 2, 2024 4
2.3 Day 3: November 3, 2024 5

3 Talks 6

3.4 Day 1 6
(1) Owens Valley Air Quality 6
(2) LADWP Lawsuits 8
(3) Desert Dust Chemistry 10
(4) Tufa Towers 12
(5) Sulfide Fractionation at Mono Lake 14
(6) Mono Lake Flies 16
3.5 Day 2 18
(7) Geologic History of the Poleta Folds 18
(8) Chalfant Valley 1986 Earthquake Series 20
(9) Lake Crowley Column Formation 22
(10) The Effects of Great Basin and Range Extension on Biodiversity 24
(11) LGM: Tioga and Tahoe Glaciations 26
(12) Walker Lane, the Hilton Creek Fault and the Earthquake of 1872 28
(13) Nuclear Theory of Radiometric Dating 30
(14) Travertine: The Superior Calcium Carbonate 32
(15) Hot Spring Brain Eating Amoeba 34
(16) Hot Creek Thermophiles 36
(17) Taq Polymerase and the reaction that changed biology 38
(18) Flintknapping 40
(19) Post-Eruption Ecology 42
(20) Snowpack-Mediated Volcanic Degassing, Earthquakes, and Tree Death at Mammoth Mountain 44
(21) Don't Eat the Pink Snow 46
(22) Shotgun Sequencing of Umbilicaria phaea: Investigations into Extant Phototrophic Diversity 48
3.6 Day 3 50
(23) Sierran magmatism: Alabama Hills & Mono-Inyo Volcanic Chain: Obsidian Dome 50
(24) Copper Carbonate Minerals of Cerro Gordo 52
(25) The Dolomitization of Carbonates 54

1. Trip Schedule

Day	Time (PDT)	Activity	Talks	Duration	Bathroom	Gas	Drive Time
Day 1 - 11/1	7:00	Meet at Arms Circle/ Caltech		1:00	X		
	7:45	Leave Arms Circle					0:55
	8:40	Vasquez Rocks - Siesmolani	Kirschvink	0:15			1:10
	10:05	ARCO in Mojave - Bathrooms and Gas		0:10	X	X	
	10:15	Drive to Owens Lake West Delta Birding Area		2:00			
	12:15	Owens Lake - Lunch and Talks	Abby/ Shriya/ Juliette	1:00			0:20
	13:35	Eastern Sierra Visitor Center - Bathroom		0:10	X		1:40
	15:25	Sierra Nevada Aquatic Research Lab - Orientation		1:00			0:40
	17:05	Mono Lake South - Talks	Tina/ Lily/ Marisa	1:00			
	18:05	Sierra Nevada Aquatic Research Lab - Dinner			X		
Day 2 - 11/2	8:30	Leave SNARL			X		0:55
	9:25	Poleta Canyon Folds	William	0:30			0:20
	10:15	Chalfant Quarry	Victor	0:20			0:10
	10:45	Bishop Paiute Gas Station		0:10	X	X	0:40
	11:35	Crowley Lake Columns	Grace / Issac	0:40			0:30
	12:45	McGee Creek - Lunch and Talks	Olivia / Simon / Tommy	1:00	X		0:20
	14:05	Hot Creek	Hemani / Eran / Jordan / Korbi	0:20	X		0:30
	14:55	Obsidian Dome Parking Spot 2	Sascha / Paolo	0:40			0:35
	16:10	Horseshoe Lake Parking Lot	Becky	0:20	X		0:20
	16:50	Sherwin Lakes Trailhead Hike / Art and chill w Jim	Richard / Forrest	1:50			0:20
	19:00	SNARL - Dinner			X		
Day 3 - 11/3	7:30	Clean SNARL		1:00	X		
	8:30	Leave SNARL					1:40
	10:10	Lone Star Bistro/Chevron - Smoothie/Coffee Stop	Amanda	0:30	X	X	0:45
	11:25	Cerro Gordo Mine/Ghost Town - Lunch	Alex / Sophia	2:00			1:45
	15:10	Indian Wells Brewing Company		0:30	X		2:33
	18:13	Arms Circle/ Caltech			X		

2. Routes

2.1 Day 1: November 1, 2024

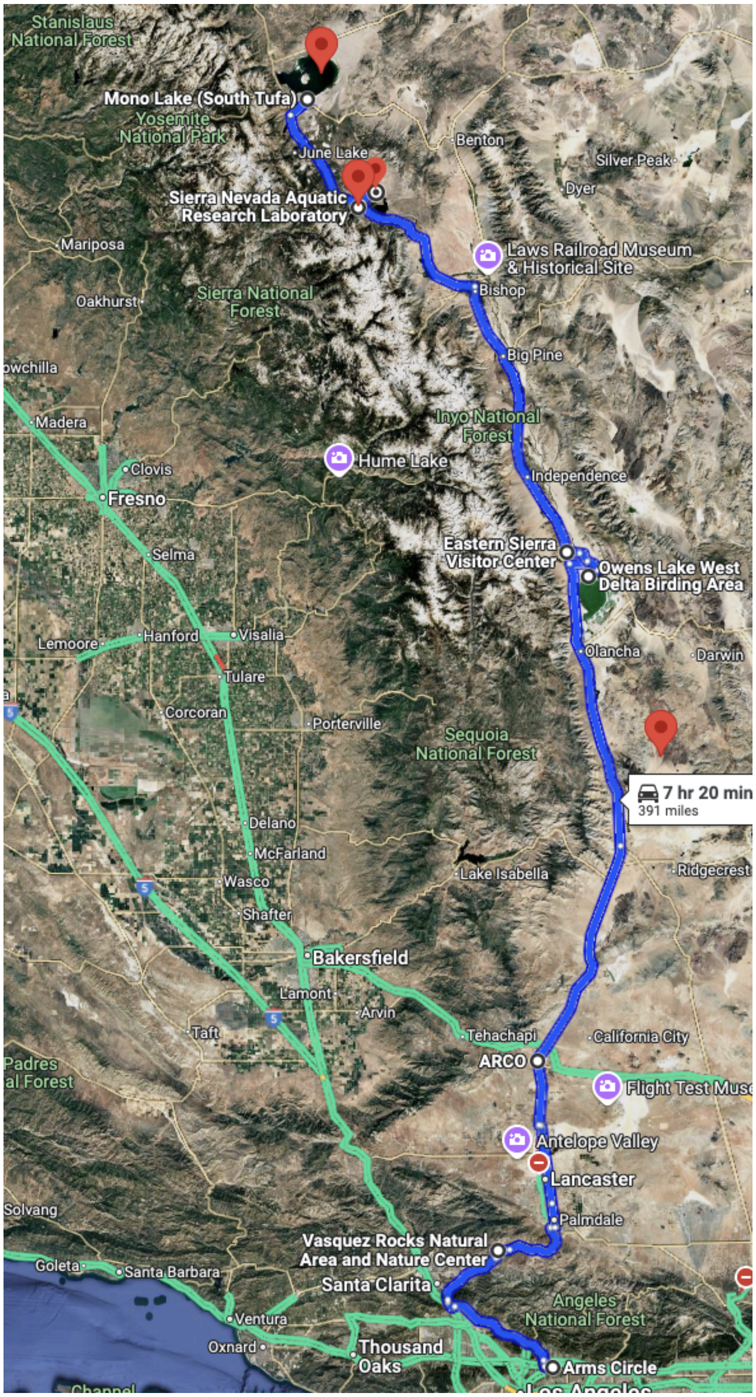
Stanislaus National Forest
Mono Lake (South Tufa)
Yosemite National Park
June Lake
Benton
Silver Peak
Dyer
Sierra Nevada Aquatic Research Laboratory
Mariposa
Laws Railroad Museum & Historical Site
Bishop
Oakhurst
Sierra National Forest
Big Pine
Madera
Inyo National Forest
Clovis
Hume Lake
Independence
Fresno
Selma
Eastern Sierra Visitor Center
Owens Lake West Delta Birding Area
Lemoore
Hanford
Visalia
Olancha
Darwin
Tulare
Corcoran
Porterville
Sequoia National Forest
7 hr 20 min
391 miles
Delano
McFarland
Wasco
Lake Isabella
Ridgecrest
Shafter
Bakersfield
Lamont
Arvin
Taft
Tehachapi
California City
ARCO
Flight Test Muse
Antelope Valley
Lancaster
Palmdale
Solvang
Vasquez Rocks Natural Area and Nature Center
Goleta
Santa Barbara
Santa Clarita
Angeles National Forest
Ventura
Oxnard
Thousand Oaks
Arms Circle
Los Angeles

2.2 Day 2: November 2, 2024

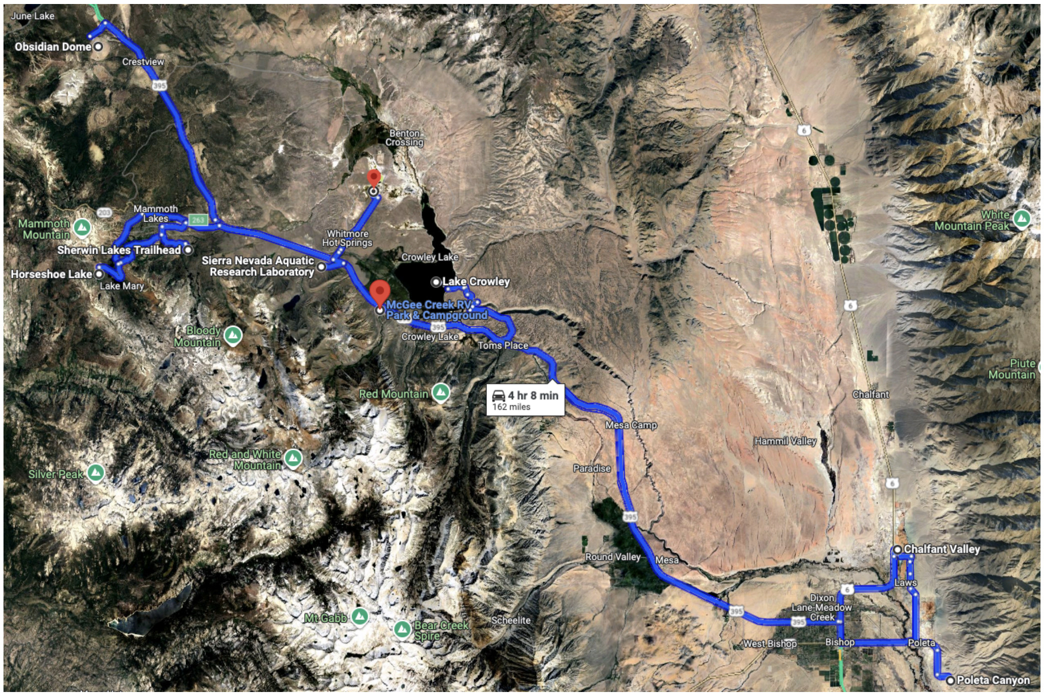
June Lake
Obsidian Dome
Crestview
395
Benton Crossing
Mammoth Mountain
Mammoth Lakes
203
Whitmore Hot Springs
Sherwin Lakes Trailhead
Sierra Nevada Aquatic Research Laboratory
Horseshoe Lake
Lake Mary
Crowley Lake
Lake Crowley
McGee Creek RV Park & Campground
Crowley Lake
Toms Place
Bloody Mountain
Red Mountain
4 hr 8 min
162 miles
Mesa Camp
Red and White Mountain
Silver Peak
Paradise
Hammil Valley
Chalfant
White Mountain Peak
Piute Mountain
Round Valley
Mesa
Chalfant Valley
Laws
Dixon Lane-Meadow Creek
West Bishop
Bishop
Poleta
Poleta Canyon
Mt Gabb
Bear Creek Spire
Scheelite
6

2.3 Day 3: November 3, 2024

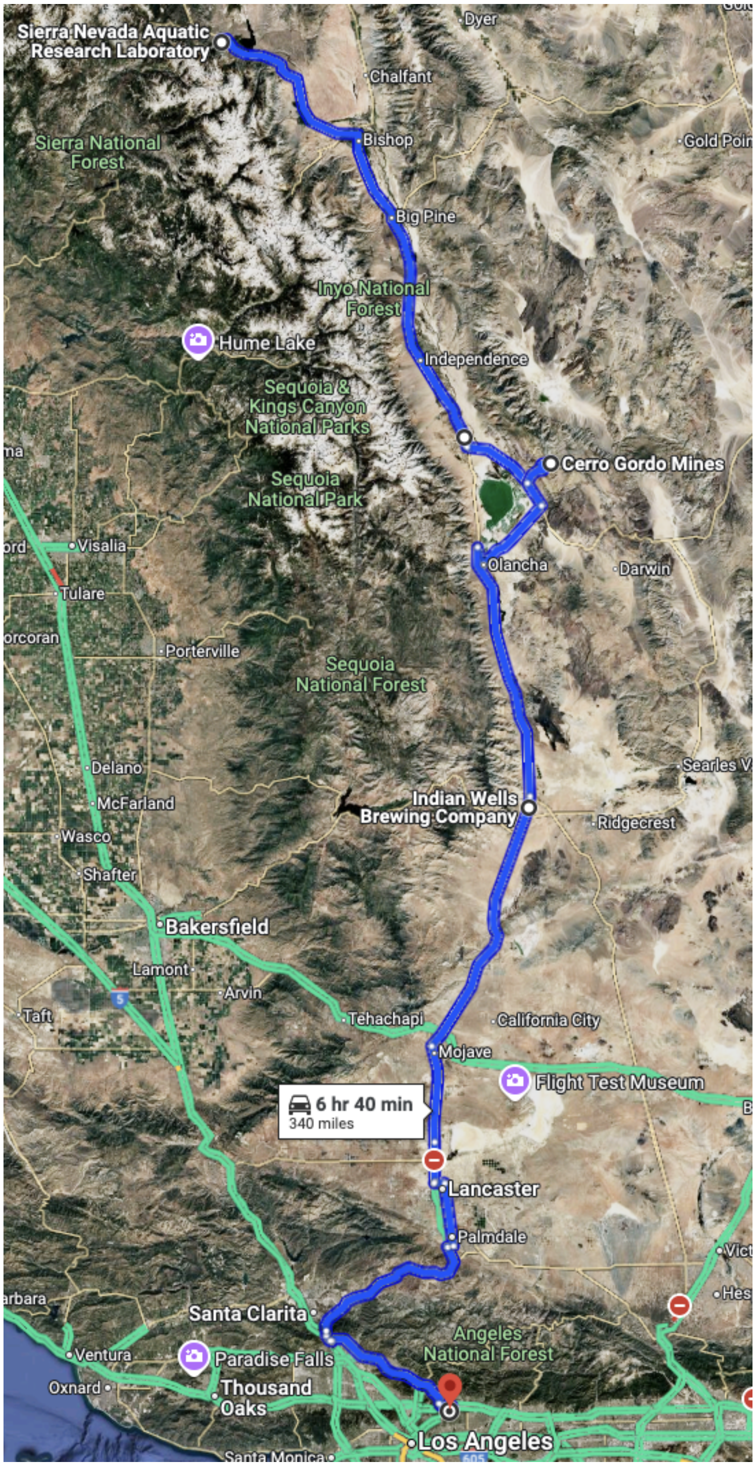
Sierra Nevada Aquatic Research Laboratory
Dyer
Chalfant
Bishop
Sierra National Forest
Gold Poin
Big Pine
Inyo National Forest
Hume Lake
Independence
Sequoia & Kings Canyon National Parks
Cerro Gordo Mines
Sequoia National Park
Visalia
Olancha
Darwin
Tulare
orcoran
Porterville
Sequoia National Forest
Delano
McFarland
Searles V
Indian Wells Brewing Company
Ridgecrest
Wasco
Shafter
Bakersfield
Lamont
Arvin
Taft
5
Tehachapi
California City
Mojave
Flight Test Museum
6 hr 40 min
340 miles
Lancaster
Palmdale
Vict
Hes
arbara
Santa Clarita
Angeles National Forest
Ventura
Paradise Falls
Oxnard
Thousand Oaks
Los Angeles
Santa Monica

Owens Valley Air Quality

Abby Keebler

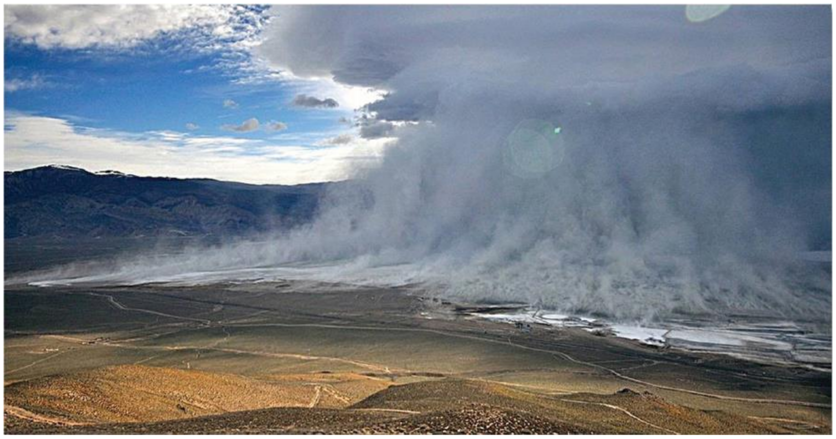

Mineral Dust and Air Quality

For the past century, Owens Valley has had poor air quality due to exceptionally high levels of aerosol particles smaller than 10 microns in diameter (PM10). In the 1980s and 1990s, levels of PM10 in the Owens Valley were measured as the highest in the USA [EPA].

Above: a major dust storm over Owens Lake, 2000 (Source: Owens Lake Scientific Advisory Panel)

Owens Lake: a Major Source of Dust Emissions

Owens lake is one of several Pleistocene lakes in the Great Basin region, in the same family as Mono Lake and basins in Death Valley. Until the late 1800s, Owens Lake was full of water, with an areal extent of over 100 square miles and a maximum depth of 50 feet. Owens Valley is called Payahuunadü, “the land of flowing water” in the language of the Paiute people. In the early 1900s, the city of Los Angeles was experiencing rapid population growth and sought sources of water to support its development. LA City Engineer Frederick Eaton purchased land in the Owens Valley and the accompanying water rights as a private citizen and then surrendered them to the city of LA, which enabled the construction of the LA aqueduct and the irrigation of the San Fernando Valley. In 1913, LA began diverting the inflow of Owens Lake to the LA aqueduct, and the lake was dry by 1928. The exposed lakebed consists of silt/clay and evaporate minerals, which are very easily entrained by saltation during frequent strong wind events [Reheis].

Impacts of Mineral Dust Pollution

Dust sourced from Owens Lake consists of fine sediments containing clay minerals, sodium carbonate, and sodium sulfate [Reheis]. Transported mineral dust interacts with many of Earth’s biogeochemical cycles, contributing to atmospheric radiative forcing, fertilizing land and coating vegetation and snow where it is deposited, reducing visibility, and most alarmingly, impacting human health. Heavy metals like arsenic, cadmium, and nickel are present in lake sediments and concentrated in the dust fraction (<10 micron) [Reheis]. Local populations report increased occurrence a suite of respiratory symptoms, including chronic cough, respiratory illness, asthma attacks, and sinus problems [Great Basin Unified Air Pollution Control District]. To reduce exposure to harmful conditions, Owens Valley residents avoid going outdoors during dust storms, but fine particles can contaminate indoor spaces as well. Indigenous and rural communities living in and near Owens Valley bear the brunt of the consequences of increased dust pollution due to the dewatering of Owens Lake by LADWP. Japanese Americans incarcerated at the Manzanar confinement center during World War II had inadequate shelter from dust storms produced by Owens Lake, with dust coming up through the floorboards of the barracks [NPS].

Dust Mitigation

In 1987 year, the EPA designated Owens Valley as failing to meet air quality standards. LADWP was directed by the Great Basin Unified Air Pollution Control District to begin constructing dust control measures on Owens Lake; construction began in 2000 [Owens Lake Scientific Advisory Panel].

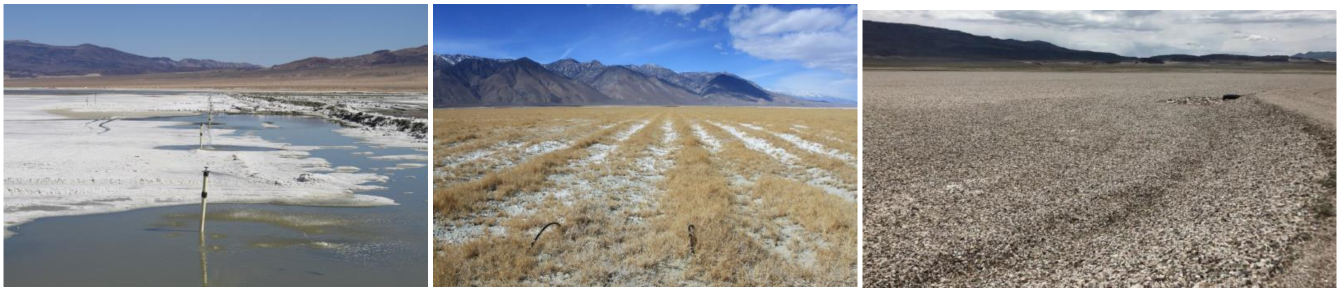

Left to right: dust mitigation techniques: shallow flooding, managed vegetation, and gravel blankets (Source: Owens Lake Scientific Advisory Panel; Chris Austin)

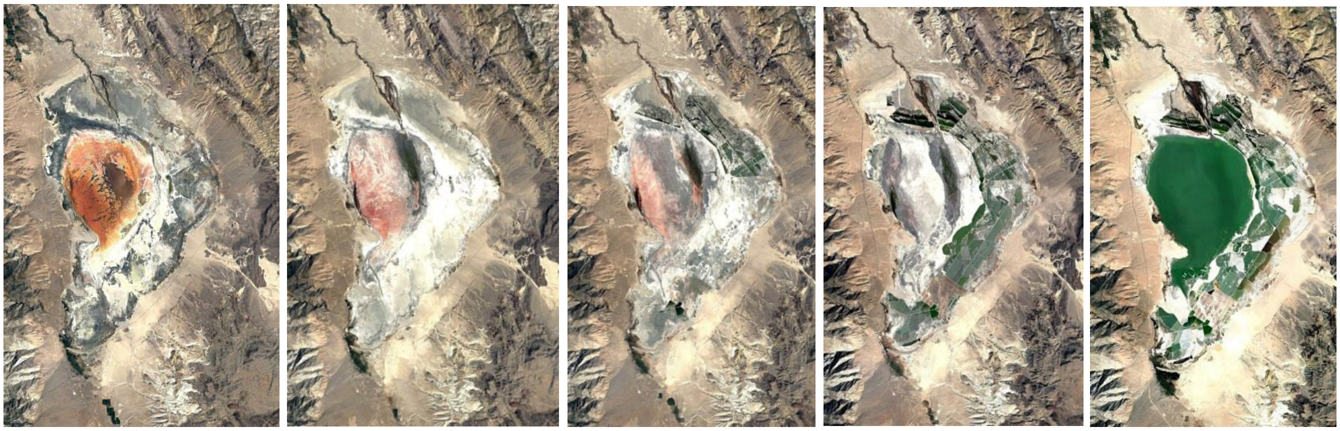

Left to right: time series satellite imagery from 1984, 1994, 2004, 2014, 2024 (Source: Google Earth). Note increasing dust mitigation infrastructure in images from 2004-2024.

A note on the 2023 floods

2023 was an abnormally wet year, and the eastern Sierra and Great Basin experienced several atmospheric rivers and a hurricane. Flooding in Owens Valley resulted in damage to the LA aqueduct and Owens Lake dust control infrastructure, estimated to cost LADWP $100 million to repair [LA Times]. The Owens Lake brine pool grew by a factor of 10 in surface area due to emergency releases of storm water.

The future of Owens Lake

Dust mitigation measures have dramatically reduced the number of days per year with unhealthy dust levels. LADWP has spent approximately $2.5 billion on dust mitigation and has reduced air pollution by approximately 99% [LADWP]. The flooded Owens Lake is also a habitat for migrating birds, with around 70 species observed each year during spring migration [Eastern Sierra Audubon Society].

Sources:
EPA (2017). Owens Valley Particulate Matter Plan: Fact Sheet; Reheis (1997). Dust deposition downwind of Owens (dry) Lake, 1991-1994: Preliminary findings. JGR: Atmospheres; Great Basin Unified Air Pollution Control District (2000). Survey of Reported Health Effects of Owens Lake Particulate Matter; NPS (2024). Japanese Americans at Manzanar; Owens Lake Scientific Advisory Panel (2020). Effectiveness and Impacts of Dust Control Measures for Owens Lake; LA Times (2024). Cost of Owens Valley Storm Damage Continues to Mount for Los Angeles Department of Water and Power; LA Department of Water and Power (2024). Owens Lake: Balancing Dust Mitigation, Water Conservation, and Wildlife; Eastern Sierra Audubon Society (2017). Owens Lake Count Data

LA Water and Power - Legal Battles

Shriya Fruitwala Ge136a Report

A *brief* history of the California Water Wars

Running along the eastern flank of the Sierra Nevadas, Owens Valley is a major source of water for Los Angeles, located 200 miles to the south. [1] The Los Angeles Department of Water and Power (DWP) has a documented history of exploiting Owens Valley as a resource colony. The advent of white settlers set in motion the pattern of dispossession and displacement that continues today through the perpetual legal battles that define the region.

The population boom in LA in the late 19th to early 20th century was unsustainably supported by the LA river, so the founder of DWP, William Mulholland sought out Owens Valley as a new water source for LA residents [3]. Quietly purchasing land in Owens Valley over a few decades, Mulholland amassed 97% of all privately owned land in Inyo and Mono counties [3].

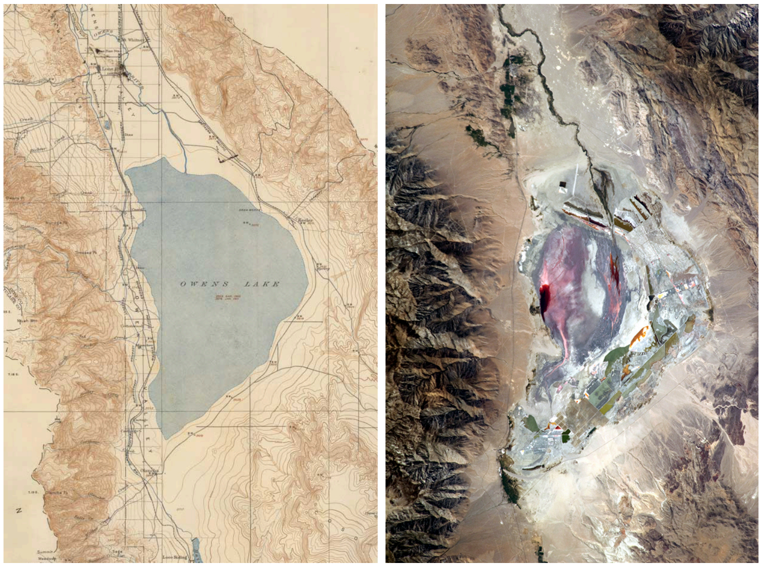

Figure 1: Owens Lake; map surveyed between 1905 and 1911 (left), and seen from space in 2011 (right). *U.S. Geological Survey; NASA*

The Second Aqueduct and Groundwater Litigation

The privatization of land and water allowed DWP to purchase this land with the intention of diverting its water to LA. By 1926, Owens lake was dry, exposing large amounts of toxic dust to surrounding communities [1]. Since DWP is municipally owned, LA residents are able to impart some influence on what projects are taken on through voting. However, residents of Inyo and Mono counties do not have access to the same processes, so they must rely on litigation to challenge DWP decisions.

The enactment of the 1970 California Environmental Quality Act (CEQA) prompted Inyo county to pursue litigation against LA, ordering them to produce an Environmental Impact Report (EIR) on their excessive groundwater pumping throughout the 70s and 80s to fill a second LA aqueduct and plans to mitigate these damages [5]. After two decades of the DWP submitting inadequate reports, an agreement was reached in 1991 to manage groundwater usage in the area, and a 1997 agreement added additional terms to restore the lower Owens River by 2003 [5]. DWP failed to meet this deadline twice, and ultimately, rewatering the lower Owens River took almost 10 years, two lawsuits, and a court ordered fine of $5000 per day for missing deadlines [2].

Mono Basin Ecosystem Lawsuits

In the 1930s, DWP began buying land in Mono Basin to divert waters that fed Mono Lake into an extension of the aqueduct [1]. Naturally, this had severe consequences on the Mono Lake ecosystem, particularly concerning several migratory bird species, which were first studied by David Gaines in 1974 [9]. His (and several other students') findings were published in a 1977 report that highlighted the ecological concerns associated with lowering Mono Lake. This report served as the basis for a 1979 lawsuit filed by the Mono Lake committee (formed by David Gaines) and the National Audubon society, arguing that water diversions were in violation of the Public Trust Doctrine, which contends that the government has a responsibility to safeguard navigable bodies of water for the benefit to all people [9]. The California Supreme Court ruled in favor of the committee. An additional lawsuit in 1984 filed by the committee argued that the DWP water diversions violated state fishery codes [11]. This eventually culminated in a 1994 decision by the State Water Board, which imposed limits on how much water could be diverted, requiring DWP to raise the lake level 17.4 feet above the then current level of 42.4 feet below the 1941 level [9]. As of 2023, the water level has risen 8.6 feet [4]. Overall, this is the largest dust control project in US history, spanning 42 square miles and costing over $1.2 billion [6]. Although dust levels have dropped significantly due to these measures, a local air quality government agency known as the Great Basin Unified Air Pollution Control District is arguing that more dust control measures are needed to meet federal standards.

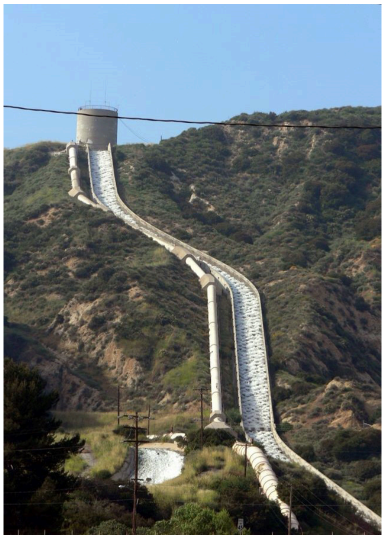

Figure 2: Second aqueduct. Waters from the first aqueduct shown on the left. *Water and Power Associates*

2012 DWP Lawsuit

In 2011, the Great Basin air district ordered DWP to extend the 42 square mile dust control region by 2.86 square miles [10]. In response, the DWP sued every federal and state environmental agency, including the US EPA, the California Air Resources Board, and the Great Basin air district, claiming that the city would be forced to waste billions of gallons of water on further dust control [10]. They argued [7] that a) ratepayers have already spent $1.2 billion on dust control measures, and that this order would mean spending up to an additional $400 million; and b) DWP is only responsible for the 42 square miles it drained to siphon water into the city and any dust emission outside of this is attributable to the environment being a “naturally dusty desert.”

The case was dismissed in 2013 in a federal court [7]. The judge ruled that liability (for polluting) cannot be determined from who owns/manages the land. Instead, the entity that controls the activities causing the pollution must be held accountable [7]. A 2014 agreement between air quality control authorities and DWP expands LA’s control to 53 square miles, but instead of re-watering the lake, a new solution involves using tractors to turn lake bed clay into furrows and clods of dirt, which will provide a way to store the dust for years before breaking down - at which point the process will be repeated [10]. Despite these agreements, the region still continues to be the center of similar legal battles, with DWP failing to control dust on patches of lake bed, citing regulatory overreach on the part of local agencies and increased costs for LA ratepayers, and air quality authorities pursuing litigation as recent as 2022 [6] to hold DWP accountable in the name of public health.

References

[1] Danskin, W. R. (1998). *Evaluation of the hydrologic system and selected water-management alternatives in the Owens Valley, California*. https://doi.org/10.3133/wsp2370H

[2] Knudson, T. (2014, January 5). *Outrage in Owens Valley a century after L.A. began taking its water*. The Sacramento Bee.

[3] Lattanzi, M. (2018, September 25). *Local Control of Land and Water Resources: Rethinking California’s Eminent Domain Standard*. UCLA Law Review.

[4] *Mono Lake Levels 1850-Present (Yearly)*. (n.d.). [Dataset].

[5] Novinska, V. (2005, October 20). Desertification As Usual: Groundwater Management Under The Inyo-LA Long Term Water Agreement. *OVC Web*. https://ovcweb.org/desertification-groundwater-management-inyo-la-long-term-water-agreement/

[6] Sahagún, L. (2022, November 8). *Legacy of dust: How Owens Valley air pollution increases LA water bills*. Los Angeles Times.

[7] Sahagún, L. (2013, May 2). *Federal judge dismisses DWP lawsuit over Owens Lake dust*. Los Angeles Times.

[8] State of California Department of Justice. (2003, December 4). *Attorney General Lockyer Files Suit to Force Los Angeles to Restore Lower Owens River Stretch* [Press release].

[9] Mono Lake Committee History. (n.d.). *Mono Lake*.

[10] Peterson, M. (700, 00:03). *LADWP takes state & federal air regulators to court*. Southern California Public Radio.

[11] Kahn, C. (2006, December 7). L.A. Returns Water to the Owens Valley. *NPR*.

Desert Dust Chemistry

Juliette Lipson

23 Oct. 2024

Introduction

Dust particles are suspended in the air by physical processes in dry desert regions and can be transported large distances[1–3]. These dust aerosols occur naturally but anthropogenic activities can create additional dust, for example, at Owens Lake (see Shriya's writeup for details)[3,4]. Dust is important to the Earth system because it provides iron to marine ecosystems and impacts the radiative balance[5,6]. Further, inhalation of dust particles is harmful to human health[1,5]. During transport, dust particles can support chemistry on their surface thus altering atmospheric composition and changing the impacts of the dust on our planet[1]. In this report, I will provide a sketch of desert dust chemistry and its ties to the Earth System.

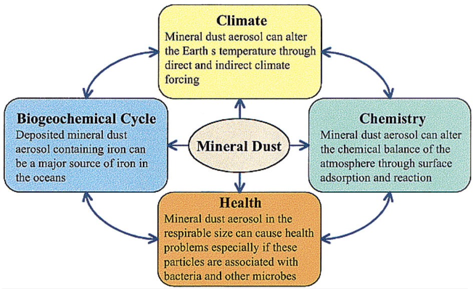
Climate
Mineral dust aerosol can alter the Earth s temperature through direct and indirect climate forcing
Biogeochemical Cycle
Deposited mineral dust aerosol containing iron can be a major source of iron in the oceans
Mineral Dust
Chemistry
Mineral dust aerosol can alter the chemical balance of the atmosphere through surface adsorption and reaction
Health
Mineral dust aerosol in the respirable size can cause health problems especially if these particles are associated with bacteria and other microbes

Figure 1: Dust interactions with the Earth System from Usher et al. 2003.

Fun sidebar 1: A Bit of Dust Physics

Dust is typically emitted when there are strong winds, but the wind itself does not lift small dust particles from the surface as the interactions between particles are too strong[2]. But if larger particles bounce onto the surface at high speeds other particles can be sent into the atmosphere[2,5]. These smaller particles travel sometimes thousands of kilometers. Owens Lake, before more recent mitigation efforts, produced large amounts of dust[3]. In the winter, the lakebed became wet with salt water such that salt was left crusted on the surface when the lakebed dried up[3]. This salt crust makes it more likely that the large particles bouncing into the surface will result in dust events[3].

Why do we want to understand Dust Chemistry?

Desert dust interacts with the Earth system and chemistry can alter these interactions. Desert dust supplies nutrients to marine environments, damages human health by depositing in our lungs, and affects the radiative budget by scattering light and contributing to cloud formation[5]. Chemistry can change the ability of iron in dust particles to dissolve and be released for biological use[5,7]. For example, adsorption of acids onto dust particles increases the solubility of the iron thus increasing the amount of nutrients supplied to the ocean[1]. The health impacts of dust could change based on the dust's chemical composition and the chemical composition of the atmosphere can change due to reactions on the surface of the dust, thus changing the health impacts of the gas phase portion of the atmosphere. That is, oxidants can be incorporated into dust particles such that they enter our blood stream when we breathe dust[7]. And, dust reactions can change amounts of gas phase compounds, such that the amount of toxic gas pollutants we breathe changes[5]. As gas phase compounds interact with and are incorporated into dust particles, the chemical and physical makeup of the dust particle is altered[1,5]. Such changes may lead to changes in the particle's ability to scatter light or nucleate clouds, thus changing the dust's effect on climate.

Fun sidebar 2: Atmospheric gas phase chem crash course! [8]

The hydroxyl radical (OH) is our major atmospheric oxidant responsible for initiating many reactions. An important example is that it begins the conversion of methane to CO_2. NO is another oxidant and is emitted by cars, amongst other sources. It reacts with organic compounds to form NO_2 which in turn photolyzes to produce O atoms. These O atoms react with O_2 to make ozone. Ozone oxidizes our lungs. (You can see current O_3 concentrations near Caltech: https://aq.caltech.edu/). NO and NO_2 are amongst several reactive nitrogen compounds that interconvert. The total amount of reactive nitrogen, and any preferences for certain reactive nitrogen species, changes atmospheric oxidation and ozone formation. Volatile organic compounds (VOCs) are emitted anthropogenically and biogenically. They are oxidized by atmospheric oxidants and thus impact cycling of atmospheric oxidants (for example they convert NO to NO_2 and sometimes are oxidized by OH to form HO_2) and can partition to the particle phase impacting aerosol.

A Whole Bunch of Chemistry

In our atmosphere, chemistry happens in the gas phase, liquid phase (within an aerosol or cloud), or on the surface of an aerosol such as desert dust (heterogeneous chemistry). We are focusing on heterogenous chemistry on dust, keeping in mind how this chemistry alters gas phase composition as well as dust properties because these will change the way dust impacts our planet. A few types of chemical processes can happen on the surface of a dust particle[1,5]:

1. Hydrolysis of mineral metal oxides by water to form terminating hydroxyl groups (-OH) on the dust surface (first step in Figure 2).
2. Adsorption of water onto the surface via hydrogen bonding with the hydroxyl groups to form a water layer (see the rightmost structure in Figure 2).
3. Adsorption of atmospheric oxidants to the surface with the metal oxides acting as Lewis Acids (see Figure 3b and Fun sidebar 3).
4. Adsorption of atmospheric oxidants or organics to the surface by interaction with hydroxyl groups (see Figure 3a).

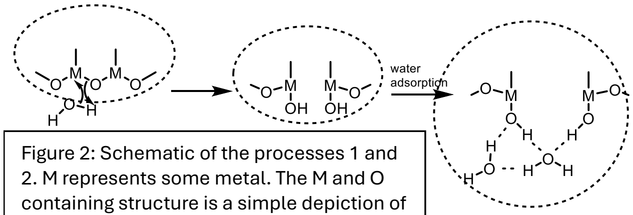

Figure 2: Schematic of the processes 1 and 2. M represents some metal. The M and O containing structure is a simple depiction of a mineral that makes up a dust particle. The number of bonds to the metal is just an example and will vary by mineral type. Do not treat any bond angles shown as being accurate to any mineral structure. Curved arrows represent the movement of electrons. Dashed lines are hydrogen bonds. Solid lines without an atom on one end represent continuation of the crystal structure.

5. Dissolution of organics into the water layer on the surface.
6. Reactions of oxidants or organics once adsorbed or dissolved.

Fun Sidebar 3: Lewis Acids[9]

When chemists talk about Lewis acids, you can totally just think of them as being acidic. We specifically call them Lewis acids because you might think of acids as H^+ donors, but Lewis acids don't donate protons. Instead, they can accept electrons. Either way acids are electron deficient but some acids deal with that by being amenable to losing a proton and others by accepting electrons.

O_3 Dust Chemistry

Desert dust can directly convert tropospheric ozone into O_2 thus removing some (some models say up to 6% globally) of this toxic oxidant from the atmosphere[1,5]. O_3 binds to the dust surface as shown in Figure 3[5]. Note Figure 3a and b show O_3 binding through processes 3 and 4, respectively. O_2 is released and leaving a bound O atom which combines with another bound O atom to form an additional O_2 or reacts with another O_3 to form two O_2[1,5]. Thus, dust converts toxic and reactive ozone into oxygen that we can breathe.

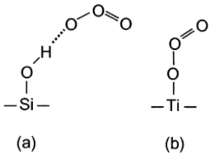

Figure 3: Ozone interacting with two minerals in desert dust via hydrogen bonding (a) and electron donation (Lewis base) (b) prior to dissociating to form O_2. From Usher et al. 2003.

Nitric Acid and Nitrogen Oxides Dust Chemistry

Tracing atmospheric reactive nitrogen compounds is necessary to understand atmospheric oxidation rates and O_3 formation. Dust samples are often found to have nitrate (NO_3^-) adsorbed to them because reactive nitrogen species can be removed from the atmosphere by reactions on dust that tend to result in nitrate formation[5]. Nitric acid (HNO_3) can adsorb to the surface of dust and release protons through reactions with hydroxyl groups that result in water and nitrate[5]. NO_2 can also be adsorbed onto dust and 2 NO_2 then react with two hydroxyl groups to form adsorbed nitrite and nitrate (Figure 4)[5,10]. Not only are reactive nitrogen species being removed from the atmosphere, but specifically NO_2 which photolyzes to produce O_3 is being removed. Two NO_2 can also react with adsorbed water to form adsorbed nitric acid and release HONO as a gas[5,10]. Again, this removes NO_2, but only removes one reactive nitrogen for every two NO_2 as HONO photolyzes to produce NO. This photolysis also releases OH, thus changing the balance of atmospheric oxidants. Nitrate can be photolyzed with 305 nm light to produce NO_2 ($NO_3^- + H^+ + h\nu \rightarrow NO_2 + OH$) thereby reversing some of the loss of reactive nitrogen[1,11]. The above discussion is not a comprehensive review of the possible heterogenous reactions of inorganic atmospheric gases on the surface of dust. I only hope that these examples give a sense of the ways in which inorganic species interact with dust and change atmospheric reactivity.

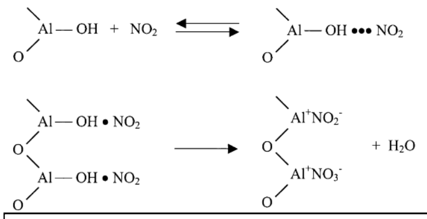

Figure 4: NO_2 reacting on the surface of Al_2O_3 mineral dust to form nitrite and nitrate from Usher et al. 2003.

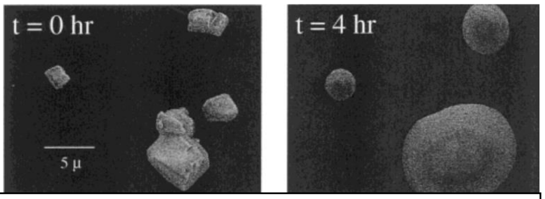

Figure 5: Images taken with a scanning electron microscope showing dust particles before and after interaction with nitric acid. Notice how the chemistry impacts the physical properties of dust. From Usher et al. 2003.

Volatile Organic Compounds

VOCs can also be adsorbed onto dust particles and react. A study of aerosols during a dust event found that adsorbed water on dust surfaces can allow for oxidation of VOCs and spectroscopy of dust samples has shown hydrocarbons in dust samples[5]. Other studies find evidence of carbonyl groups and carboxylic acids[5,12]. The carbonyl groups hydrogen bond to hydroxyl groups on the dust surface[12]. Two such carbonyl containing compounds then can undergo a reaction called an aldol condensation whereby they combine into one molecule[5]. Uptake of alcohols and organic acids onto dust aerosols has also been observed[5,12]. Thus, interactions of VOCs on dust surfaces can change the organic composition of the atmosphere which in turn can change the cycling of atmospheric oxidants.

Works Cited

1.Cwiertny, D. M., Young, M. A. & Grassian, V. H. Chemistry and Photochemistry of Mineral Dust Aerosol. *Annu. Rev. Phys. Chem.* **59**, 27–51 (2008).
2.Kolesar, K. R., Schaaf, M. D., Bannister, J. W., Schreuder, M. D. & Heilmann, M. H. Characterization of potential fugitive dust emissions within the Keeler Dunes, an inland dune field in the Owens Valley, California, United States. *Aeolian Research* **54**, 100765 (2022).
3.Reheis, M. C. Owens (Dry) Lake, California: A Human- Induced Dust Problem.
4.Reheis, M. C., Budahn, J. R., Lamothe, P. J. & Reynolds, R. L. Compositions of modern dust and surface sediments in the Desert Southwest, United States. *Journal of Geophysical Research: Earth Surface* **114**, (2009).
5.Usher, C. R., Michel, A. E. & Grassian, V. H. Reactions on Mineral Dust. *Chem. Rev.* **103**, 4883–4940 (2003).
6.Myhre, G. *et al.* 8 Anthropogenic and Natural Radiative Forcing.
7.Tong, H. *et al.* Reactive oxygen species formed in aqueous mixtures of secondary organic aerosols and mineral dust influencing cloud chemistry and public health in the Anthropocene. *Faraday Discussions* **200**, 251–270 (2017).
8.Seinfeld, J. H. & Pandis, S. N. *Atmospheric Chemistry and Physics: From Air Pollution to Climate Change*. (John Wiley & Sons, 2016).
9.Lewis Concept of Acids and Bases. *Chemistry LibreTexts* https://chem.libretexts.org/Bookshelves/Physical_and Theoretical Chemistry_Textbook_Maps/Supplemental_Modules_(Physical_and_Theoretical_Chemistry)/Acids_and_Bases/Acid/Lewis_Concept_of_Acids_and_Bases (2013).
10.Ma, T. *et al.* Comparison of the heterogeneous reaction of NO2 on the surface of clay minerals and desert dust particles. *Environmental Pollution* **334**, 122134 (2023).
11. Rubasinghege, G., Elzey, S., Baltrusaitis, J., Jayaweera, P. M. & Grassian, V. H. Reactions on Atmospheric Dust Particles: Surface Photochemistry and Size-Dependent Nanoscale Redox Chemistry. *J. Phys. Chem. Lett.* **1**, 1729–1737 (2010).
12. Carlos-Cuellar, S. *et al.* Heterogeneous Uptake Kinetics of Volatile Organic Compounds on Oxide Surfaces Using a Knudsen Cell Reactor: Adsorption of Acetic Acid, Formaldehyde, and Methanol on α-Fe2O3, α-Al2O3, and SiO2. *J. Phys. Chem. A* **107**, 4250–4261 (2003).

Mono Lake Tufa Towers: Formation and Ecological Impacts

Tina Seeger

One of the most distinctive features at Mono Lake is the towering blocks of tufa that rise up from the lake bottom and create unique and personable islands. These towers are a fundamental part of alkaline lake environments, and the land surface they create plays a large role in local ecosystem—one that is in peril due to falling lake levels as a result of climate change and thirsty Angelinos.

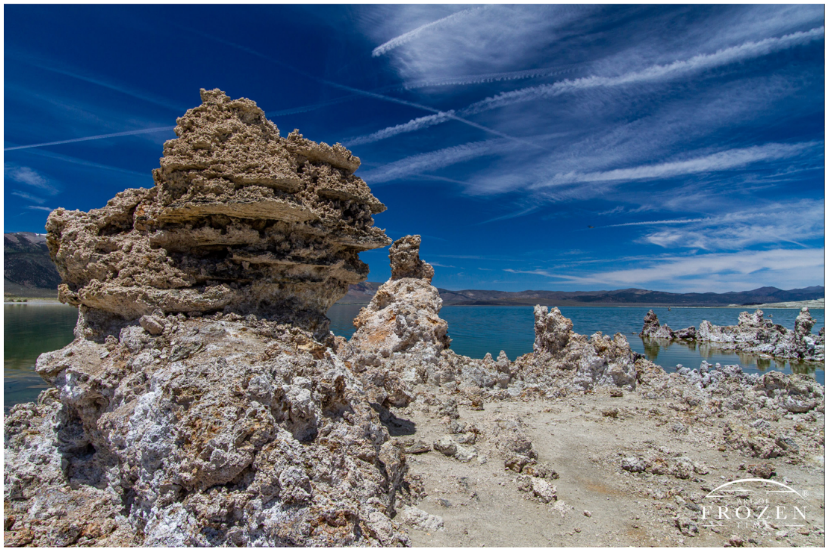

Figure 1. Tufa towers at Mono Lake margins with sequential layers of precipitation visible. Photo: Jeff, Art of Frozen Time

Formation: Mono Lake is an alkaline lake with a pH of 10, and its waters are rich in carbonates (Dunn, 1953). It was once about 5 times as large with outlet channels, but lake level decrease after the last glacial maximum reduced its size and concentrated salts. Calcium-rich springs seep into the lake and mix with the lake water to precipitate limestone ($CaCO_3$) in the form of tufa. Compositionally, these precipitates are the same as travertine (which form in warm to hot water), but form at ambient temperatures. Tufas build up over time at spring locations, creating towers in the water column (Keevil et al., 2022). Therefore, the tallest towers we see provide a lower limit on lake level depth when they were still forming, and provide a very visible metric of how much lake level has fallen.

Water Diversion & Ecological Impacts: The large population of tufa exposed along the lakeshore records a period of dramatic lake level fall, spurred by the water diversions of Mono Lake's tributary streams by LA Department of Water and Power that began in 1941. For the next 40 years, the lake level dropped by 45 vertical feet, lost half its volume, and doubled in salinity. This was bad news!! Especially for the California Gulls, which nest on the islands of Mono Lake—both volcanic and the tufa towers (Figure 2). The islands of Mono Lake are extremely attractive nesting grounds for numerous bird species, and even host one of the largest California Gull rookeries in North America (50,000 gulls nest every year!). Osprey will carry 6-foot-long sticks to their nests atop tufa towers. The saline moat around the islands provides protection from hungry shorebound mammals. However, lake level lowstands (in the 1970s, and again recently due to drought) can open land bridges to these islands, allowing coyotes to decimate the nesting bird population (Burnett et al., 2021) (Figure 3). In 2017, temporary electric fences were erected across the land bridges to deter coyotes from invading Gull colonies (Figure 4). Further initiatives to keep Mono Lake levels high are essential to protect the residents of Tufa Towers.

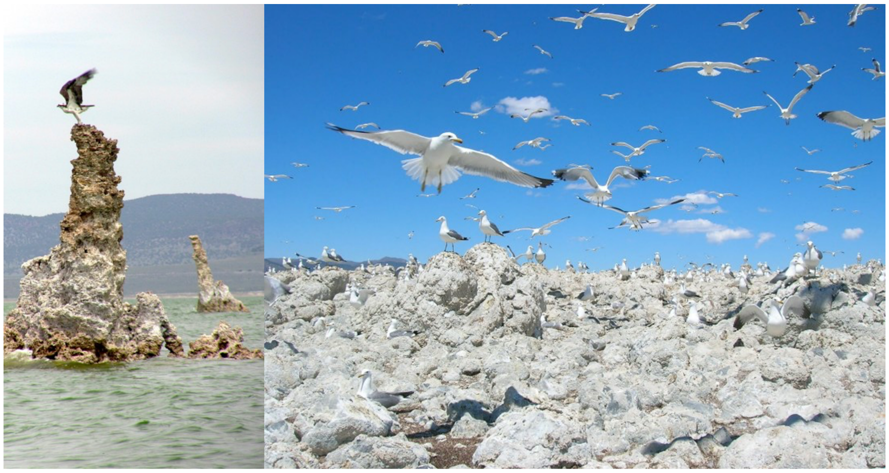

Figure 2. Bird nesting at Mono Lake. (a) Osprey departing a lunch spot, photo by Miles Clark. (b) California Gulls nesting on islets, photo by Nora Livingston.

Figure 3.

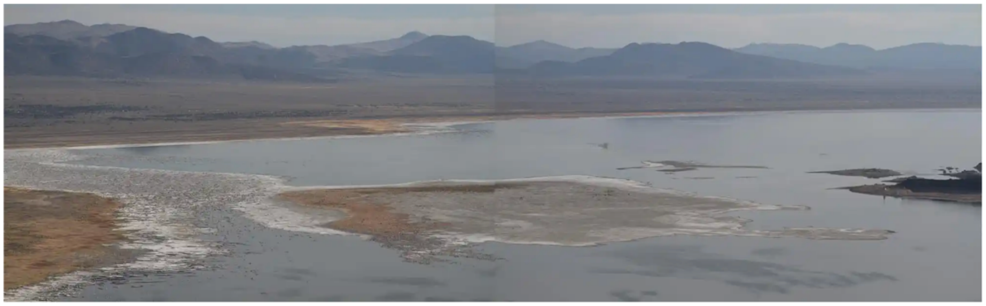

This composite of two photos from the October 18, 2022 Eared Grebe survey flight shows the current extent of the landbridge (center), which is becoming increasingly exposed between the mainland (left) toward Negit Island and the California Gull nesting islets (right). Photos by Robbie Di Paolo.

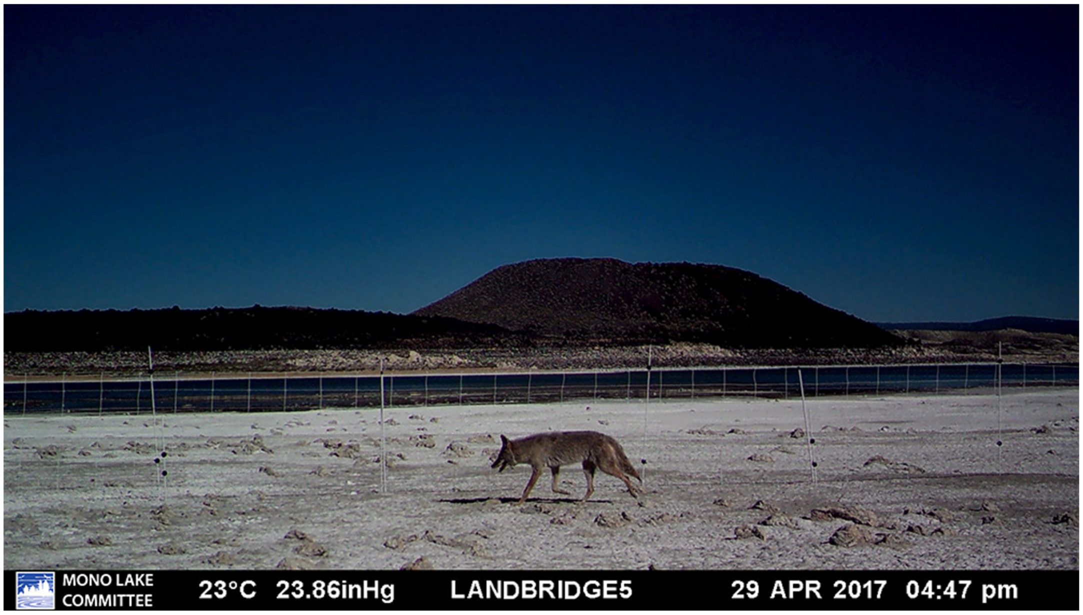

Figure 4. Coyote successfully thwarted by community-installed wildlife electric fence, captured by wildlife camera. Photo: Mono Lake Committee

References

Burnett, R. D., Nelson, K., & Schmidt, A. E. (2021). Population size and reproductive success of California Gulls at Mono Lake, California.

Dunn, J. R. (1953). The origin of the deposits of tufa in Mono Lake [California]. *Journal of Sedimentary Research*, *23*(1), 18-23. https://doi.org/10.1306/D4269530-2B26-11D7-8648000102C1865D

Keevil, C. E., Rogerson, M., Parsons, D. R., Mercedes-Martín, R., Brasier, A. T., Reijmer, J. J., & Matthews, A. (2022). The geomorphological distribution of subaqueous tufa columns in a hypersaline lake: Mono Lake, USA. *Journal of Sedimentary Research*, *92*(6), 530-545.

Biosignature Detection and Sulfide Fractionation at Mono Lake

Lily Coffin

Isotopic Fractionation

All elements have a characteristic isotope abundance. Atomic weight is determined by taking a weighted average of all naturally occurring isotopes by percent abundance. One might expect that these characteristic abundances are approximately constant in nature, however, certain processes can sequester particular isotopes and change the observable relative abundances. Although isotopes of the same element will have identical chemical properties, the slight difference in mass affects the vibrational, rotational, and translational motion of atoms. In bonding, the vibrational energy tends to be lower for heavier atoms, producing a stronger bond. Chemical processes can show preference for specific isotopes, and isotope abundances can be preserved in the rock record to give clues about biological and environmental factors of the past[6].

Sulfur Reducing Bacteria at Mono Lake

Mono Lake is a hypersaline soda lake with a pH of 9.8. This is considered an extreme environment, and organisms that are able to thrive here are an excellent model for organisms that could survive in other extreme environments like the surface of Mars or the subsurface ocean of Europa. Within the lake sediment where oxygen is limited, some species of bacteria reduce sulfate instead of oxygen to perform respiration anaerobically. *Desulfovibrio vulgaris* is a common example of a sulfate-reducing bacteria (SRB), and its mechanism for sulfate metabolism is shown to the right[3].

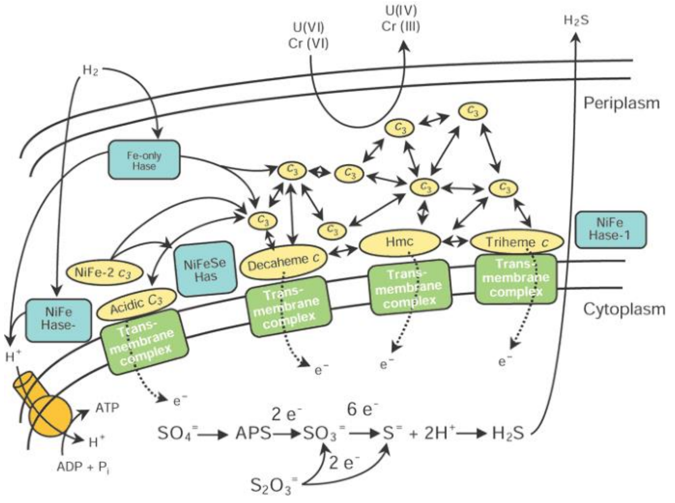

Fig 1 Sulfate reduction pathway for cellular respiration by *Desulfovibrio vulgaris.*

Biological Fractionation

Biological enzymes carryout the chemical reactions necessary to reduce sulfate for anaerobic respiration. At each step in this pathway, the enzymes exhibit a preference for lighter isotopes, so H_2S produced by these organisms will have an isotope signature that is different from abiotically generated H_2S. Fractionated isotope signatures preserved in the rock record have been used to follow the origin of sulfur metabolisms and the introduction of abundant oxygen in Earth's atmosphere. In a laboratory setting, the difference in abundance of ^{34}S between the SO_4^{2-} reactant and the H_2S product exceeded 65%, which shows that biogenic sulfur metabolism is a strong driver of sulfur fractionation. Variations in ^{34}S fractionation can be caused by biogenic sulfate reduction, sulfide oxidation, disproportionation of intermediate sulfur compounds as well as abiotic atmospheric photochemistry or thermochemical sulfur reduction. Abiotic factors tend to have little effect on less abundant isotopes, so ^{33}S or ^{36}S can be more helpful in determining the fractionation contribution of different biotic and abiotic factors[5].

Biosignature Detection on Mars?

Sulfur is widely abundant on Mars, making sulfur metabolizing organisms a distinct possibility on the red planet. There is mineralogical evidence that suggests a past presence of evaporitic, acidic, sulfate enriched brines similar to the environment of Mono Lake, indicating Mars may have supported similar SRBs.

Large sulfur isotope fractionations have been measured by the Curiosity rover on Mars. A -47 to 28% depletion of ^{34}S was recorded at Gale crater, which is a similar magnitude to an analogous environment on Earth. Biogenic sulfur cycling could explain this phenomenon; however, the large fractionation can also be explained by abiotic processes characteristic of an impact-generated hydrothermal system. It is proposed that the atmospheric processing and equilibrium fractionation are responsible, rather than biogenic sulfur processing[2]. This data has not been dismissed as evidence of biosignature detection, even if there are other explanations.

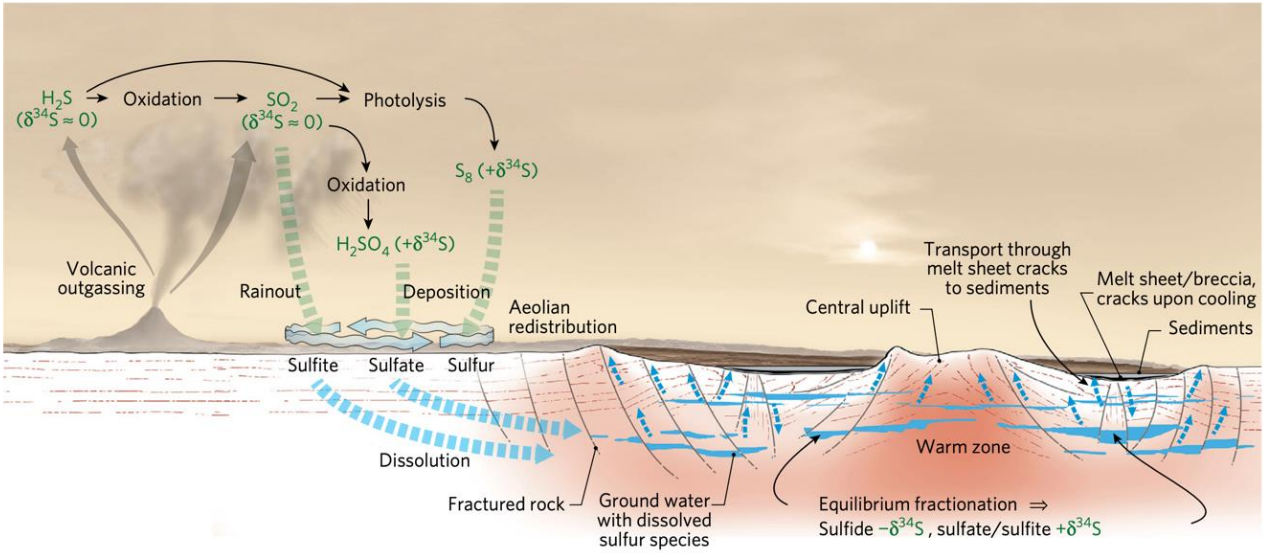
H_2S $(\delta^{34}S \approx 0)$
Oxidation
SO_2 $(\delta^{34}S \approx 0)$
Photolysis
Oxidation
S_8 $(+\delta^{34}S)$
H_2SO_4 $(+\delta^{34}S)$
Volcanic outgassing
Rainout
Deposition
Aeolian redistribution
Sulfite
Sulfate
Sulfur
Dissolution
Fractured rock
Ground water with dissolved sulfur species
Central uplift
Transport through melt sheet cracks to sediments
Melt sheet/breccia, cracks upon cooling
Sediments
Warm zone
Equilibrium fractionation ⇒
Sulfide $-\delta^{34}S$, sulfate/sulfite $+\delta^{34}S$

Fig 2 Possible mechanism for abiotic 34S fractionation at Gale crater.

Future Biosignature Detection on Europa

The composition of Europa's oceans is less certain than the composition of Mars, but it is theorized that sulfur ions are significantly represented from exogenous sulfur deposits from Io[1]. The MASPEX instrument on the Europa Clipper mission will be able to distinguish isotopes and hopefully collect data about sulfur fractionation that may support theories of sulfur metabolizing life[4].

References

1. Arola Moreras-Marti, et al. "Sulfur Isotopes as Biosignatures for Mars and Europa Exploration." Journal of the Geological Society, vol. 179, no. 6, 23 Aug. 2022, https://doi.org/10.1144/jgs2021-134.
2. Franz, H. B., et al. "Large Sulfur Isotope Fractionations in Martian Sediments at Gale Crater." Nature Geoscience, vol. 10, no. 9, 7 Aug. 2017, pp. 658–662, https://doi.org/10.1038/ngeo3002. Accessed 4 Mar. 2023.
3. Heidelberg, John F, et al. "The Genome Sequence of the Anaerobic, Sulfate-Reducing Bacterium Desulfovibrio Vulgaris Hildenborough." Nature Biotechnology, vol. 22, no. 5, 11 Apr. 2004, pp. 554–559, https://doi.org/10.1038/nbt959.
4. "MASPEX | Instruments." NASA's Europa Clipper, europa.nasa.gov/spacecraft/instruments/maspex/#otp_how_it_works.
5. Stam, Marjolijn C., et al. "Sulfate Reducing Activity and Sulfur Isotope Fractionation by Natural Microbial Communities in Sediments of a Hypersaline Soda Lake (Mono Lake, California)." Chemical Geology, vol. 278, no. 1-2, Nov. 2010, pp. 23–30, https://doi.org/10.1016/j.chemgeo.2010.08.006. Accessed 14 Oct. 2021.
6. White, William M. *Isotope Geochemistry*. Chichester, Wiley Blackwell, Cop, 2015, pp. 263–265.

Mono Lake’s Hypersalinity and Its Effect on Flies

Marisa Langley

Acknowledgements: This report was inspired by a lecture given by Professor Michael Dickinson in “The Biomechanics of Organismal Design.” I’m incredibly grateful to Professor Dickinson for always being so passionate about flies.

The flies of Mono Lake

Mono Lake is inhabited by a large population of flies. Although the species Ephydra hians (commonly known as the ”alkali fly”) resembles the housefly, it has vastly different qualities. Unlike the isolated flies in our everyday experiences, the Mono Lake flies cluster together, mingling on the shoreline in vast numbers [1]. In his 1872 book *Roughing It*, Mark Twain describes the flies as follows:

> “. . . any time, you can see there a belt of flies an inch deep and six feet wide, and this belt extends clear around the lake—a belt of flies one hundred mile long. If you throw a stone among them, they swarm up so thick they look dense, like a cloud.” [2]

The hypersalinity of Mono Lake

Salts build up easily in Mono Lake because it is a closed lake, with no way for water to leave except by evaporation. Thus, the concentration of salt in the lake gets higher and higher over time. By one estimate, if all the solids currently dissolved in the lake were taken out, they would collectively weigh around 280 million tons [3]. Although the exact values depend on the water level of the lake, Mono Lake has a salinity of around 81 grams/liter and an alkalinity of around 10 pH [3, 4].

Mono Lake contains a variety of different salts, such as sodium chloride (NaCl), sodium sulfate ($Na_2\,SO_4$), and sodium bicarbonate ($Na\,H\,CO_3$) [4]. Unlike other lakes with high salinity, Mono Lake contains a significant amount of sodium carbonate ($Na_2\,CO_3$) [4]. In fact, out of the $\sim$81 grams/liter salt concentration, there are about $\sim$32 grams/liter of sodium carbonate in Mono Lake.

The flies and the hypersalinity

Surviving in a lake with such high salinity is a challenge. For example, consider fish. Although fish are found oceans, which are about a third as salty, fish cannot survive the salt of Mono Lake. Not only are there no fish native to the lake, attempts to introduce fish into the lake have failed [5].

Even among flies, the Mono Lake flies are unique. Thanks to a project done by Francis van Breugel and Michael Dickinson at Caltech, we know that if you dip a typical fly in a solution filled with sodium carbonate, it becomes sopping wet, even if it has adaptations to guard against water [4].

The flies of Mono Lake have no such issues. They can survive being dipped in Mono Lake and will still come out “as dry as a patent office report,” in the words of Mark Twain [2]. When a Mono Lake fly enters the water, it is encapsulated by a bubble of air which protects its body from becoming wet. The act of pushing against the surface tension and entering the water takes a great deal of force on the fly's part; in fact, the maximum force it exerts was calculated to be 18 times its body weight.

Once it has entered the water, the only parts of the fly's body that are exposed to the water are its eyes, so that it can see underwater, and its tarsal claws, so that it can grip rocks and crawl underwater. When the fly decides to leave the water, it doesn't need to crawl to the beach, but can instead release its grip on the rock, float to the surface in its bubble, and fly off. The fly's anti-wetness adaptation is crucial in this last step, since a wet fly would not be able to get above the surface of the water, but would instead helplessly bob around. However, since the Mono Lake fly remains dry, it is able to get upon the surface of the lake, and the surface tension of the lake pushes against the fly, helping it leave the water. In their study, van Breugel and Dickinson dipped flies in solutions containing different salts found in Mono Lake, and they discovered the salt that was most effective at trapping flies was sodium carbonate. (Their paper includes some fascinating explanations of why the sodium carbonate makes the water so sticky.)

As we discussed above, Mono Lake has a high concentration of sodium carbonate, so it is no surprise that, out of the seven species they tested, the only fly that was able to stay dry in sodium carbonate solutions was the Mono Lake fly [4]. Surprisingly, the super-hydrophobicity of the Mono Lake fly does not use a different mechanism as the regular hydrophobicity of other flies. Other flies also employ hair and waxy cuticles for hydrophobicity. What makes the Mono Lake fly special is simply the degree to which it is hairy and the degree to which its wax protects against water [4].

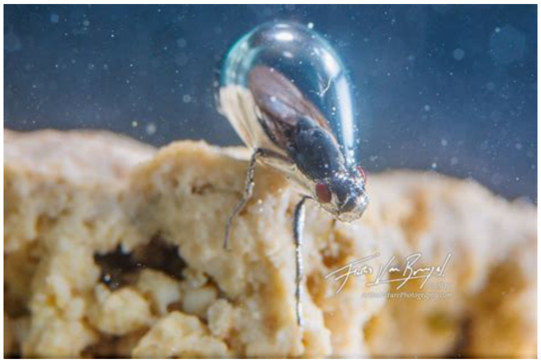

The flies and the ever-increasing salinity

Although Mono Lake is guaranteed a water right by law, the water level was over a foot below the target level in 2022 [6]. The water levels of Mono Lake have been lowering for decades, leading to a rapid increase in the salinity of Mono Lake [6].

The Mono Lake fly spends most of its life underwater. The eggs are laid and hatch underwater, the larvae live underwater, and the adults gather food underwater. Although the diving ability we discussed above is not particularly affected by increasing salinity, other aspects of the flies' lives are highly affected.

In particular, the rising salinity has a major impact on osmoregulation. Osmoregulation is the regulation of the internal osmotic concentration, which is very important for creatures in extremely saline environments like Mono Lake. In general, a rise in salinity has a huge impact on the energy required for osmoregulation, and it leads to less growth and reduced size in aquatic creatures. A study from 2023 found that similar results hold for the Mono Lake fly when the larvae were raised in different salinities [7].

References

1. *Alkali Flies* `https://www.monolake.org/learn/aboutmonolake/naturalhistory/alkaliflies/`.
2. Twain, M. *Roughing It* `https://gutenberg.org/cache/epub/3177/pg3177-images.html` (1872).
3. *Water Chemistry* `https://www.monolake.org/learn/aboutmonolake/naturalhistory/chemistry/`.
4. Van Breugel, F. & Dickinson, M. H. Superhydrophobic diving flies (¡i¿Ephydra hians¡/i¿) and the hypersaline waters of Mono Lake. *Proceedings of the National Academy of Sciences* **114,** 13483–13488. eprint: `https://www.pnas.org/doi/pdf/10.1073/pnas.1714874114`. `https://www.pnas.org/doi/abs/10.1073/pnas.1714874114` (2017).
5. *Frequently Asked Questions About Mono Lake* `https://web.archive.org/web/20170418210400/http://www.monolake.org/about/faq`.
6. *Conservation Plan for Wilson's Phalarope* 2024. `https://whsrn.org/wp-content/uploads/2024/01/plan_wiph_2024_final_en.pdf`.
7. Herbst, D. B. Developmental and reproductive costs of osmoregulation to an aquatic insect that is a key food resource to shorebirds at salt lakes threatened by rising salinity and desiccation. *Frontiers in Ecology and Evolution* **11.** ISSN: 2296-701X. `https://www.frontiersin.org/journals/ecology-and-evolution/articles/10.3389/fevo.2023.1136966` (2023).

Geologic History of the Poleta Folds

Will Lawrence, Ge 136A

Field camp is a rite of passage for undergraduate geology students, and I was lucky to have had my own field camp experience in the Poleta Folds. Having never camped for an extended period, one month in the desert was quite a step up from anything that I was used to. Our time mapping rocks and analyzing structures in the field would mercifully end at around half past noon each day, avoiding the hellishly hot summer temperatures that swung through in the early afternoon. One colleague brought a cornhole set to the campground, resulting in our bean-bag-tossing skills improving significantly over the course of a month (in great excess of our mapping skills). Weekends were spent taking dips in the Owens River, or trips down to the local bar in Bishop aptly named the “Rusty Saloon”. Apart from having a fantastic experience, I walked away with an appreciation for the importance and difficulty of geologic mapping and field observation. A quote by Caltech’s own Jason Saleeby attests to this: “Perhaps one of the unique aspects of the science of geology is the time transcendence of sound field observations and descriptions regardless of the paradigm in genetic lines of thought.” (Saleeby, 1999).

Moving Rocks and Making Mountains

The rocks exposed in the White-Inyo Range hold important clues to the complex evolution of the western margin of the North American continent (Nelson et al., 1991). Neoproterozoic to Cambrian marine sediments (~700–550 Ma) were deposited adjacent to the continental margin, and these were deformed by a protracted series of mountain building events triggered by continental collisions, termed orogenies. To the west of the White-Inyo Range lies the Sierra Nevada, remnants of the magmatic arc that formed in most recent episode of collisional evolution (~150 Ma) recorded in the rocks of western California.

The Poleta Folds lie in a structural depression situated on a regional N/NW-trending anticlinorium traced by the White and Inyo mountains (Fig. 1). In contrast to the geometry of the White-Inyo anticline, the structures the Poleta Folds comprise smaller NE-trending folds and low-angle thrust faults. These clearly distinguish two episodes of compressional folding and faulting in the White-Inyo Range (Morgan and Law, 1998). Tectonic compression leaves its imprint at smaller scales in the development of cleavage fabrics in rocks, and detailed outcrop observations have locally shown that NE-striking cleavages overprint N/NW-striking cleavages. This conclusively documents a relatively older age of the NE-trending structures ubiquitous in the Poleta region.

Similar NE-trending folds to those observed at Poleta are found in Nevada, and as far as 120 km to the NW near the Eastern Sierras (Morgan and Law, 1998). These are associated with the ~340 Ma Antler orogeny, and thus the deformation observed in the Poleta Folds has been attributed to the same event. On the other hand, the N/NW-trending structures associated with the White-Inyo anticlinorium have been associated with the

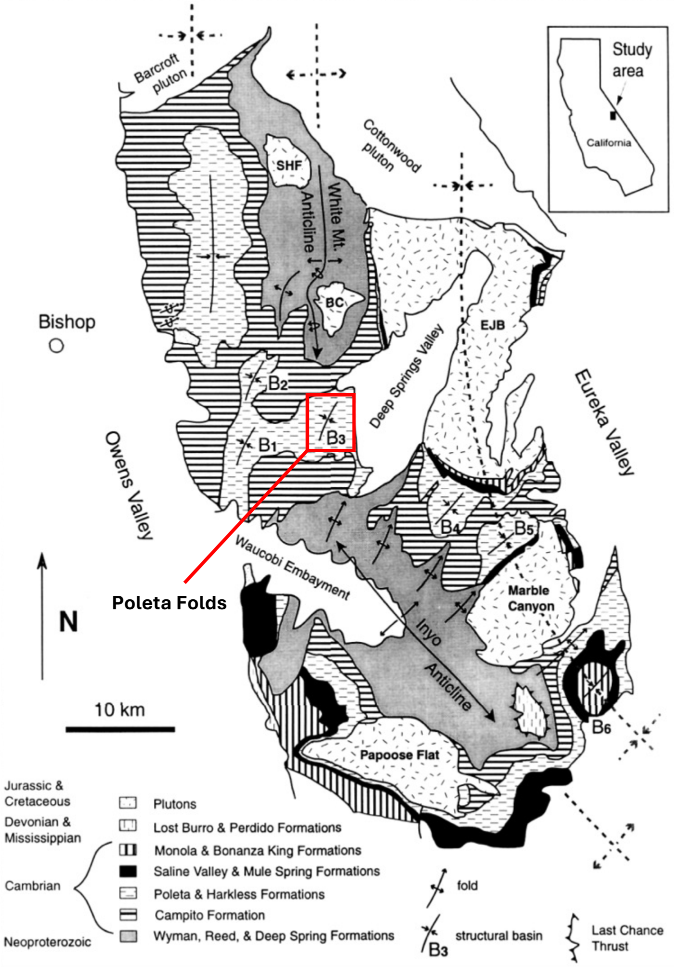
Barcroft pluton
Cottonwood pluton
Study area
California
SHF
White Mt. Anticline
BC
Bishop
EJB
Deep Springs Valley
Eureka Valley
B2
B1
B3
Owens Valley
B4
B5
Waucobi Embayment
Poleta Folds
Marble Canyon
Inyo Anticline
N
10 km
Papoose Flat
B6
Jurassic & Cretaceous
Plutons
Devonian & Mississippian
Lost Burro & Perdido Formations
Cambrian
Monola & Bonanza King Formations
Saline Valley & Mule Spring Formations
Poleta & Harkless Formations
Campito Formation
Neoproterozoic
Wyman, Reed, & Deep Spring Formations
fold
structural basin
Last Chance Thrust

Figure 1. Geologic Map of the White-Inyo Range adapted from Morgan and Law, (1998).

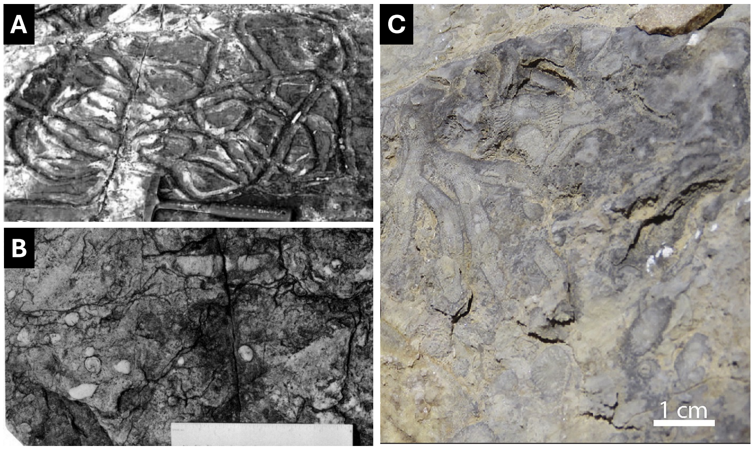

Figure 2. Fossils in rocks of the Poleta Formation. Trace fossils of A) *Taphrhelminthopsis* and B) *Skolithos* (circular) and *Planolites* (tubular). C) Branching archaeocyathids in a carbonate reef. Images from Hagadorn et al. (2000), Alpert (1975), and Pruss et al. (2019).

~225 Ma Sonoma orogeny. Remarkably, this folding event appears to have been linked with regional movement along a large thrust fault (the Last Chance thrust); a structural window through this fault puts the entire ~7 km thick Neoproterozoic to Cambrian sequence of the White-Inyo Range on top of younger Devonian and Carboniferous rocks. This suggests that the rocks of the White-Inyo Range originated at a minimum of 75 kilometers to the west of their present location!

Life in the Oceans of the Cambrian

Untangling the rocks of the Poleta Folds gives a snapshot of a near-shore marine environment during the Cambrian period. The varied appearance of limestone, sandstone and mudstone rocks reflect their deposition in tidal and subtidal settings, along with reef and shoal environments (Nelson et al., 1991). These rocks preserve evidence of a remarkable 'explosion' of life that occurred at the Precambrian-Cambrian boundary, marked by the sudden appearance of a diverse range of invertebrates in the fossil record. Included are some of the oldest trilobite faunas in North America, and primitive molluscs (e.g., *Wyattia*), along with abundant 'trace' fossils. These trace fossils are often observed as crisscrossing tracks or trails left behind by ancient arthropods and molluscs as they scurried about the seafloor. Whichever animal left behind the enigmatic *Taphrhelminthopsis*, might have spent a little too much time at the Cambrian equivalent of the Rusty Saloon as its drunken meanderings show little evidence of rhyme or reason in its motion (Fig. 2A). *Skolithos* are observed as vertical pipe-like features cutting down into sediment layers and are often accompanied by horizontal burrows called *Planolites* (Fig. 2B), both traces left behind by an unknown worm-like animal.

An important member of the fossil record preserved in limestone rocks of the Poleta Formation are archaeocyathids. These sponge-like creatures have a brief appearance in the geologic record, but they served an important role as the first carbonate reef builders, providing structures that housed complex and biodiverse ecosystems (Pruss et al., 2019). They can be observed as concentric circular and tubular features in limestones, usually in abundance as larger reef-like structures (Fig. 2C). While relatively common in carbonate rocks deposited as the Poleta Formation, they disappear from the fossil record after this time. The extinction of the archaeocyathids appears to have coincided with a significant change in the global carbon cycle, although the exact cause of this remains unknown (Pruss et al., 2019).

It is hard to envision the Cambrian environment captured by the rocks of the Poleta Folds, especially in contrast to the current barren landscape. If hanging out in the desert on a geology field trip isn't for you, maybe try imagining that you're wading through the chest-deep waters of an early Paleozoic sea. You'll probably want to avoid stepping on the makers of *Skolithos*…

References

Alpert, S. P. (1975). Planolites and Skolithos from the Upper Precambrian-Lower Cambrian White-Inyo Mountains, California. *Journal of Paleontology*, *49*(3), 508-521.

Hagadorn, J. W., Schellenberg, S. A., & Bottjer, D. J. (2000). Paleoecology of a large Early Cambrian bioturbator. *Lethaia*, *33*(3), 142-156.

Morgan, S. S., & Law, R. D. (1998). An overview of Paleozoic-Mesozoic structures developed in the central White-Inyo Range, eastern California. *International Geology Review*, *40*(3), 245-256.

Nelson, C. A., Hall Jr, C. A., & Ernst, W. G. (1991). Geologic history of the White-Inyo Range. *Natural History of the White Inyo-Range, Eastern California*, 42-74.

Pruss, S. B., Smith, E. F., Leadbetter, O., Nolan, R. Z., Hicks, M., & Fike, D. A. (2019). Palaeoecology of the archaeocyathan reefs from the lower Cambrian Harkless Formation, southern Nevada, western United States and carbon isotopic evidence for their demise. *Palaeogeography, Palaeoclimatology, Palaeoecology*, *536*, 109389.

Saleeby, J. B., Moores, E. M., Sloan, D., & Stout, D. L. (1999). On some aspects of the geology of the Sierra Nevada. In *Classic Cordilleran concepts: a view from California* (Vol. 338, pp. 173-184).

The 1986 Chalfant Valley Earthquake Series

Victor Vescu · G3 · MCE/GPS · FT24 · Ge136a · Owens Valley · Nov 1st-3rd 2024

Introduction:

At 7.72 AM, on July 21, 2024, a M_w *6.2 earthquake struck West of Chalfant Valley, North of Bishop, California. The mainshock occurred at a depth of 10 km. It had one large foreshock a day before and one large aftershock 10 days later. There were numerous well-measured aftershocks, with many so small that their total number is uncertain. All three events, the foreshock, the mainshock, and the largest aftershock, were strike-slip with a small normal slip component. The fault planes were steep to moderately dipping and oriented approximately North-South. The main rupture resulted in a peak ground acceleration of 0.46g.*

Damages:

High-rise buildings were swayed in Los Angeles, San Francisco, and Salt Lake City. The earthquake caused an estimated \$2.7 million in damages. The most affected communities were Bishop and Chalfant, where two people were injured. Significant damages were observed in pipe and road infrastructure, mobile homes, and building facades. A Burger King lost its ceiling, prompting the company to divest from the area.

Aftershocks:

Shortly following the mainshock, the USGS deployed 120 vertical-component seismometers to obtain dense array recordings of aftershocks. The aftershocks were studied to obtain high-resolution crustal models beneath Chalfant Valley. The average aftershock stress drop tends to increase as the sequence progresses, suggesting that the faulted volume is equilibrating to the regional stress.

Field Observations:

The earthquake resulted in widespread surface faulting in the Volcanic Tablelands north of Bishop. In many locations, surface cracks had a left-stepping en-echelon pattern. The cracks were found mainly in loose sand. This, in combination with rainy weather a few days after the earthquake, made measurements difficult.

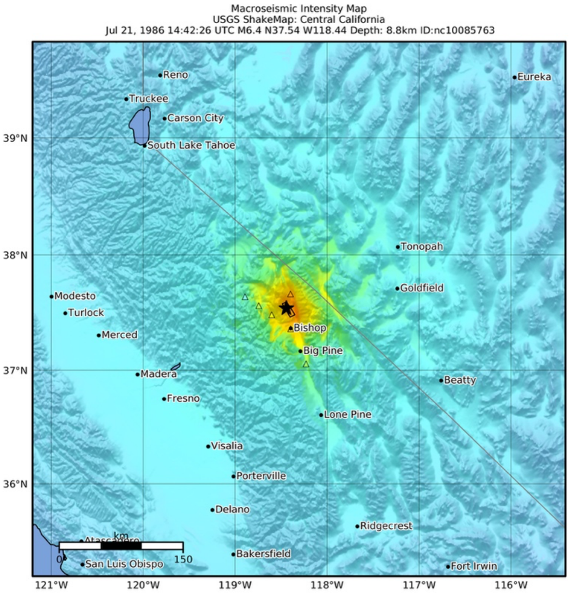
Macroseismic Intensity Map
USGS ShakeMap: Central California
Jul 21, 1986 14:42:26 UTC M6.4 N37.54 W118.44 Depth: 8.8km ID:nc10085763
Reno
Eureka
Truckee
Carson City
South Lake Tahoe
Tonopah
Goldfield
Modesto
Turlock
Merced
Bishop
Big Pine
Madera
Beatty
Fresno
Lone Pine
Visalia
Porterville
Delano
Ridgecrest
Atascadero
San Luis Obispo
Bakersfield
Fort Irwin
km
0
150
39°N
38°N
37°N
36°N
121°W
120°W
119°W
118°W
117°W
116°W

SHAKING	Not felt	Weak	Light	Moderate	Strong	Very strong	Severe	Violent	Extreme
DAMAGE	None	None	None	Very light	Light	Moderate	Moderate/heavy	Heavy	Very heavy
PGA(%g)	<0.05	0.3	2.76	6.2	11.5	21.5	40.1	74.7	>139
PGV(cm/s)	<0.02	0.13	1.41	4.65	9.64	20	41.4	85.8	>178
INTENSITY	I	II-III	IV	V	VI	VII	VIII	IX	X+

Scale based on Worden et al. (2012) Version 1: Processed 2019-09-25T23:51:25Z

△ Seismic Instrument ○ Reported Intensity ★ Epicenter ▭ Rupture

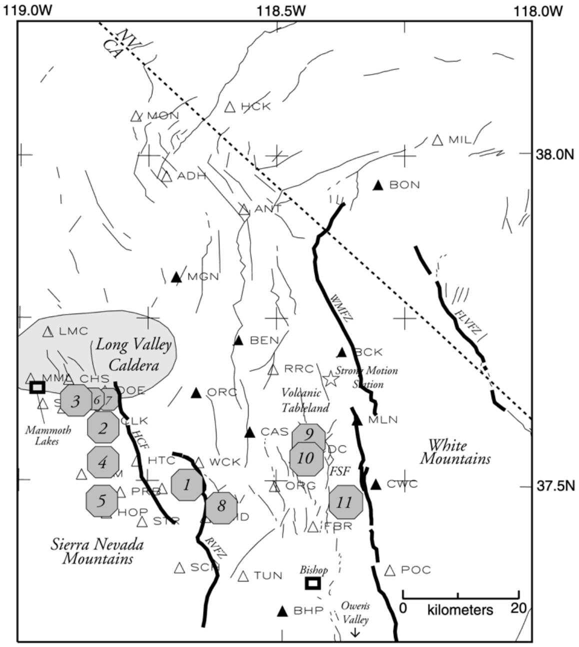
119.0W
118.5W
118.0W
38.0N
37.5N
NV
CA
MON
HCK
MIL
ADH
BON
ANT
MGN
WMFZ
FLVFZ
LMC
Long Valley Caldera
BEN
BCK
RRC
Strong Motion Station
MMC
CHS
DOE
ORC
Volcanic Tableland
Mammoth Lakes
CLK
CAS
MLN
HCF
HTC
WCK
DC
FSF
White Mountains
PRB
ORG
CWC
HOP
STR
FBR
Sierra Nevada Mountains
RVFZ
SCH
TUN
Bishop
POC
BHP
Owens Valley
0
kilometers
20
1
2
3
4
5
6
7
8
9
10
11

1. M 5.7 October 1978 Wheeler Crest earthquake.
2-5. Four M 6+ earthquakes, May 1980.
6-7. M 5 events in Caldera's south moat, January 1983.
8. M 5.8 November 1984 Round Valley earthquake.

CHALFANT

9. Event I M 5.7, 14:29 - July 20
10. Event II M 6.3, 14:42 - July 21
11. Event III M 5.4, 07:22 - July 31

△ Network Stations

▲ (Filled used in Stress Drop Analysis)

— Quaternary Faults

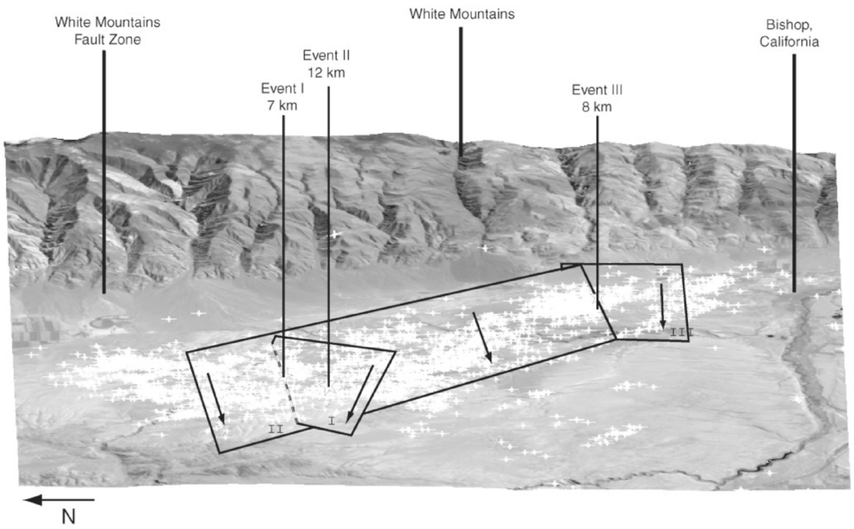

Tectonic Setting:

Owens Valley was the scene of the 1872 M_w *7.4-7.9 Lone Pine Earthquake, which generated surface ruptures over a 100 km-long region. The region is part of the Eastern California–Central Nevada seismic zone, also known as the Walker Line. No other large earthquake (*$>M_w$ *7) has occurred between the Southern edge of the 1932 Cedar Mountains rupture and the Northern extent of the 1872 Lone Pine Earthquake. The 1986 Chalfant Valley event and the 1934* M_w *6.3 Excelsior Mountains earthquake have been the most significant events in this seismic gap. However, studies suggest that they cannot fully account for the relaxation of the stress build-up. Studies of focal mechanisms and aftershocks suggest that the Chalfant sequence appears to have transferred strike-slip motion away from the White Mountains front, contributing to the observed increase in the relative normal offset along the White Mountains.*

Dust clouds:

Due to the arid region in which it occurred, the mainshock had an interesting consequence. Immediately following the shaking, dust was dislodged by slope failures along the White Mountains and the Chidago Canyon, creating large clouds throughout the landscape.

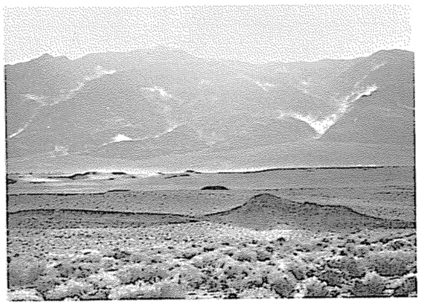

References:

[1] Brewer, L. (1989). The Intensity of the July 21, 1986, Chalfant Valley, California, Earthquake (No. 89-135). US Geological Survey.

[2] Bryant, William A., Canon, Ted J., Hart, Earl W., Horstman, Nancy G., Kahle, James E., Love, R. Jay, McCormick, David L., Shakal, Anthony F., and Urhammer, Robert A., Report on the Chalfant Valley, California, Earthquake July 21, 1986, in Earthquake Engineering Research Institute Special Report, Newsletter, November 1986, v. 20, no. 11, p. 1-8.

[3] Smith, K. D., & Priestley, K. F. (2000). Faulting in the 1986 Chalfant, California, sequence: Local tectonics and earthquake source parameters. Bulletin of the Seismological Society of America, 90(4), 813-831.

[4] Rietbrock, A., & Scherbaum, F. (1994). Acoustic imaging of earthquake sources from the Chalfant Valley, 1986, aftershock series. Geophysical Journal International, 119(1), 260-268.

[5] Lienkaemper, J. J., Pezzopane, S. K., Clark, M. M., & Rymer, M. J. (1987). Fault fractures formed in association with the 1986 Chalfant Valley, California, earthquake sequence: Preliminary report. Bulletin of the Seismological Society of America, 77(1), 297-305.

[6] dePolo, C. M., & Ramelli, A. R. (1987). Preliminary report on surface fractures along the White Mountains fault zone associated with the July 1986 Chalfant Valley earthquake sequence. Bulletin of the Seismological Society of America, 77(1), 290-296.

The Lake Crowley Columns

Grace Otos

Introduction:

The Lake Crowley Columns are a geologic formation on the east side of what is now Lake Crowley, formed as a result of water downwelling into the ash and rock that came to form the Bishop Tuff almost 760,00 years ago. The columns are made of morenite, and have been etched into the landscape as surrounding softer rhyolite eroded away. Due to their proximity to Lake Crowley, much of the year the columns remain underwater due to high water levels in the lake, but during low-level times, the columns are accessible by foot, boat, or all-terrain vehicles.

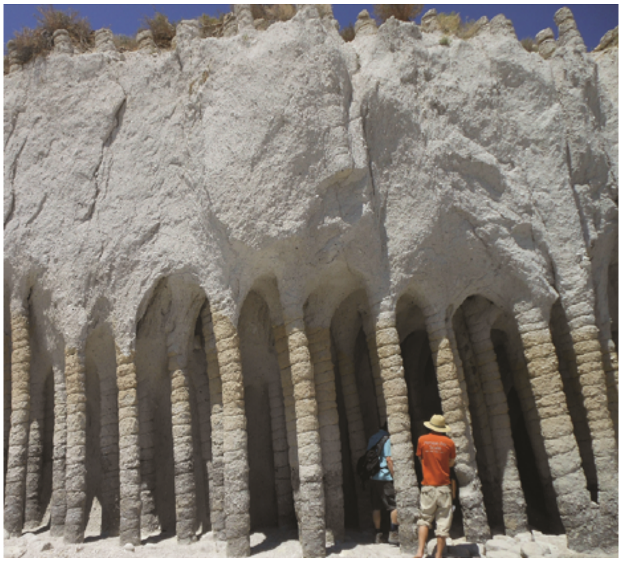

Fig. 1 A section of the Lake Crowley Columns. The columns vary in diameter, ranging from about 0.3-1 m in diameter. The columns form archways as the higher layers of rock have yet to have the rhyolite in between the columns erode. (Randolph-Flagg, 2017)

How did the columns form?

During the formation of the Bishop Tuff, the settling volcanic rock took years to cool. The rock cooled quickly on the surface due to air exposure, but under the surface, the rock remained hot for several years. During this time, rain and snow fell on the developing tuff and seeped into the rock, with low lying parts of the tuff forming lakes. As the water got deeper into the dense hot rock, it boiled. The steam would congregate into columnal vents. Before reaching the surface and creating a proper vent, the water cooled enough once again to condense, which prevented the columns from breaking the surface. The water once again moved down through the rock, boiled and moved up, and condensed. While in the liquid phase, the water transported ions through the rock, incorporating the water and ions into the crystal structure along these columnar structures, thus creating morenite, a zeolite formed at these relatively low temperatures (100 C-130 C). Zeolite rocks incorporate water into their crystal structure, creating a porous, but relatively strong and erosion resistant silica based material. This process continues as the ions are allowed to accumulate while the water is in the liquid form, while the column is being built upwards by the steam. Eventually this process halts as the rock cools and the water no longer boils as it moves through the layer, leaving behind the morenite structures as fossils of this hydrothermal activity. The columns reveal themselves as water erodes the surrounding rhyolite but not the stronger morenite. The columns today are revealed on the very edges of the tuff since this is the only available spot to be able to see geologic formations at the very base of the tuff.

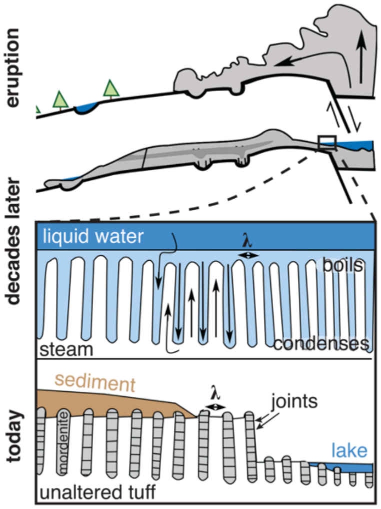
eruption
decades later
today
liquid water
λ
boils
steam
condenses
sediment
λ
joints
mordenite
lake
unaltered tuff

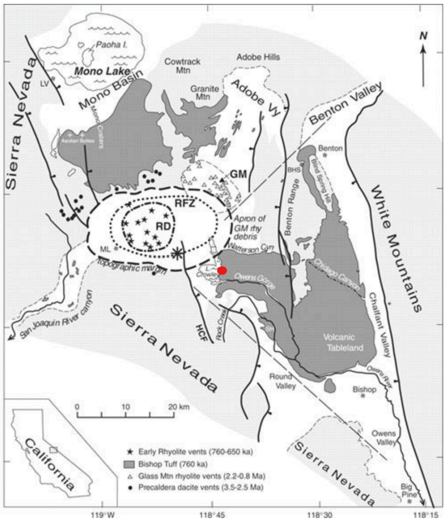
N
38°N
37°45
37°30
37°15
119°W
118°45
118°30
118°15
Paoha I.
Mono Lake
LV
Mono Basin
Mono Craters
Aeolian Buttes
Sierra Nevada
Cowtrack Mtn
Granite Mtn
Adobe Hills
Adobe Vy
Benton Valley
Benton
BHS
Blind Spring Hill
GM
RFZ
RD
ML
Apron of GM rhy debris
Watterson Cyn
Topographic margin
L. Crowley
Owens Gorge
Benton Range
White Mountains
Chidago Canyon
Chalfant Valley
San Joaquin River canyon
Sierra Nevada
HCF
Rock Creek
SH
Volcanic Tableland
Round Valley
Owens River
Bishop
0
10
20 km
California
★ Early Rhyolite vents (760-650 ka)
▨ Bishop Tuff (760 ka)
△ Glass Mtn rhyolite vents (2.2-0.8 Ma)
● Precaldera dacite vents (3.5-2.5 Ma)
Owens Valley
Sierra Nevada
Big Pine

Fig 2. (Left) A schematic of the formation of the columns. Water boils and condenses through the rock in a columnal formation producing the mordenite columns, revealed by the erosion by the local modern lake (Lake Crowley). (Randolph-Flagg, 2017)
Fig 3. (Right) The location of the Lake Crowley Columns formation (marked in red) relative to the Bishop tuff. Its placement on the edge correlates to why the columns have now been exposed. (Hildreth, 2007)

Why do they look like that?
The column's spacing varies through the region based on the relative permeability of the original rock in which it formed. Highly vertically permeable rock made more stable but more spaced columns since the water could easily travel up to form columns. Highly horizontally permeable rock creates less stable columns since the steam was not constrained to proper columns to form. Since the permeability, determined in part by the local silica content, is relatively uniform in any given region, it results in relatively uniform spacing between the columns in any given region of the formation. It is theorized that there may be more columns that have yet to be revealed lower in the basin of the tuff. There are still questions about why exactly the columns formed with clear horizontal joints.

Citations

Randolph-Flagg, N. (2017, Oct 2). Evenly spaced columns in the Bishop Tuff (California, USA) as relics of hydrothermal cooling. Geology 2017, 45 (11): 1015–1018. https://doi.org/10.1130/G39256.1

Hildreth, W. (2007). Compositional zoning of the Bishop Tuff. Journal of Petrology, Volume 48, Issue 5, May 2007, Pages 951–999, https://doi.org/10.1093/petrology/egm007

Kordala, N., & Wyszkowski, M. (2024). Zeolite Properties, Methods of Synthesis, and Selected Applications. Molecules (Basel, Switzerland), 29(5), 1069. https://doi.org/10.3390/molecules29051069

The Effects of Great Basin and Range Extension on Biodiversity

Ge 136a; Fall 2024 | Isaac N. Aguilar Rivera

Background

The diversity of life on Earth is a fundamental, yet poorly understood, feature of the planet. The biosphere includes multifaceted properties that can be quantified as the number of species and their variation in phylogeny, form, and function that evolve over geological time. Understanding how and why diversity varies over time, environment, and geography is central to describing the reciprocal relationship between biodiversity and geological processes. Distinguishing the elusive roles of tectonic activity, paleoelevation, and climate in determining patterns of the distribution and richness of multiple dimensions of biodiversity requires an interdisciplinary examination of the geologic and biotic record. The extant and fossil record of biodiversity in the Great Basin and Range of Western North America demonstrates elevated taxonomic, ecological, and phylogenetic richness in mountainous regions with increased topographic complexity (1). However, the mechanisms shaping this Topographic Diversity Gradient (TDG) over deep time remain elusive and motivate observations of regional species richness and turnover along gradients of basin sediment area, extensional strain rate, (paleo)elevation, and topographic ruggedness.

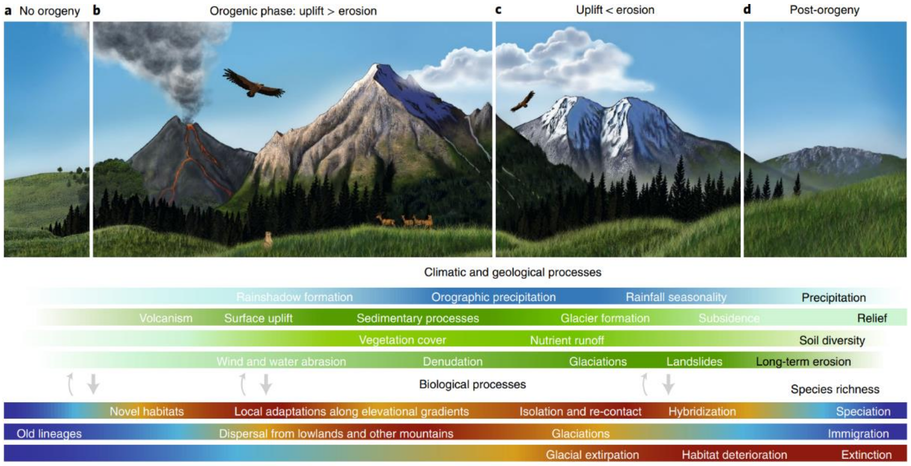
a No orogeny
b Orogenic phase: uplift > erosion
c Uplift < erosion
d Post-orogeny
Climatic and geological processes
Rainshadow formation
Orographic precipitation
Rainfall seasonality
Precipitation
Volcanism
Surface uplift
Sedimentary processes
Glacier formation
Subsidence
Relief
Vegetation cover
Nutrient runoff
Soil diversity
Wind and water abrasion
Denudation
Glaciations
Landslides
Long-term erosion
Biological processes
Species richness
Novel habitats
Local adaptations along elevational gradients
Isolation and re-contact
Hybridization
Speciation
Old lineages
Dispersal from lowlands and other mountains
Glaciations
Immigration
Glacial extirpation
Habitat deterioration
Extinction

Fig. 1: Linking the evolution of mountains and biodiversity. *Climatic (blue bar) and geological (green bars) variables influence species richness through speciation, immigration, and extinction (lower bars) through different orogenic phases. Lighter/colder colors in the bars indicate high and low levels, respectively. (Antonelli* et. al.*, 2018; figure from I. Voet)*

Observe: While driving through the Basin and Range landscape, note the environmental conditions and geological features that could influence patterns of species richness and distribution. *Are some of these features more important than others, and for which species?* As the geological landscape changes throughout Earth's history, elevational gradients can act as refugia and dispersal corridors (2), unless the rate of change outpaces the ability of species to adapt or track their preferred climate (3).

Biodiversity-Geology Phases of the Great Basin and Range

[Phase 1] From 30 to 20 Ma ago: Species richness was low and steady with low to moderate faunal turnover. The collapsing Nevadaplano and Mogollon highlands were a topographic barrier to immigration from the east and south, whereas large areas of low relief constrained opportunities for geographic speciation. A potential underestimation of species richness may be due to the comparatively smaller area of basin sediments reducing fossil preservation.

[Phase 2] From 19 to 14 Ma ago: Elevated rates of tectonic extension and widespread fault activation developed an increasing land area and topographic ruggedness which coincided with the rapid rise in regional species richness. In combination with mid-Miocene Climate Optimum (MMCO) dynamics, the landscape reorganization initiated geographic and ecological speciation, elevational range shifts, and immigration into the region. An implied non-linear biodiversity response to landscape change is concentrated during intervals of rapid and large elevational change and suggest that richness responds to the rate of landscape change more than to the specific properties themselves.

[Phase 3] From 13 to 1 Ma ago: Following the MMCO, species richness declined with low to moderate faunal turnover as the land surface reached a dynamic steady-state phase. Although ruggedness remained high, the processes generating biodiversity are subdued without marked changes to the relief structure or climate warming.

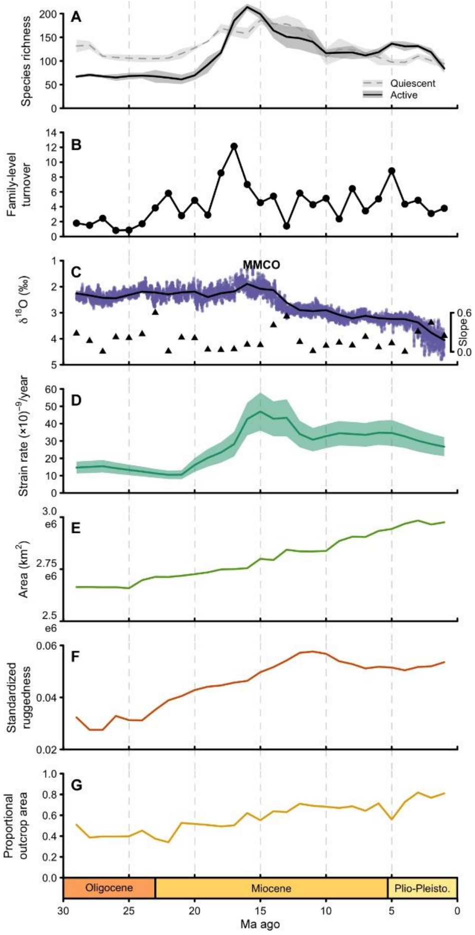

***Fig. 2:* Mammalian biodiversity trends in relation to geohistorical variables.** (A) Species richness of western N. America contrasted against the tectonically quiescent eastern region and (B) family-level turnover are compared to (C) oxygen isotope proxies for global temperature within 1 Ma bins shown as black triangles; (D) strain rate, (E) total area, and (F) median standardized ruggedness; and (G) the proportional outcrop area of the rock record in the tectonically active region of western N. America. (Smiley *et al.*, 2024)

Mechanisms and Processes of Biodiversity

Mountains and the geological processes in their orogeny as sources of biodiversity for adjacent low-relief regions during cooling periods of Earth's climate has been documented for other taxonomic groups and regions (4). During Miocene cooling, dispersal from tectonically active regions of Western North America into the low-relief Great Plains likely contributed to contemporary patterns of biodiversity and its geographic distribution. A changing climate on a dynamic landscape developed orographic gradients in precipitation and rain shadow effects that would have served to further isolate populations, limit species ranges, and lead to high spatial turnover across the landscape and elevated regional diversity. Speciation processes are facilitated by stronger elevational zonation that create barriers to dispersal in mountainous regions. It is also possible for periods with warmer and more stable climates to also see higher species richness across a topographically complex landscape.

In the Mojave subregion, mammals likely underwent in situ speciation during the middle Miocene period of rapid elevation gradients and climate warming. In particular, small mammal species experienced high turnover and reflect elevated rates of speciation and endemism on a rapidly changing landscape. Small mammals are more susceptible than large, mobile and migratory mammals to landscape changes that fragment and isolate populations. Interestingly, the rodent record shows evidence for increased hypsodonty earlier than the relatively well-described ungulate record. Rodents and other small mammals may exhibit earlier and stronger eco-evolutionary responses to landscape change. Future evaluation of individual clade dynamics should include differences in ecology, taphonomy, and sampling in a comparative framework to help discern the complex processes and interactions between species biology and landscape change. The inclusion of an improved Mesoamerican fossil record as well as coupled topographic-climate-landscape models are needed to identify the spatial configuration and timing of effective intercontinental corridor formation in the past. Given the variable spatial distribution of fossil localities through the Neogene, the challenges of scaling from regional to global drivers may provide a poor fit to temporal turnover data if spatial turnover is also high. In conclusion, the study of topographic and climatic features within the Basin and Range will be necessary to further characterize the causes of faunal turnover.

References

1. T.M. Smiley, Bahadori A., Troy Rasbury E., Holt W.E., and Badgley C., 2024, Tectonic extension and paleoelevation influence mammalian diversity dynamics in the Basin and Range Province of western North America, *Science Advances* **10**(25): eadn6842.
2. N.A. Hazey, J.S. Moreno, C. Ortiz-Movliav, R.D. Palacio, 2018, Biogeographic regions and events of isolation and diversification of the endemic biota of the tropical Andes, *PNAS USA* **115**: 7985-7990.
3. M.T. Burrows *et al*., 2014, Geographical limits to species-range shifts are suggested by climate velocity, *Nature* **507:** 492–495.
4. D. Esquerré *et al.*, 2018, How mountains shape biodiversity: The role of the Andes in biogeography, diversification, and reproductive biology in South America's most species-rich lizard radiation (Squamata: Liolaemidae). *Evolution* **73**: 214–230.

The Tahoe and Tioga Glaciations in the Sierra Nevada

Olivia Alcabes

The Milankovitch Cycles

Glaciations occur due to periodic variations in Earth's orbit that bring Earth into a colder climate state. In particular, small variations in the obliquity and eccentricity can lead to these glaciations. In the past, glacial episodes occurred roughly every 40,000 years. More recently, there has been a shift to 100,000 years between glaciations, likely a result of Earth entering a different climate state sometime during the Pleistocene. The last glacial maximum (LGM) occurred roughly 20,000 years ago.

image taken from Tapio's ESE 101 slides of glaciations during the Pliestocene

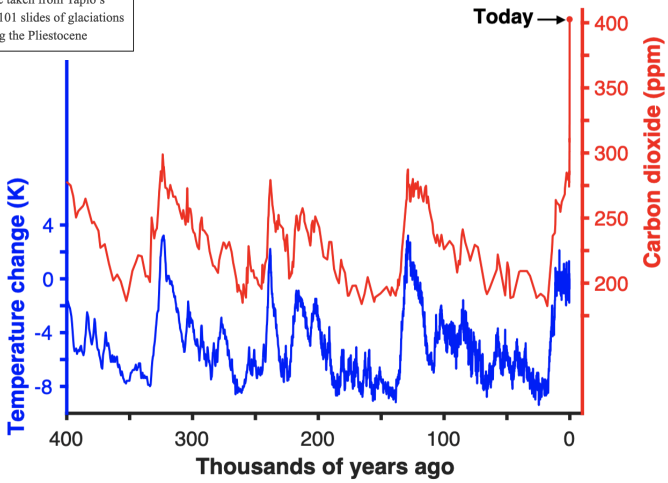

Glaciations in the Sierra Nevada

When temperatures are cold enough for long enough, accumulated snow packs down into ice and becomes a glacier. Typically glaciers form at the poles and at high altitudes, where conditions sustain snowpacks for the longest. During Earth's glacial maxima, massive glaciers formed in the Sierra Nevada and flowed down from the peaks. The most recent glaciation during the LGM is called the Tioga glaciation. Before that, the Sierra Nevada experienced Tahoe, Mono Basin, Sherwin, and McGee glaciations (see Table 1).

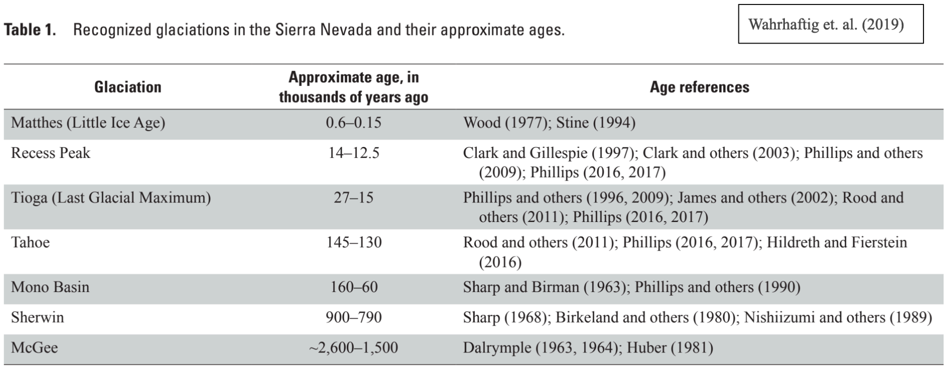

Table 1. Recognized glaciations in the Sierra Nevada and their approximate ages.

Wahrhaftig et. al. (2019)

Glaciation	Approximate age, in thousands of years ago	Age references
Matthes (Little Ice Age)	0.6–0.15	Wood (1977); Stine (1994)
Recess Peak	14–12.5	Clark and Gillespie (1997); Clark and others (2003); Phillips and others (2009); Phillips (2016, 2017)
Tioga (Last Glacial Maximum)	27–15	Phillips and others (1996, 2009); James and others (2002); Rood and others (2011); Phillips (2016, 2017)
Tahoe	145–130	Rood and others (2011); Phillips (2016, 2017); Hildreth and Fierstein (2016)
Mono Basin	160–60	Sharp and Birman (1963); Phillips and others (1990)
Sherwin	900–790	Sharp (1968); Birkeland and others (1980); Nishiizumi and others (1989)
McGee	~2,600–1,500	Dalrymple (1963, 1964); Huber (1981)

How can we use geology to learn about the glaciations?

After glaciers melt, they leave behind signatures of their movement and extents in the rocks. Rocks deposited by a glacier are called *till,* and mounds of till are called *moraines.* Because multiple glaciations happen in the same place, most of the moraines that we currently see are from the most recent glaciation, Tioga, with some remnants from the earlier glaciations like Tahoe. Dating of moraines can thus be difficult, as they don't usually have fossils. Some ways that moraines can be dated include cosmogenic-nuclide-exposure dating. Along with moraines, glaciers can also gouge, polish, or sharpen the rocks that they flow through or over, depending on how soft the rocks are. When glaciers carve out soft rocks in valleys, they tend to sharpen the valley walls and deepen the valley floor, forming a "U" shape. Lakes that form in the carved out sections of glaciers are called *tarns.*

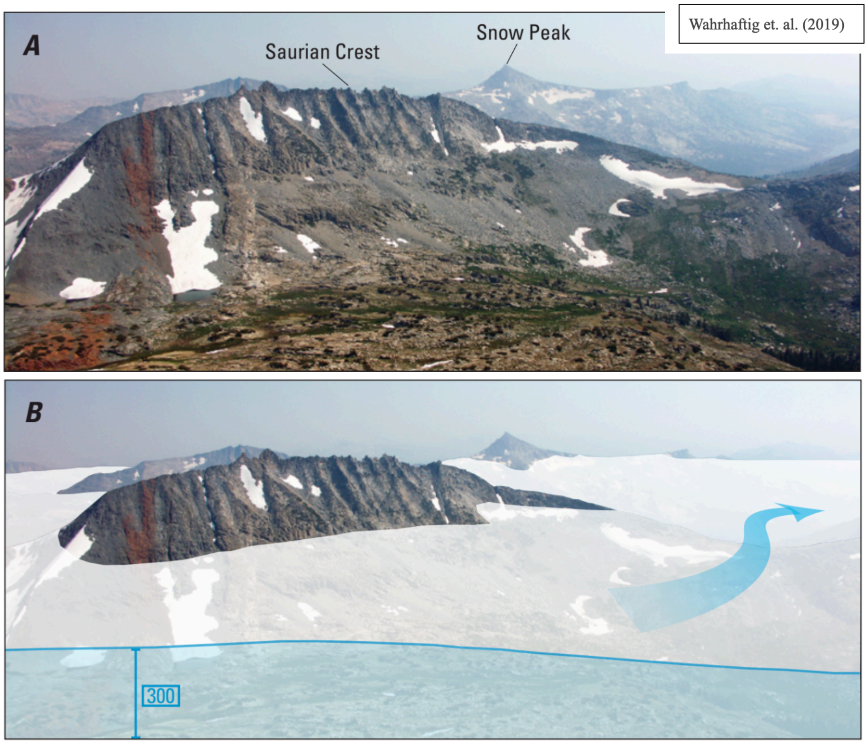
A
Saurian Crest
Snow Peak
B
300

Wahrhaftig et. al. (2019)

Figure 6. View to south from summit of Forsyth Peak, showing features mapped in field that were used to help determine Tioga-age ice extent in Yosemite National Park. Glacial arête of Saurian Crest is in foreground, and Snow Peak is in background. *A*, Transition between serrated arête crest and smoother ridges on either side provides approximate sense of height of past glaciers. Glacial trimline, identified by prominent break in slope and abrupt truncation of avalanche chutes, marks height of Tioga-age ice surface on north side of Saurian Crest. *B*, Same view as in *A*, with overlay showing approximate extent (transparent white shading) and direction of flow (blue arrow) of Tioga-age ice. Transparent blue shading in lower part of image shows approximate thickness of ice; height of trimline on Saurian Crest indicates glacier thickness of about 300 m, suggesting that ice completely surrounded it and flowed from northeast to southwest across pass to west.

Impacts of Glaciers

The effects of glaciers can be felt much farther from where they're actually located. For example, the way that glaciers carve the landscape can lead to changes to previous directions of rivers, which can heavily impact climates in the valleys below them depending on how meltwater will now flow. Glaciers are also important climatically because of their high albedo. Their reflectivity will lead to less absorbed sunlight, which leads to cooling.

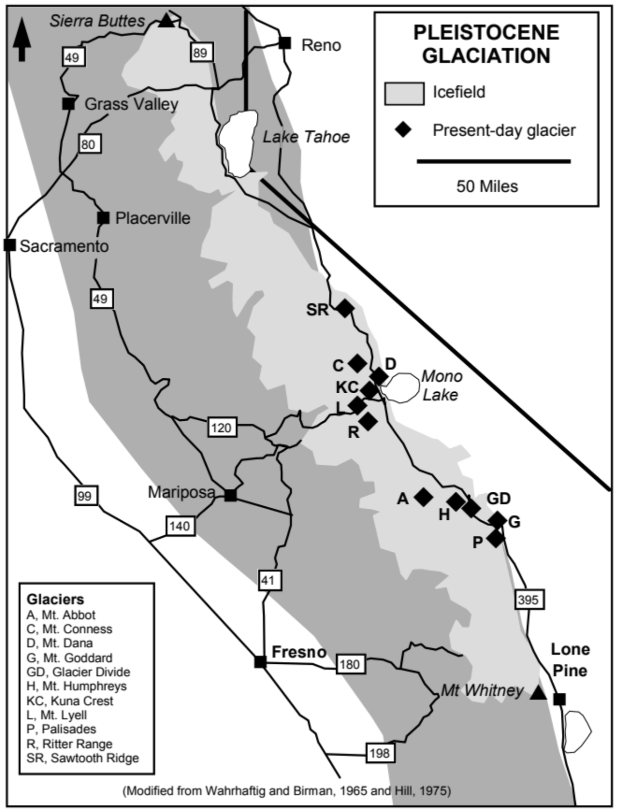
PLEISTOCENE GLACIATION
Icefield
Present-day glacier
50 Miles
Sierra Buttes
Reno
49
89
Grass Valley
80
Lake Tahoe
Placerville
Sacramento
49
SR
C
D
KC
L
R
Mono Lake
120
99
Mariposa
140
A
H
GD
G
P
41
395
Fresno
180
Lone Pine
Mt Whitney
198
Glaciers
A, Mt. Abbot
C, Mt. Conness
D, Mt. Dana
G, Mt. Goddard
GD, Glacier Divide
H, Mt. Humphreys
KC, Kuna Crest
L, Mt. Lyell
P, Palisades
R, Ritter Range
SR, Sawtooth Ridge

(Modified from Wahrhaftig and Birman, 1965 and Hill, 1975)

References

Milankovitch, M., 1941: Kanon der Erdbestrahlung und seine Anwendung auf das Eiszeitenproblem. Königlich Serbische Akademie.

SHARP, ROBERT P. "Pleistocene Glaciation, Bridgeport Basin, California."*GSA Bulletin* 83, no. 8 (August 1, 1972): 2233–60.

Wahrhaftig, Clyde, Greg M. Stock, Reba G. McCracken, Peri Sasnett, and Andrew J. Cyr. "Extent of the Last Glacial Maximum (Tioga) Glaciation in Yosemite National Park and Vicinity, California." Report. Scientific Investigations Map. Reston, VA, 2019. USGS. Publications Warehouse.

Konigsmark, Ted. *Geologic Trips Sierra Nevada*. Mendocino, CA: GeoPress, 2002.

WALKER LANE, THE HILTON CREEK FAULT AND THE EARTHQUAKE OF 1872

Simon Andren - GE136a

Introduction

This old map of a map from the 1650s shows California as an Island separated from mainland America. We all know from the Ge136 trips that this is **not** the case. However, this map might actually be a good prediction of what this land will look like in millions of years, thanks to the existence of Walker Lane.

Walker lane

Walker Lane is a geological trout roughly aligned with the Nevada-California border. It's +500 miles in length and 100 miles in width extending from Mexico to Oregon. The Walker Lane takes roughly 15-25% of the boundary motion between the Pacific and North American planes with the infamous San Andreas accommodating the rest. Instead of being one continuous fault, the zone consists of multiple discontinuous right-lateral strike-slip faults (Two plates moving horizontally past each other where an observer would see the opposite side moving to the right). The extent of the shear averages around 10 mm/yr. I don't know how, but it's hypothesized that it might eventually replace the faster-moving San Andreas fault as the new boundary between the Pacific and North American Place giving the people living in Reno beachfront houses.

Key facts about the Walker Lane

1. **Size: 500 miles in length, 100 miles in width**
2. **Accommodates 15-25% of Pacific/north American plate motion**
3. **Major transform fault zone**
4. **Seismically active with famous earthquakes being Ridgecrest in 2019 and Owens Valley Earthquake in 1872**
5. **Death Valley, Owens Valley, Pyramid Lake, & Walker Lake all lie within Walker Lane**
6. **Could be new tectonic plate boundary in ~10 million years**

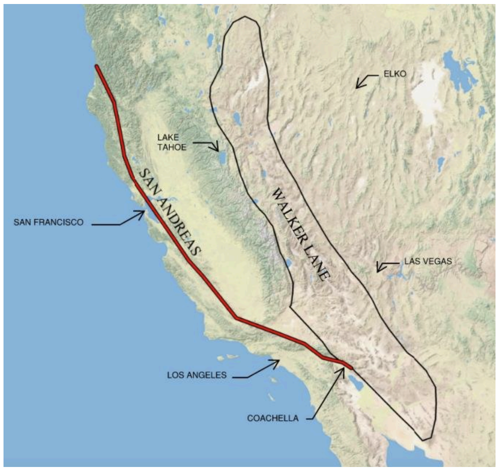

Milton Creek

Milton Creek flows through the Bodie hills, and has through its erosion, exposed multiple faults and rock formations which gives a direct view of the processes that are taking place over geological time. For example, Milton Creek intersects the Milk Ranch fault zone, where we can see fault scarps (step-like breaks in the ground) and offset stream channels (helping us quantify slip-rate), caused by the right lateral strike-slip. In addition, it has exposed both rhyolitic tuffs (Silica-rich volcanic ash) and andesitic lava flows, which are associated with the volcanic activity of the region. Most importantly, there are hot springs that intersect with Milton Creek providing relaxation and joy.

1872 Lone Peak Earthquake

The lone peak earthquake is one of largest seismic earthquakes to have been recorded in california with an approximate 7.5 magnitude. The earthquake, occurring along the Owens Valley fault, resulted on an average of 6 meters right-lateral offset and 1 meter of vertical offset. Below, you can see an amazing fault scarp sling the fault line. The earthquake also caused large damaged in the town of lone peak (Thereby the name) killing 10% of the population. It was a small town though. Luckily, it’s believed that the lone peak earthquake is about as big as any fault along the walker lane can produce. However, there are relatively frequent large earthquakes happening along walker lane with some examples being 1992 Landers earthquake, 1999 Hector Mine earthquake, the 2019 Ridgecrest earthquakes sequence.

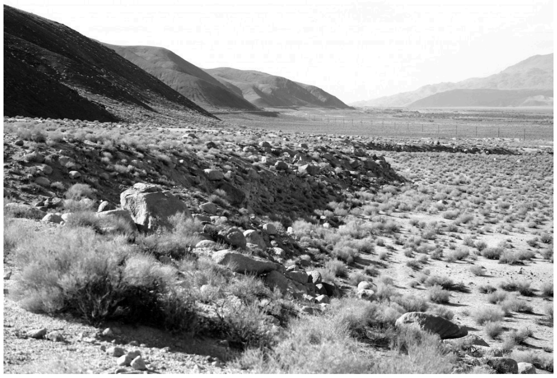

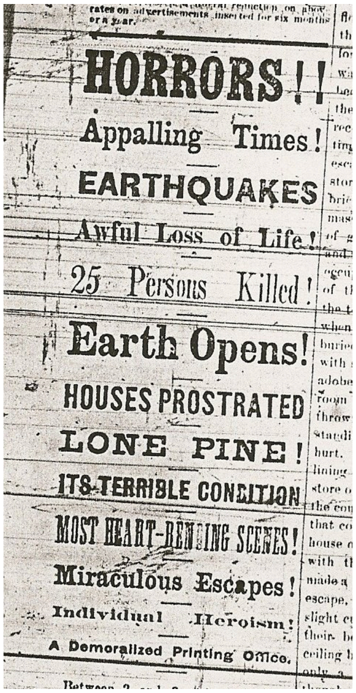

HORRORS!!

Appalling Times!

EARTHQUAKES

Awful Loss of Life!

25 Persons Killed!

Earth Opens!

HOUSES PROSTRATED

LONE PINE!

ITS TERRIBLE CONDITION

MOST HEART-RENDING SCENES!

Miraculous Escapes!

Individual Heroism!

A Demoralized Printing Office.

References

Faulds, J. E., Henry, C. D., Hinz, N. H., Drakos, P. S., & Delwiche, B. (2005). Transect across the Northern Walker Lane, Northwest Nevada and Northeast California: An incipient transform fault along the pacific–north american plate boundary. *GSA Field Guide 6: Interior Western United States*, 129–150. https://doi.org/10.1130/0-8137-0006-x.129

Wesnousky, S. G. (2005). The San Andreas and Walker Lane Fault Systems, western North America: Transpression, transtension, cumulative slip and the structural evolution of a major transform plate boundary. *Journal of Structural Geology*, *27*(8), 1505–1512. https://doi.org/10.1016/j.jsg.2005.01.015

Wolterbeek, M. (2020, February 18). *Finding faults: How the burgeoning Walker Lane may split the American west*. University of Nevada, Reno. https://www.unr.edu/nevada-today/nevada-stories/walker-lane

Nuclear Theory of Radiometric Dating

Thomas Sievert

Broadly, radiometric dating refers to the use of radioactivity to measure ages, [1] where "ages" refers to the amount of time elapsed between the measurement and the formation or deposition of a material. At first glance, radiometric dating seems to give so-called "absolute" ages because of the direct relationship between isotope abundance and time – this is in contrast to other forms of dating that use proxy measurements to date things *relative* to other events. However, radiometric dating has its own caveats which we will discuss later-on when talking about Owens Valley. I'll begin by giving an overview of nuclear physics theory in order to understand *why* some isotopes are radioactive and then we'll discuss *how* we relate isotope abundance to time by applying radiometric dating techniques to Owens Valley in the form of Ar^{40}-Ar^{39} dating.

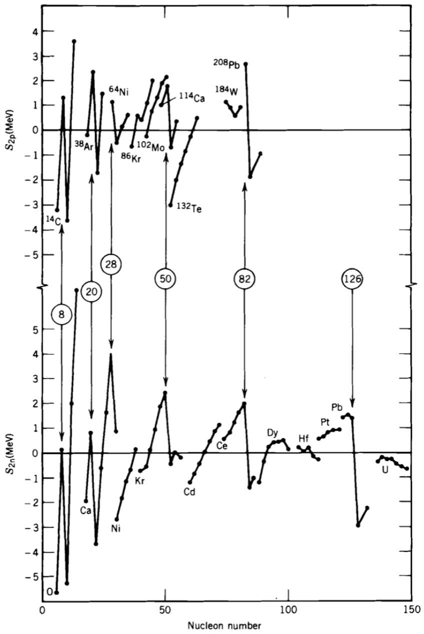

Figure 1 Separation energies of two protons at constant N (top) and two neutrons at constant Z (bottom). The energies peak at the same numbers, which represent filled valence shells [2].

Radioactivity was discovered by Becquerel in 1896 [2] – this is the same year electrons were discovered by Thomson and Rutherford[1]. In other words, radioactivity is old news. But what even *is* radioactivity? Radioactivity is fundamentally caused by nuclear interactions, so to understand radioactivity we must understand the nucleus[2]. In nuclear theory, a nucleus is not modeled as a collection of nucleons (protons and neutrons), but rather as a composite object with some overall properties we can measure and predict[3]. Building on the success of the Bohr model in atomic physics, we can model the nucleus[4] as a set of "shells" which are filled with weakly-interacting point particles (i.e. the "protons" and "neutrons") [2]. The Shell model of the nucleus is well-justified as it explains the sharp jumps in nucleon binding-energy (Fig. 1) observed at specific numbers of protons and neutrons[5]; the jumps are caused by the filling of a valence shell. For nuclei with an odd atomic number (odd-A), the shell model correctly predicts the energy and spin spectra – and just like atomic spectra the properties are entirely determined by the valence and near-valence nucleons[6]. For even-A nuclei the spectra are more complicated due to additional "collective modes" resulting from the vibration and/or rotation of the nucleus as a whole. Even-A nuclei with A < 150, typically vibrate around a spherical nucleus, whereas nuclei with 150 < A < 190 and A > 220 typically rotate a non-spherical nucleus[7] (Fig. 2). Through the shell model we can understand the energy spectra of nuclei as excitations of valence nucleons and rotation/vibration of the nucleus. We're left with a remarkable fact: the spectra of a nucleus behaves remarkably similar to the spectra of the atom itself[8]! And just like excited states in an atom decay by emitting photons, so too do excited states of nuclei decay by emitting high-energy photons (aka γ radiation). Through the analogy with atomic spectra, we've described how an excited state of a nucleus would decay via γ radiation. However, we still need to explain why the ground-state of a nucleus might *itself* be unstable; said another way, what causes β-decay, α-decay, and fission?

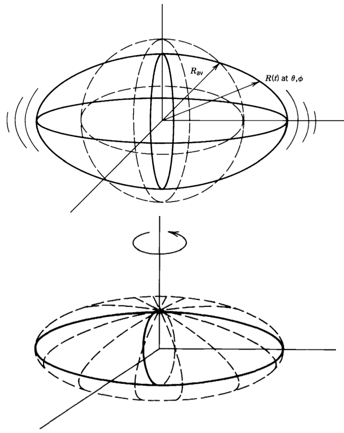

Figure 2 Vibration around a spherical nucleus seen in A < 150 (top), and rotation of an oblate nucleus seen in 150 < A < 190 and A > 220 (bottom) [2].

In order to figure out the cause of nuclear *instability*, lets start by explaining *stability*. The first thing we notice about stable isotopes is that they have approximately equal numbers of protons (Z) and neutrons (N); (Fig. 3) this is due to the Pauli Exclusion principle[9]. As we add nucleons, the nucleons must take on higher and higher energies and become more and more loosely bound with the nucleus, just like electrons in orbitals. The key difference with nuclei is that protons and neutrons fill in *separate* shells, so if I add too many protons or neutrons such that there's a large[10] difference in the valence energies of the two, it becomes energetically favorable for the high-shell, high-energy protons (neutrons) to β-decay[11] to lower energy neutrons (protons). The Pauli Exclusion principle, via β-decay, pushes nuclei to have approximately equal numbers of protons and neutrons. The second thing we notice about stable isotopes is that the majority of them have *more* neutrons than protons – how can this be if the Pauli Exclusion principle wants the numbers equal? The answer lies in the interplay of two forces: the Strong force[12] and the Coulomb force. The Strong force is ~100x stronger than the Coulomb force, but the former only extends to ~1fm whereas the Coulomb force extends to infinity. The attractive strength of the Strong force grows roughly linearly with A, the number of nucleons, but the repulsive strength of the Coulomb force grows quadratically with Z, the number of protons. Essentially, we have two competing forces and the only stable isotopes are those where the Strong force *wins*. For light nuclei (Z ≤ 30), the Strong force can win while fulfilling N=Z (pleasing Pauli) because the Coulomb force is much weaker to start. However, for heavier nuclei, (Z > 30) the Coulomb force begins to overtake the Strong force and at a given Z, we need *more neutrons* for the Strong force to win (Fig. 3). Lets try to understand more concretely what it means for the Strong force to lose by imagining what would happen if we stay on the N=Z line. For Z ≈ 30 nuclei, as we add protons the Coulomb repulsion grows quickly, and it becomes energetically favorable to change protons into neutrons at higher shells (energies). For heavy nuclei, the added protons are so energetic and so loosely bound that they deform and stretch the nucleus. The combination of the Strong force and Coulomb force means the protons and trapped in the nucleus (Fig. 4) until the nucleus can gain enough energy to break apart, either via α-decay or fission. The energetic, repulsive protons create energetic, unstable nuclei that are on the edge of breaking apart. If instead we try to over-saturate a nucleus with neutrons something different happens. As neutrons don't feel the Coulomb repulsion (Fig. 4), they aren't in the same trap as the protons are, so adding energetic neutrons (while it does increase the energy of the nucleus and can cause deformation) often simply results in the energetic neutrons flying out of the nucleus. This is why there's slightly fewer unstable isotopes on the N-enriched side of stable, as compared to the Z-enriched side, the energetic neutrons aren't trapped (Fig. 3).

---

[1] Thomson used the discovery of electrons as evidence towards the "plum-pudding" model of the atom, which was quickly overturned by Rutherford in 1911 with the gold-foil experiment and replaced with Bohr's model in 1913 [3].

[2] Useful size scales for reference: an atom is $\mathcal{O}(10^{-10}m)$ or 0.1nm, protons and neutrons are $\mathcal{O}(10^{-15}m)$ or 1fm, and a nuclei are typically a few fm. Note that size is not a well-defined quantity for atoms nor nuclei, but it loosely refers to the length at which interactions with the object start to be observed.

[3] There are two main reasons why we do this simplistic modeling. The first reason is combinatorics: a nucleus with 50 nucleons has ~$\mathcal{O}(50!)$ or 10^{64} pair-wise interactions to account for [2], let alone nuclei with 200 nucleons. The second reason has to do with the size of nucleons vs. a nucleus: in the non-quantum world you can't pack 50 1fm balls into a few fm bag, which means these nuclei aren't actually sitting *next* to each other, they're overlapping. This overlapping means to accurately model the interactions of the nucleons we would need to model the interactions of the quarks and gluons that *make up* the nucleons, and we can't even model these interactions well for a single proton.

[4] The nuclear potential (the nuclear equivalent of the Coulomb potential) of the shell model is described by two terms: $\frac{-V_0}{1+e^{(r-R)/a}}$ and $V_{so}(r)\ \ell \cdot s$. The first term describes a logistic curve, capturing the fast and strong "turn-on" effect of the Strong force. The second term is the spin-orbit contribution – akin to the spin-orbit effect responsible for the fine-structure splitting of atomic spectra – which is necessary to give the correct numbers of protons and neutrons in each valence-shell.

[5] The fact that nucleons and electrons fill in energy shells is a direct result of the Pauli exclusion principle, which states that two *identical* particles cannot be in the same state at the same time. The fact that the principle only applies to identical particles means that protons and neutrons fill in *separate shells*!

[6] By using high-energy electrons to penetrate deep into the nucleus we can confirm that the shell-model holds even for those deep-interior nucleons by measuring the charge density of deep nucleons and comparing to the shell model predictions [2].

[7] Nuclei with 190 < A < 220 have proton and neutron numbers near the 82 and 126 valence shells and are therefore better modeled with shells.

[8] Nuclear theory fun fact: The point-particles used in the shell model to represent the protons and neutrons are orbiting around the nucleus at a speed of 25% of the speed of light on average.

[9] The Pauli Exclusion principle states that identical particles (i.e. protons, neutrons, or electrons) cannot have the same position and momentum. In a nucleus the nucleons are all on top of each other, so the Pauli Exclusion principle requires nucleons to fill shells with higher and higher kinetic energy.

[10] In this case "large" doesn't have a specific meaning, it varies by isotope. But it roughly means "a few energy levels of difference".

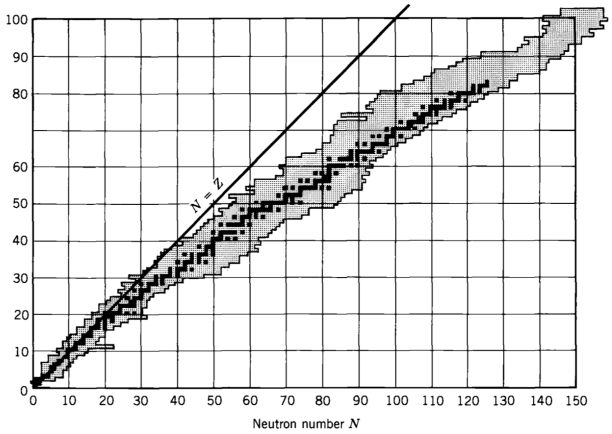

Figure 3 Chart of all known isotopes. Stable isotopes are in black and unstable are in grey [2].

Now that we have a thorough understanding of nuclear theory and radioactivity, lets move on to radiometric dating. If we assume that a decay has a constant probability (i.e. the decay probability is something intrinsic to the isotopes), then we can extract a simple exponential equation governing the number of an isotope over time: $N(t) = N_0 e^{-\lambda t}$. By measuring the ratio of the number of parent-daughter isotopes we can determine t without N_0. However, things get complicated once we try to account for the fact that the thing we're measuring has interacted with the world for the intervening time, and thus there are many possible ways the number of parent and/or daughter isotopes could be contaminated. For the dating of the Big Pine volcanic field (see Olivia's talk), conventional $^{40}K/^{40}Ar$ (parent-daughter) dating couldn't be used well due to these contamination concerns. First, in the basalt itself there are trace amounts of Ar with an unknown isotopic composition, which can easily mask the ^{40}Ar signal in young, low-^{40}K rocks [4]. Second, the basalt is often contaminated with (potentially ^{40}Ar-rich) granite, which can again mask the true ^{40}Ar signal [4]. The solution is to step-wise heat the samples and measure the ratios at every temperature. The minimum plateau on the age-curves (Fig. 5) measured over the temperatures shows the upper-bound on the age.

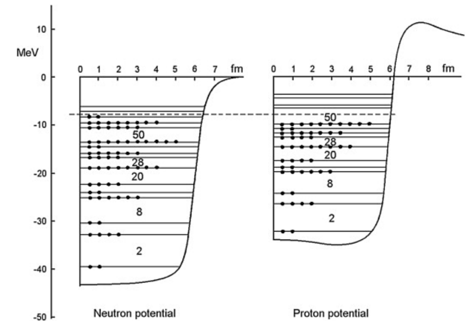

Figure 4 Plots showing the nuclear (Strong + Coulomb) potentials seen by neutrons and protons [5].

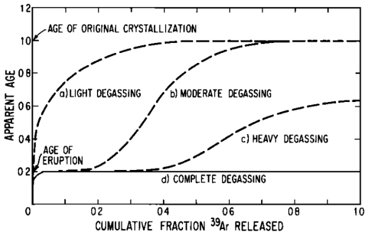

Figure 5 Age curves of ^{40}Ar–^{39}Ar analysis [4]

Citations

[1] Gopalan K. Radioactivity and Radiometric Dating. In: Principles of Radiometric Dating. Cambridge University Press; 2017:40-79.

[2] Krane, K.S. (1988) Introductory Nuclear Physics. Wiley John & Sons, New York.

[3] Stewart, K. (2023, November 17). atomic model. Encyclopedia Britannica. ***https://www.britannica.com/science/atomic-model***

[4] Gillespie, A. R., et al (1983), Eruption age of a Pleistocene basalt from ^{40}Ar–^{39}Ar analysis of partially degassed xenoliths, J. Geophys. Res., 88(B6), 4997–5008

[5] Radiochemistry and nuclear chemistry. (2013). In Elsevier eBooks. https://doi.org/10.1016/c2011-0-07260-5

---

[11] I'm not describing here how its *possible* particles can β-decay at all, merely why they do assuming they can. In order to understand β-decay we would need to discuss the Weak force in full, relativistic detail – something that people spend whole courses understanding.

[12] The Strong force is what binds quarks and gluons into protons and neutrons. It also holds the nucleus together through an equivalent of the Van der Waals force (i.e. the exchange of π particles, whose mass actually causes the 1fm size scale of a nucleus) The Strong force is called as such because it is much stronger than the other forces.

Travertine, the superior calcium carbonate

Hemani Kalucha

Travertine ($CaCO_3$) is one of the most active sedimentary systems and represents a modern analog for ancient stromatolites [1]! Travertine is precipitated from rapid CO_2 degassing from turbulent water. Contrary to ordinary fluvial systems, where rapid flow erodes sediment, travertine remains resistant to erosion in flows as fast as 2 m/s [1]. Sedimentation of travertine occurs at the interface of water and sediment substrate and in favourable geochemical conditions, travertine precipitation rates can reach tens of centimetres per year! Tufa growth, for comparison, doesn't exceed 10 mm/year [1].

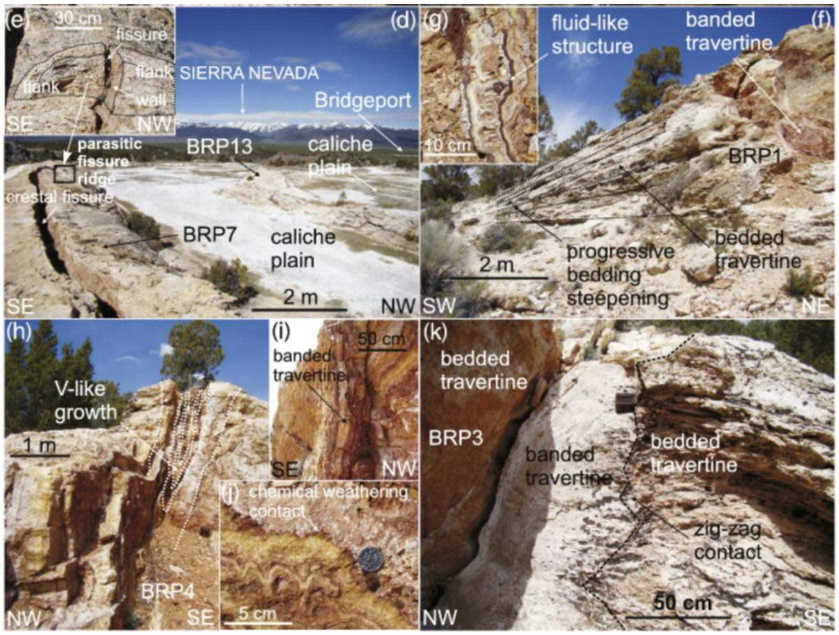
(e)
30 cm
fissure
flank
flank
wall
SE
NW
parasitic fissure ridge
crestal fissure
(d)
SIERRA NEVADA
Bridgeport
BRP13
caliche plain
BRP7
caliche plain
2 m
SE
NW
(g)
fluid-like structure
10 cm
banded travertine
(f)
BRP1
bedded travertine
progressive bedding steepening
2 m
SW
NE
(h)
V-like growth
1 m
BRP4
NW
SE
(i)
50 cm
banded travertine
SE
NW
(j)
chemical weathering contact
5 cm
(k)
bedded travertine
BRP3
banded travertine
bedded travertine
zig-zag contact
50 cm
NW
SE

Figure 1: Travertine terraces at Bridgeport, Mono Basin [2].

Travertine is found in multiple spots in the area: Bridgeport Reservoir [2], Mono Lake [3], and Birch Creek in the White Mountains [4]. The Bridgeport travertine system is Pleistocene in age and a result of hydrothermal fluids (50-65C) seeping out from fissures in Tertiary volcanic rocks (66 – 2.6 Ma). The travertine forms terraces here at elevations between 2010 and 2065 m, pictured in Figure 1 [2]. The volcanic islands, Paoha and Negit, in the centre of Mono Lake host travertines due to hydrothermal ground water circulation in the Mono Basin [3]. Ground water seepage supplies Birch Creek with the CO_2 saturation levels required to precipitate travertine and the creek is only 3 inches deep remarkably [4]!

Differentiating Tufa versus Travertine in the field and in the lab [7]

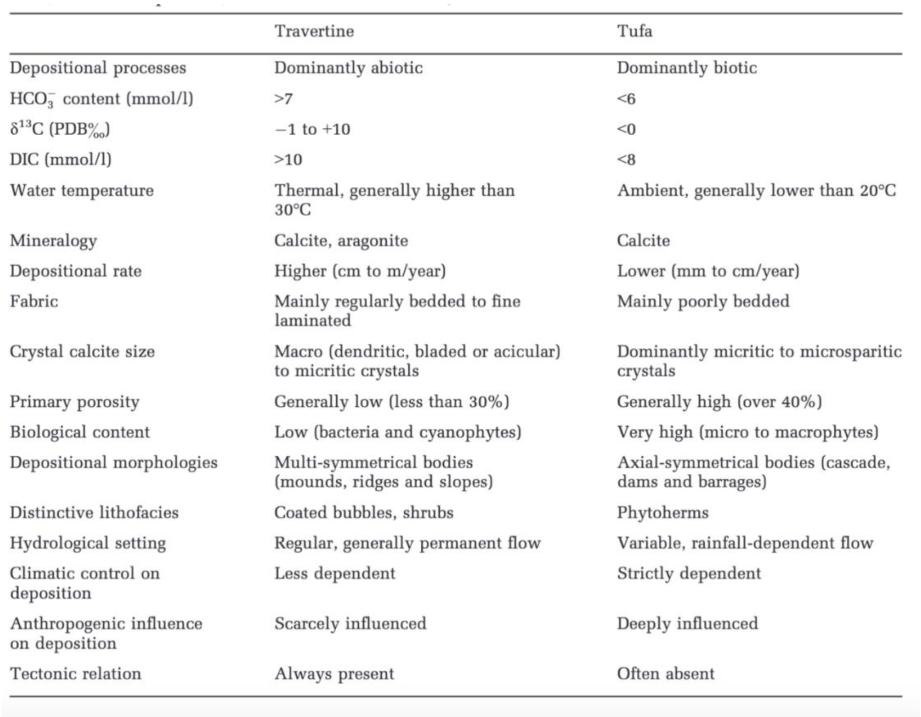

	Travertine	Tufa
Depositional processes	Dominantly abiotic	Dominantly biotic
HCO_3^- content (mmol/l)	>7	<6
$\delta^{13}C$ (PDB‰)	−1 to +10	<0
DIC (mmol/l)	>10	<8
Water temperature	Thermal, generally higher than 30°C	Ambient, generally lower than 20°C
Mineralogy	Calcite, aragonite	Calcite
Depositional rate	Higher (cm to m/year)	Lower (mm to cm/year)
Fabric	Mainly regularly bedded to fine laminated	Mainly poorly bedded
Crystal calcite size	Macro (dendritic, bladed or acicular) to micritic crystals	Dominantly micritic to microsparitic crystals
Primary porosity	Generally low (less than 30%)	Generally high (over 40%)
Biological content	Low (bacteria and cyanophytes)	Very high (micro to macrophytes)
Depositional morphologies	Multi-symmetrical bodies (mounds, ridges and slopes)	Axial-symmetrical bodies (cascade, dams and barrages)
Distinctive lithofacies	Coated bubbles, shrubs	Phytoherms
Hydrological setting	Regular, generally permanent flow	Variable, rainfall-dependent flow
Climatic control on deposition	Less dependent	Strictly dependent
Anthropogenic influence on deposition	Scarcely influenced	Deeply influenced
Tectonic relation	Always present	Often absent

Travertine Fabrics have a huge variety and changes of microfacies reveal changes in environmental conditions [5, 6]

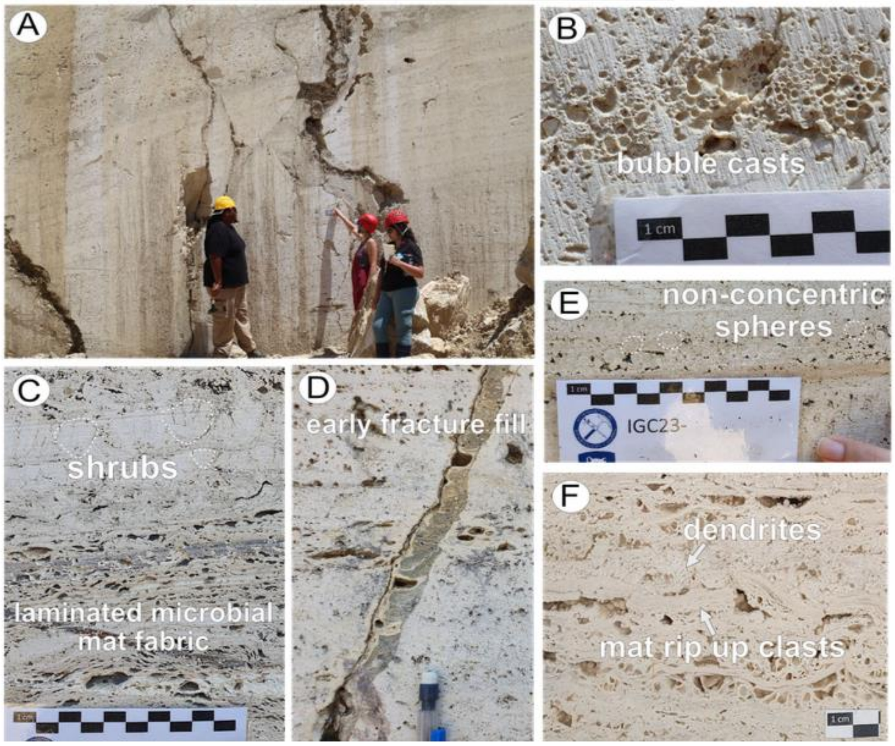

Figure 2: Interglacial travertine terrace (210.5 kya) in the Appenine Range, Italy [6]. A) Capotti Quarry cut wall with decimetre scale bedding. B-E) microfacies of travertine ranging from abiotic to microbially mediated precipitation

Facies observed can be (i) microbial-influenced when the microbial growth rate is greater than the precipitation rate and flow energy is not above the threshold value tolerated by microbes, or (ii) inorganic-dominated if the precipitation rate exceeds that of the microbial growth rate and/or flow energy is above the threshold tolerated by microbes [8]. Travertine facies show changes, variations and alternations on a mm-scale, suggesting great sensitivity than tufas to changes in environmental conditions [8].

Controlling factors and implications for travertine and tufa deposition in a volcanic setting [8]

$^{87}Sr/^{86}Sr$ ratios indicate that the origin of waters forming travertines and tufas is the same. Travertine precipitates include aragonite-calcite mixtures, which are more likely to precipitate in waters with higher Mg/Ca ratios, or stronger CO_2 degassing. Lower CO_2 degassing and higher degree of re-equilibrium between DIC species and water, often occurring in distal environments with higher biological photosynthetic activity, preferentially precipitate tufa over travertine.

References:

[1] Kano, A., Okumura, T., Takashima, C., & Shiraishi, F. (2019). Geomicrobiological properties and processes of travertine. *Springer Geology*, *176*, 9-41.

[2] De Filippis, L., & Billi, A. (2012). Morphotectonics of fissure ridge travertines from geothermal areas of Mammoth Hot Springs (Wyoming) and Bridgeport (California). *Tectonophysics*, *548*, 34-48.

[3] Whiticar, M. J., & Suess, E. (1998). The Cold Carbonate Connection Between Mono Lake, Californiaand the Bransfield Strait, Antarctica. *Aquatic Geochemistry*, *4*(3), 429-454.

[4] Barnes, I. (1965). Geochemistry of Birch Creek, Inyo County, California a travertine depositing creek in an arid climate. *Geochimica et Cosmochimica Acta*, *29*(2), 85-112.

[5] Gandin, A., & Capezzuoli, E. (2014). Travertine: distinctive depositional fabrics of carbonates from thermal spring systems. *Sedimentology*, *61*(1), 264-290.

[6] Kalucha, H., van Wieren, C., Greidanus, C., Amos, E., Lloyd, M. K., Ingalls, M., ... & Freeman, K. H. (2023, December). Travertine deposits reveal a range of biotically and abiotically precipitated microfacies. In *AGU Fall Meeting Abstracts* (Vol. 2023, No. 1195, pp. PP11C-1195).

[7] Capezzuoli, E., Gandin, A., & Pedley, M. (2014). Decoding tufa and travertine (fresh water carbonates) in the sedimentary record: The state of the art. *Sedimentology*, *61*(1), 1-21.

[8] Rodríguez-Berriguete, Á., & Alonso-Zarza, A. M. (2019). Controlling factors and implications for travertine and tufa deposition in a volcanic setting. *Sedimentary Geology*, *381*, 13-28.

HOT SPRING BRAIN EATING AMOEBA

Eran Funaro

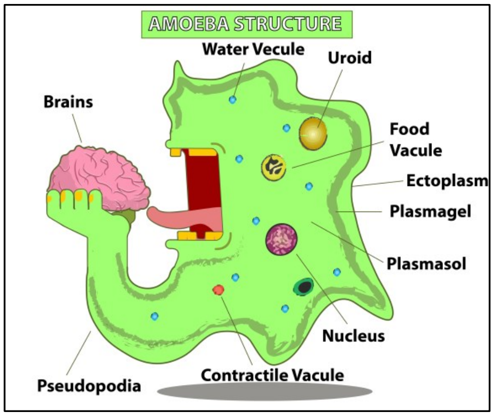
AMOEBA STRUCTURE
Water Vecule
Uroid
Brains
Food Vacule
Ectoplasm
Plasmagel
Plasmasol
Nucleus
Pseudopodia
Contractile Vacule

Brain Eating Amoeba

Amoebic encephalitis, an Amoeba caused infection of the central nervous system, comes in two human afflicting flavors. Primary amoebic meningoencephalitis (PAM) and granulomatous amoebic encephalitis, both are extremely uncommon but often lethal. Amoebic encephalitis is caused by free-living amoebae (FLA), which are microorganisms found naturally in freshwater environments, such as lakes, rivers, and springs. Naegleria fowleri, a FLA ubiquitous in the environment is the only species known to cause PAM. *N*amed after Malcolm Fowler, the first to describe a PAM infection (Australia 1965). It is thermophilic, thriving in warm freshwater, especially when soil contaminated. Its life cycle has three stages—cyst, trophozoite, and flagellate—and it can alternate these given specific conditions and is able to exist as both parasitic organisms and free living.

The Culprit - Naegleria Fowleri

N. fowleri has three stages: cyst, trophozoite (the infectious stage), and flagellate. It is a FLA of the Super Group Excavata: Heterolobosia: Vahlkampfiidae. In adverse conditions, trophozoites convert temporarily into the flagellated form. If conditions for feeding and growth improve, they can return to the trophozoite form; if not, they can enhance their long-term survival by transforming into environmentally resistant cysts. FLA are considered cosmopolitan as a group, and they live inside hosts, in soils, freshwater, marine waters, and on the aerial parts of plants and animals. These microbes, feed on bacteria and are spread by wind and water currents.

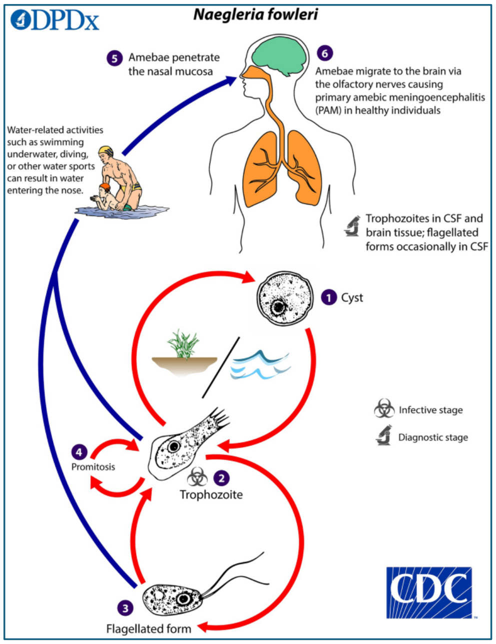
DPDx
Naegleria fowleri
5 Amebae penetrate the nasal mucosa
6 Amebae migrate to the brain via the olfactory nerves causing primary amebic meningoencephalitis (PAM) in healthy individuals
Water-related activities such as swimming underwater, diving, or other water sports can result in water entering the nose.
Trophozoites in CSF and brain tissue; flagellated forms occasionally in CSF
1 Cyst
Infective stage
Diagnostic stage
4 Promitosis
2 Trophozoite
3 Flagellated form
CDC

How And Where To Get It - Human Infection

PAM begins when the amoebae, in the trophozoite form, enter the nose and attach to the nasal mucus. The trophozoites then travel along the olfactory nerve to the olfactory bulbs in the central nervous system (brain and spinal cord). PAM primarily is caused by exposure to warm freshwater, *N. fowleri* has been isolated from other sources, including treated tap water and chlorinated swimming pools. Infections primarily occur after exposure to warm freshwater that is untreated and susceptible to changes in temperature. Increasing water temperatures of smaller bodies of water in the summer in combination with nutrient-filled runoff provides a favorable environment for the amoeba. Patients who are infected typically have participated in recreational water sports in southern states in the summer. Although nearly 80% of PAM cases between 1962 and 2008 were associated with exposure to infected freshwater, tap water has been traced to many cases. Still, *N. fowleri* is not a regulated contaminant. In 2002, two cases of PAM were linked to water from a geothermal well that was untreated by the usual methods of disinfection. A 2013 case occurred, when a 4-year-old boy contracted PAM after playing on a lawn water slide with municipal water that ultimately tested positive. Nasal rinsing with *N. fowleri*-infected water has been linked to cases of PAM.in both cases *N. fowleri* colonization of the home plumbing was revealed. Nasal ablution was linked to 13 PAM cases in Karachi, Pakistan, between 2008 and 2009. A case in St. Thomas, US Virgin Islands, was shown to be caused by ritual ablution using water from an untreated well and rainwater.High-risk travel areas include hot water springs in Yellowstone and Grand Teton national parks and hot springs surrounding Lake Mead. The fact that only a few individuals, among all of the hosts exposed to these amoebae, develop infections suggests the possible presence of underlying predisposing factors.

The Disease - Primary Amoebic Meningoencephalitis (PMA)

Upon reaching the brain, the trophozoites activate the immune system, resulting in an influx of macrophages and neutrophils. The amoebae are able to evade the immune system by removing part of the membrane-attack complex and resisting cytokines. In addition to tissue damage caused by the secretions from immune cells, structures present on the trophozoites cause nerve and brain tissue damage. Resulting cerebral edema and necrosis can progress to herniation of the cerebellum or uncus. Even tough the acute infection lasts only a few days it is almost universally leading to death. Symptoms include headache, nausea, vomiting, photophobia and nuchal rigidity in early stages, followed by Confusion, lack of attention to people and surroundings, loss of balance, seizures, and hallucinations .

Sites of infection of PAM due to *Naegleria fowleri,* Extensive hemorrhage and necrosis is present, mainly in the frontal cortex. Given the nasal route of entry, *N. fowleri* is likely to have an intimate correlation with the frontal lobe, due to the anatomical proximity of the olfactory bulb to the frontal lobe; the olfactory bulb is terminal to the olfactory neuroepithelium of the nasal passage, traversing the cribriform plate to the brain. More cases involved the frontal lobe, followed by the parietal lobe and the corticomedullary junction. Hydrocephalus was observed in 27% of cases.

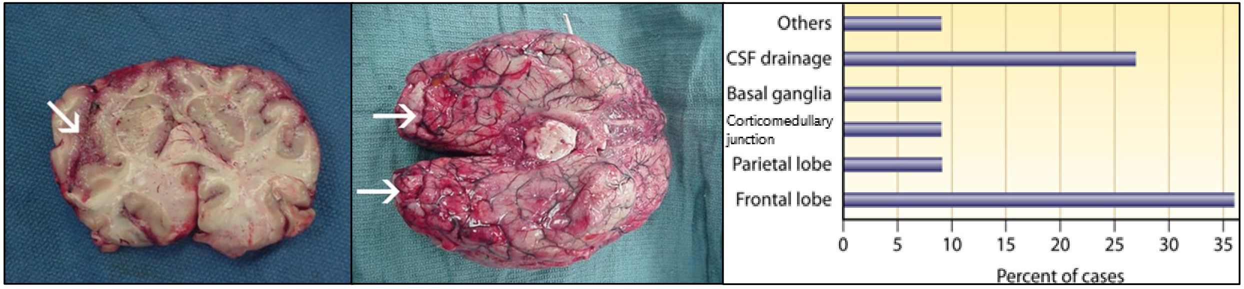

Detection & Treatment

Among cases of PAM due to *N. fowleri*, 63.7% were diagnosed postmortem. Among the postmortem cases, microscopy was used successfully in 36.4% of cases, IFAs were used effectively in 18.2% of cases, and PCR was used positively in 9.1% of cases. Among the premortem cases, CSF observations of amoebae were made in 36.4% of cases (using microscopy [18.2%] and culture [18.2%]). Overall, for PAM due to *N. fowleri*, observation of parasites in CSF samples using microscopy or IFAs was the most widely used premortem diagnostic method.

Only three survivors were documented before 2013. However, new developments call for a reassessment of the disease. Two recent cases of survival have been reported using miltefosine, a new investigational drug available through the FDA's investigational drug protocol. Recent cases in the northern United States demonstrate an expanding geographic range.

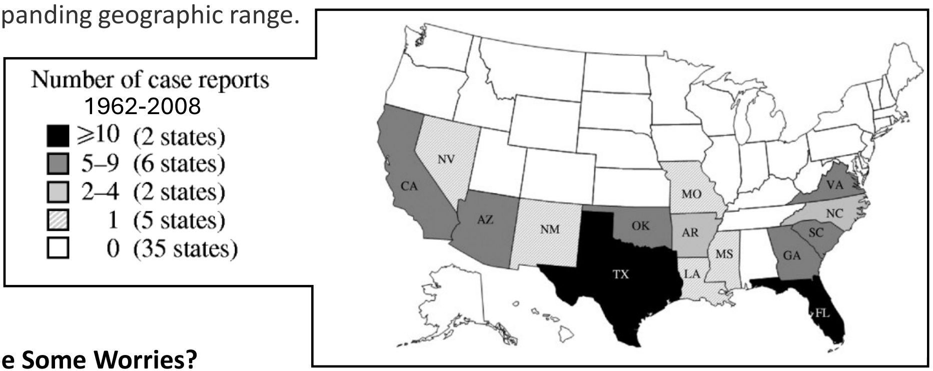

No Worries? Maybe Some Worries?

Between 1962 and 2016, the registry documented 143 cases of PAM in the United States. However, cases of are often underreported, misreported, and underrecognized globally, due to lack of awareness, lack of available diagnostic tools, lack of wide distribution of knowledge regarding public health issues and risk factors, especially in developing countries, and the similarity of symptoms to those of other common CNS infections, such as viral and bacterial meningitis.

amoebae are ubiquitous in the environment and nonresponsive to antibiotics and even with an early Diagnosis treatment has rarely been successful though some advancement have been made lately.

1. Rodríguez-Zaragoza, S. (1994). Ecology of Free-Living Amoebae. *Crit. Rev. Microbiol*, 20(3), 225–241. https://doi.org/10.3109/10408419409114556
2. Borkens, Y. (2024). The Pathology of Naegleria fowleri. *Indian J. Microbiol*, 64, 1384–1394. https://doi.org/10.1007/s12088-024-01218-5
3. Ahmad Zamzuri, M. A. I., Abd Majid, F. N., Mihat, M., Ibrahim, S. S., Ismail, M., Abd Aziz, S., Mohamed, Z., Rejali, L., Yahaya, H., Abdullah, Z., et al. (2023). Systematic Review of Brain-Eating Amoeba: A Decade Update. *Int. J. Environ. Res. Public Health*, 20, 3021. https://doi.org/10.3390/ijerph20043021
4. Ong, T. Y. Y., Khan, N. A., & Siddiqui, R. (2017). Brain-Eating Amoebae: Predilection Sites in the Brain and Disease Outcome. *J. Clin. Microbiol*. https://doi.org/10.1128/jcm.02300-16
5. Cooper, A. M. P. A.-C., Aouthmany, S. M. D., Shah, K. M. D., & Rega, P. P. M. D., FACEP. (2019). Killer amoebas: Primary amoebic meningoencephalitis in a changing climate. *J. Am. Acad. Physician Assistants*, 32(6), 30–35. https://doi.org/10.1097/01.JAA.0000558238.99250.4a

Hot Creek Thermophiles

By: Jordan Chastain

Organisms that are adapted to live in high temperature environments are called thermophiles. Geothermal hot springs around Little Hot Creek have temperatures up to 80°C,[1] which is far above most organisms' optimal temperatures, so thermophiles dominate these communities. Most enzymes in the cells of organisms not adapted to these extreme environments are destabilized and denatured in high temperatures. High temperatures can also lead to increased membrane fluidity, which can be a problem for maintaining a barrier against the environment. Through evolution, thermophiles have developed solutions to these problems, shown to the right.[2] While this figure specifically mentions proteins, most adaptations apply to lipids in cell membranes as well.

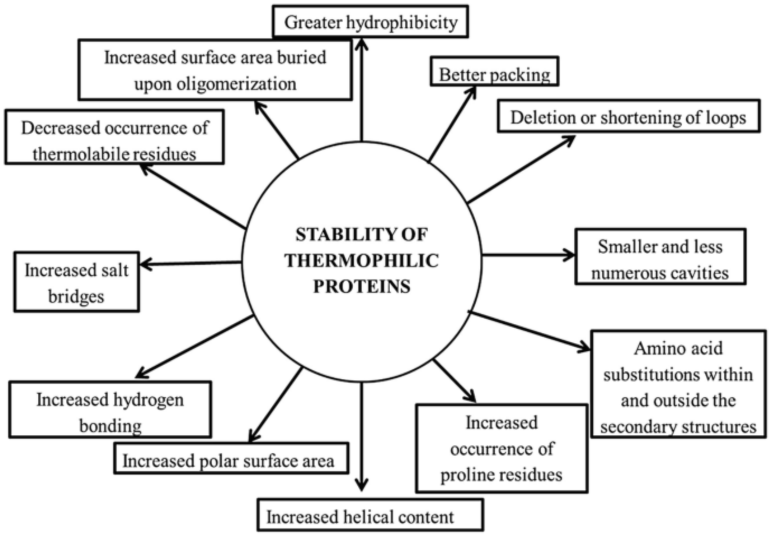
STABILITY OF THERMOPHILIC PROTEINS
Greater hydrophibicity
Better packing
Deletion or shortening of loops
Smaller and less numerous cavities
Amino acid substitutions within and outside the secondary structures
Increased occurrence of proline residues
Increased helical content
Increased polar surface area
Increased hydrogen bonding
Increased salt bridges
Decreased occurrence of thermolabile residues
Increased surface area buried upon oligomerization

Structural adaptations commonly found in thermophilic proteins[2]

Thermophily can be found in all three domains of life (Bacteria, Archaea, and Eukaryotes). However, eukaryotic thermophiles are typically limited to temperatures below 60°C.[3] In hot springs as extreme as Little Hot Creek, most of the thermophilic organisms are bacteria and archaea, both of which are single-celled microbes. Archaea have a different membrane structure than bacteria that seems to be naturally less fluid in thermophiles, allowing thermophilic archaea to survive even higher temperatures than most thermophilic bacteria.[3]

Along with maintaining protein and membrane structures, thermophiles must also find a way to get energy for metabolism. All life needs an energy source to survive. The figure to the right shows many of the redox (reduction-oxidation) reactions available in nature for organisms to utilize.[4] Metabolism is based on pairing two of these reactions together to move electrons from an electron donor (reduced species) to an electron acceptor (oxidized species) and storing the energy released through this transfer. The further apart the redox couples are on this tower, the more energy an organism obtains from the reaction. Aerobic respiration, which we use to get energy from our food, pairs the very top reaction to the to the very bottom reaction, transferring electrons from sugars and other reduced carbon sources to dioxygen (O_2). However, some organism had to create those sugars from an inorganic source, which is called primary production. Most of our reduced carbon ultimately comes from photosynthesis, whether we are eating plants or animals that eat plants. In photosynthesis, plants get their energy from the Sun rather than a naturally electron-rich compound. In extreme environments such as Little Hot Creek, the biological machinery that carries out photosynthesis cannot remain stable and function efficiently.[1] Chemolithotrophy is a type of metabolism in which energy is obtained from inorganic compounds, which includes most of this redox tower. Photosynthesis is extremely good at generating energy, so chemolithotrophy is usually only found where photosynthesis is not possible, including extreme environments, as well as deep water and deep soil.

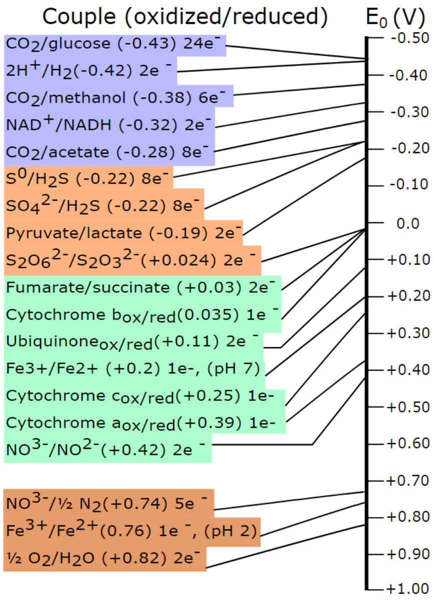

A "redox tower"[4] of biologically relevant redox couples

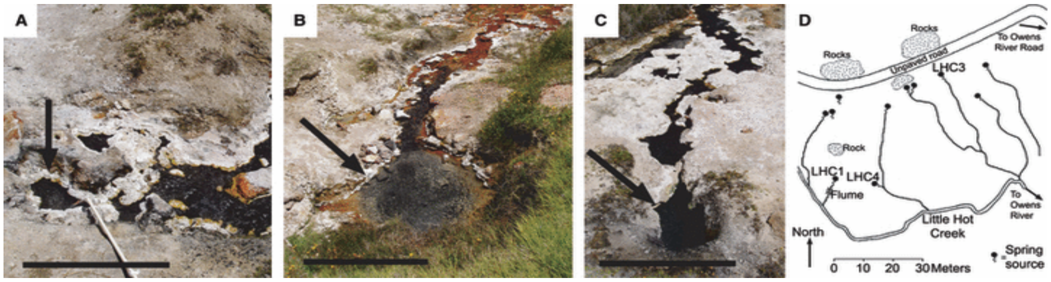

Spring sources of LHC 1(A), 3(B), and 4 (C), as well as their locations (D) relative to Little Hot Creek[1]

Little Hot Creek and other hot springs within the Long Valley Caldera host a wide variety of thermophiles and other microbes. These communities are very diverse in their metabolisms, showcased by the wide variety of taxa found through sampling. The figures above and to the right come from Vick et al., 2010.[1] The majority of these microbes are thermophiles, including any with "therm" in their name in the figure. Most microbes detected use H_2 as their electron donor, though one species within *Archaeoglobales* is mentioned to be able to use H_2S and Fe^{2+} as well. A more recent study also isolated organisms from Little Hot Creek and demonstrated that multiple can use arsenite (commonly defined as any As^{3+} oxyanion) as an electron donor.[5] Electron acceptors able to be used by Little Hot Creek microbes include Fe^{3+}, S^0, thiosulfate ($S_2O_3^{2-}$), NO_3^-, and possibly O_2 near the surface, though most of the archaea detected are anaerobic are harmed by oxygen presence. Not only is there extreme diversity within each sample site, but also across different springs within Little Hot Creek, despite them all being fed by the same geothermal fluid reservoir. The authors of this study suggest that this is due to differing amounts of oxygen in the different springs. Hot springs in Little Hot Creek host thriving and diverse communities of organisms, despite (or due to) the high temperatures. While thermophile research has progressed greatly over the last decades, developing genomics and molecular techniques show us that we still have much more to learn.

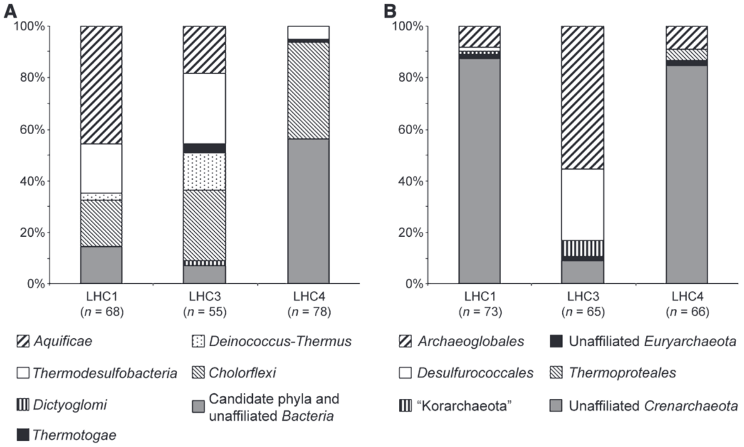

Taxa identified through metagenomic analysis at multiple springs in Little Hot Creek[1]

References:

1) VICK, T.J., DODSWORTH, J.A., COSTA, K.C., SHOCK, E.L. and HEDLUND, B.P. (2010), Microbiology and geochemistry of Little Hot Creek, a hot spring environment in the Long Valley Caldera. Geobiology, 8: 140-154. https://doi.org/10.1111/j.1472-4669.2009.00228.x
2) Eswari, J.S., Dhagat, S., Sen, R. (2019). Proteins and Amino Acids from Thermophilic Microorganisms: Current Research Trends and Applications. In: Thermophiles for Biotech Industry. Springer, Singapore. https://doi.org/10.1007/978-981-32-9919-1_3
3) Bhattacharya, D., Friedl, T., Schmidt, H. (1999). The Phylogeny of Thermophiles and Hyperthermophiles and the Three Domains of Life. In: Seckbach, J. (eds) Enigmatic Microorganisms and Life in Extreme Environments. Cellular Origin and Life in Extreme Habitats, vol 1. Springer, Dordrecht. https://doi.org/10.1007/978-94-011-4838-2_23
4) S2023_Bis2A_Singer_Redox. (2023, March 22). https://bio.libretexts.org/@go/page/106444
5) Zhou, EM., Adegboruwa, A.L., Mefferd, C.C. *et al.* Diverse respiratory capacity among *Thermus* strains from US Great Basin hot springs. *Extremophiles* **24**, 71–80 (2020). https://doi.org/10.1007/s00792-019-01131-6

Taq Polymerase and the reaction that changed biology

Korbi Thalhammer

Mushroom Pool, Yellowstone: the source of the first lab-cultured *Thermus aquaticus* strain, isolated by Brock and Freeze in 1976

Modern biology relies on the controlled manipulation of genes. The identification, amplification, and replication of specific DNA sequences underpins diverse biological advances like:

- **gene therapy** (in which a missing or disrupted gene is replaced by a functional copy)
- **diagnostics** (including detection of Huntington's and other hereditary disorders)
- **personalized medicine** (including targeting specific cancer cell lines with bespoke drug cocktails)
- **synthetic biology**, which inserts non-native genes into plants or microbes to confer new capabilities. Notable examples include provoking brewer's yeast to produce hop flavor molecules and eliciting herbicide resistance in food crops.
- **Forensics**, in every case where DNA evidence is cited.
- **Natural science** also benefits when microbiologists can easily manipulate gene expression in model organisms to learn new principles of developmental biology, metabolism, gene regulation, antimicrobial resistance, and responses to environmental stressors.

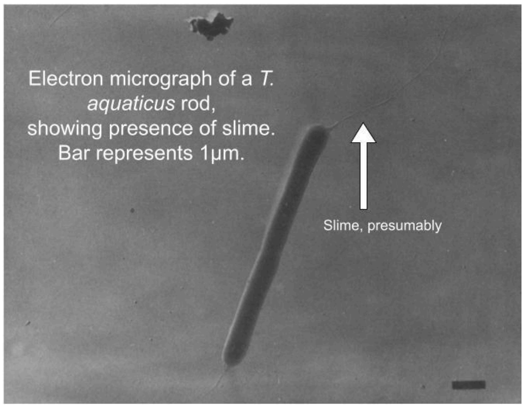

Electron micrograph of a *T. aquaticus* rod, showing presence of slime. Bar represents 1μm.

Slime, presumably

But how do people actually work on genes, which are far too small to see with even the well-aided eye? The first step is amplification by a step called PCR, short for **polymerase chain reaction**, which requires just a few reagents and a few hours to produce millions of copies of a single gene from a sample of bulk DNA. Bulk DNA contains thousands of genes *and* non-coding sequences. **Extracting a typical gene from bulk genomic DNA is similar to pulling exactly one 500-word article from an encyclopedia containing 50 million words…if the encyclopedia were small enough to fit in one microliter of water.**

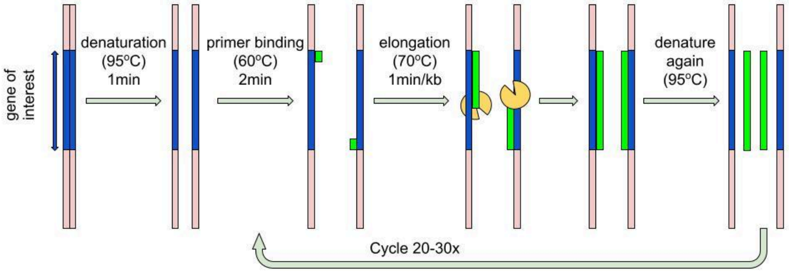

gene of interest
denaturation (95ºC) 1min
primer binding (60ºC) 2min
elongation (70ºC) 1min/kb
denature again (95ºC)
Cycle 20-30x

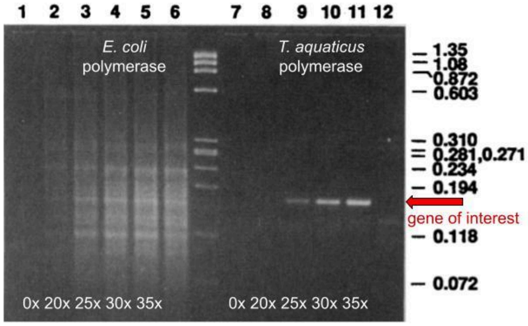

1 2 3 4 5 6 7 8 9 10 11 12
E. coli polymerase
T. aquaticus polymerase
1.35
1.08
0.872
0.603
0.310
0.281,0.271
0.234
0.194
gene of interest
0.118
0.072
0x 20x 25x 30x 35x
0x 20x 25x 30x 35x

PCR allows the amplification of a single gene by a factor of >10^6 in just a few hours by repeatedly melting the DNA and then copying the gene of interest using specific DNA primers and a polymerase enzyme.
A thermostable enzyme both reduces copying errors and allows the entire process to be automated.

Before PCR, gene amplification relied on cutting and pasting DNA into plasmids (scraps of circular DNA that can be taken up by bacteria), then waiting (hours to days) for the microbes to replicate in large volumes of growth medium, then lysing the cells and extracting the DNA chemically. This process was slow, arduous, and prone to error.

In 1985, Kary Mullis, who later received a Nobel Prize for his contribution and subsequently made some wildly unsubstantiated claims about AIDS, realized that if double stranded DNA were melted in the presence of primers that could bind to the gene of interest, an enzyme could elongate the primers based on the complementary DNA strands to which they were bound, doubling the copies of the gene. Furthermore, the process could be targeted precisely and repeated indefinitely, doubling the number of copies each cycle, to produce a sufficient quantity of DNA to use in further experimental steps (often several hundred thousand to several million copies). **The only problem with Mullis's procedure was that the enzyme used to elongate the DNA degraded during the necessary melting step** at the beginning of each new reaction cycle. To allow the reaction to continue, a scientist had to be present every 10-20 minutes to add fresh enzyme. Apart from the inconvenience, the commonly employed E. coli polymerase required low temperatures for elongation, which decreased primer specificity and increased the possibility of primer-dimers and other misamplifications.

In 1988, Mullis and others began **replacing the E. coli polymerase with the thermostable Taq polymerase enzyme from the extremophile *Thermus aquaticus*[3]**. Years earlier, in a study that would never have been funded today, Brock and Freeze had isolated *Thermus aquaticus* from the Mushroom Pool hot spring in Yellowstone, where it lived a quiet, contemplative life at about 70ºC, replicating its genomic DNA approximately every 45 minutes.

Studies of extremophiles continue to bring joy to scientists and laypeople alike, while simultaneously broadening our understanding of life's fundamental limits. The current hottest known microbe🥵was found on a black smoker in the Gulf of California and can grow and divide at 122ºC.

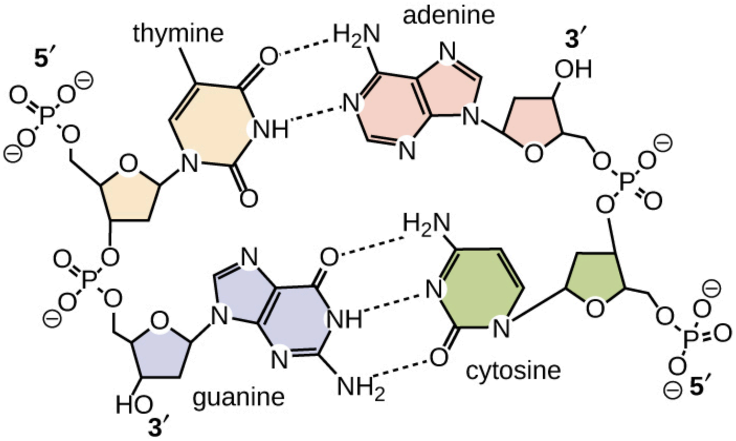

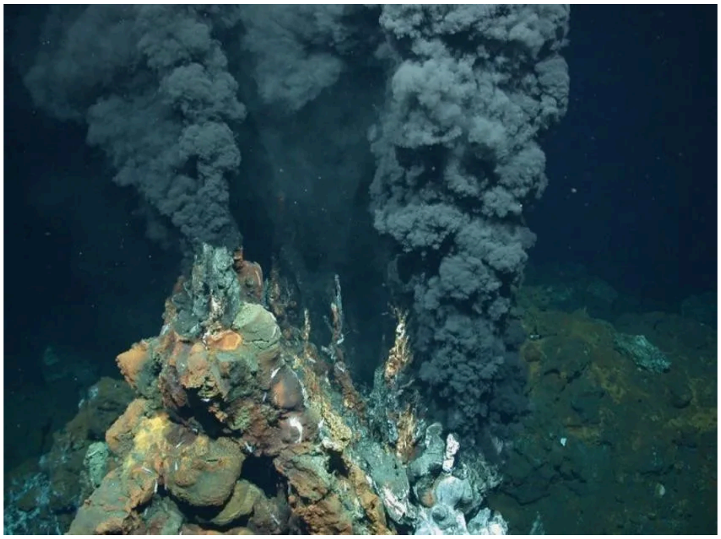

Microbial adaptations to life at high temps

- Thermostable Proteins
- Higher G-C content in DNA
- More rigid membrane lipids

References

1. Brock TD, Freeze H. *Thermus aquaticus gen. n. and sp. n.*, a nonsporulating extreme thermophile. J Bacteriol. 1969 Apr;98(1):289-97. doi: 10.1128/jb.98.1.289-297.1969. PMID: 5781580; PMCID: PMC249935.
2. https://www.usgs.gov/media/images/mushroom-pool-lower-geyser-basin-yellowstone-national-park-pool
3. https://geologyscience.com/geology/black-smokers/
4. Randall K. Saiki *et al.* ,Primer-Directed Enzymatic Amplification of DNA with a Thermostable DNA Polymerase.*Science***239**,487-491(1988).DOI:10.1126/science.2448875

Flintknapping: From Rocks to Tools

Paolo Sanchez | Ge 136a | Fall 2024

Flintknapping is the process by which certain materials such as chert, flint, glass and obsidian, are fractured to manufacture stone tools such as points (i.e., arrowheads and spear points), drills and scrapers. It is argued that flintknapping (shortened to "knapping") was first developed by hominids along the East African Rift ~3 million years ago, and for a majority of human history[1], knapping was one of the key methods for tool production. In the Old World, knapping has been attributed to the Stone Age (c.30,000-3,000 B.C.E.) and has largely been phased out by the advent of metal tools[1]. In the Americas, indigenous peoples have utilized knapping as a major toolmaking process from the arrival of humans in the Americas until the late 1800's. The availability of material, various tool functions and the cultural significance of tools has led to a wide diversity of lithic traditions across the New World, from projectile points of different morphologies to simple hide scrapers to large Mayan flint ornaments for ceremonial purposes. Today, flintknapping is widely regarded as an art and a hobby (Fig.1), but it is also integral in studying lithic technologies through the discipline of experimental archaeology.

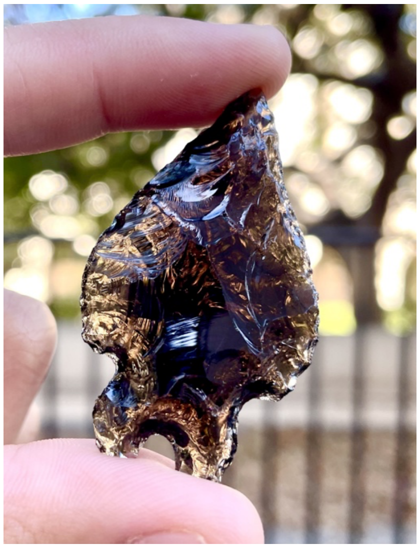

Figure 1: Obsidian arrowhead flintknapped by the author in 2018.

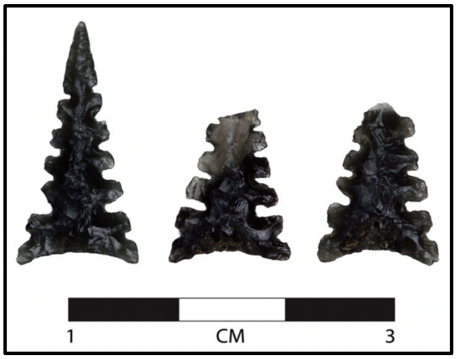

Figure 2: Historical Californian arrowheads made from obsidian north of Mono Lake, from Panich, 2016.

What materials are used? Ideally, any solid amorphous or polycrystalline material that exhibits a conchoidal (shell-shaped) fracture can be used for knapping. The most common material to work with for knapping is obsidian, however, other forms of natural silica, such as chert and flint, are often also used and are more durable than glassy materials. Some historical archaeology digs in the Midwest and Western United States have uncovered knapped glass bottles and glass telegraph insulators dating to the 19th century[2]. Some flintknapping artists today have also utilized agate, petrified wood, slag and even tektite glass for their material. Any leftover flakes and shards from the flintknapping process are known as *debitage* and can provide great use in understanding the context surrounding archaeological sites.

How do you flintknapp and what are the tools? Although there are many ways to break a stone, there are three common methods for knapping: 1) hard hammer percussion, 2) soft hammer percussion and 3) pressure flaking.

1.*Hard hammer percussion* (Fig. 3a): Simply striking a rock with another rock. The tool is a hard, tough stone (usually a palm-sized cobble of granite or other rock) used to directly strike a nodule or large flake. The first ever knapped tools are hypothesized to be constructed solely by this method[1]. This technique is usually done on large cobbles or nodules and is meant to produce the raw flakes from a central *corestone* for further processing.

2.*Soft hammer percussion* (Fig. 3b): Used to generally break off longer and thinner flakes than in hard hammer percussion. A tool known as a *billet* is used to ident the stone is used to make these flakes. Billets are made of either a thick antler, bone, hard dense wood or nowadays copper. Because longer flakes are generally produced, soft hammer percussion is ideal for making *flutes* (long flaked surfaces that runs down the long axis of a point) and *preforms* for producing points[1].

3.*Pressure flaking* (Fig. 3c): A detailed process which involves pressing a pointed tool onto a flake or slab to create a cutting edge as well as notches and groves. Traditionally the tool used is a sharpened antler or bone, though today copper nails are often used. Having a steady yet firm hand and knowing where exactly to apply pressure to control the shape of the resulting flake is necessary. This is the last step in making a point, drill, or cutting tool, and from experience it is also the most frustrating part of flintknapping. Many a nearly finished point has been broken and an unsuspecting finger cut from this difficult step.

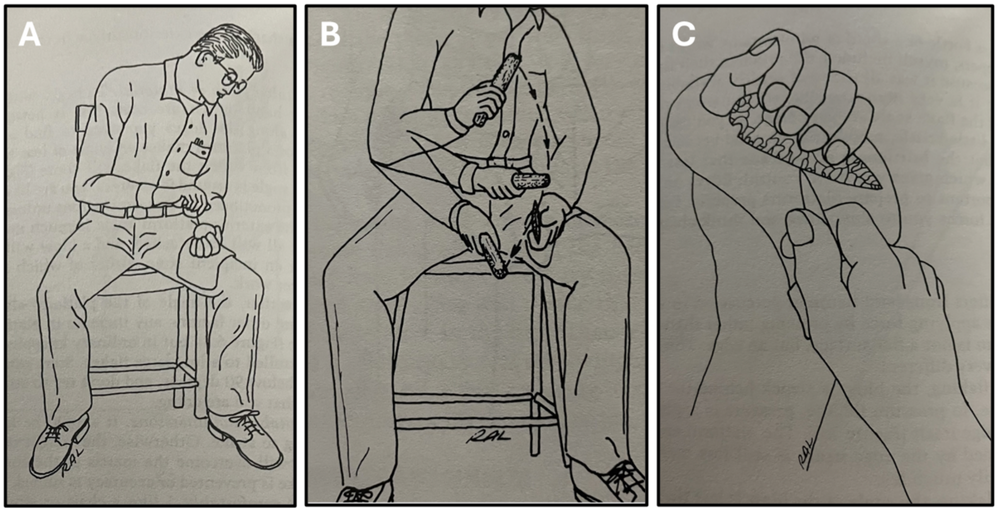

Figure 3: Various knapping techniques from Witttaker, 1994. A) Hard hammer percussion. B) Soft hammer percussion. C) Pressure flaking.

Flintknapping in California and Owens Valley: The first presence of stone tools in California came with the advent of human occupation[3] and has persisted well into the colonial period, resulting in a lithic tradition spanning around ten thousand years. This is well-evidenced by the discovery of points from the Clovis culture (c.11,000 years ago) in the Southern Sierras[4] and tools in archaeological excavations of indigenous villages in 1800's Spanish missions[5] (Fig. 2). Deposits of chert along the central coast and numerous obsidian deposits in Napa, Modoc, Inyo and Mono counties have been the main sources of knappable material.

The unique rhyolitic volcanism in areas around Owens Valley has made the valley a central hub for the obsidian trade (Fig. 4) in California and the Basin and Range provinces for over 2,000 years. During the Hawiee (ca. 1500-600 years ago) and Marana (600 years ago to colonial contact) periods, the development of extensive trade networks surrounding obsidian has resulted in the formation of complex socioeconomic structures and the establishment of obsidian quarries for trading with tribes in the Sierras and modern-day Nevada[6].

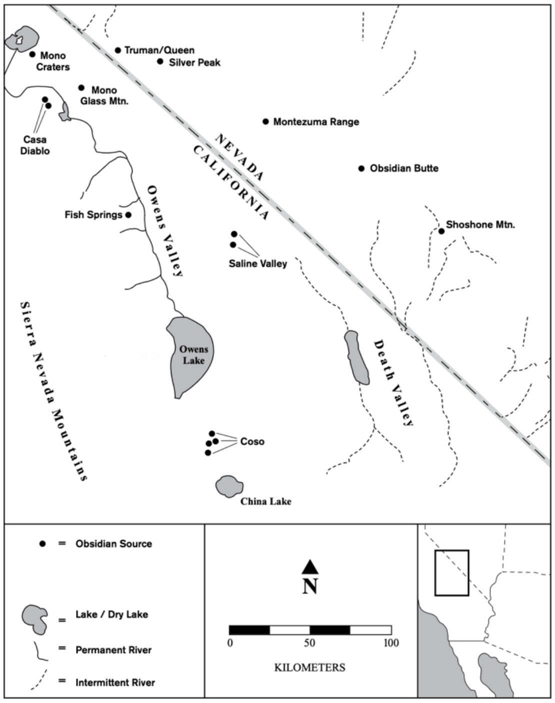
Mono Craters
Truman/Queen
Silver Peak
Mono Glass Mtn.
Casa Diablo
Montezuma Range
NEVADA
CALIFORNIA
Obsidian Butte
Fish Springs
Owens Valley
Shoshone Mtn.
Saline Valley
Sierra Nevada Mountains
Owens Lake
Death Valley
Coso
China Lake
● = Obsidian Source
= Lake / Dry Lake
= Permanent River
= Intermittent River
N
0
50
100
KILOMETERS

Figure 4: Locations of various obsidian quarries around Owens Valley during the Marana Period, from Vellanoweth et al., 2003.

References:

[1] Whittaker, J.C. 1994. *Flintknapping: Making and Understanding Stone Tools*. [2] Wacket, J. M. n.d. *The Post Hole*, n.42. P.20-27. [3] Vellanoweth et al., 2003. *J. of Arch. Sci.* n.30, p.1161-1173. [4] Zimmerman et al., 1989. *J. of CA and Great Basin Anth.,* v.11, p.89-91. [5] Panich, L.M. 2016. *J. of Arch. Sci. Reports 5*. p.521-530. [6] Eerkens and Spurling, 2008. *J. of CA and Great Basin Anth*. v.28, p.111-126.

Post Eruption Ecology

Sascha Goldsmith

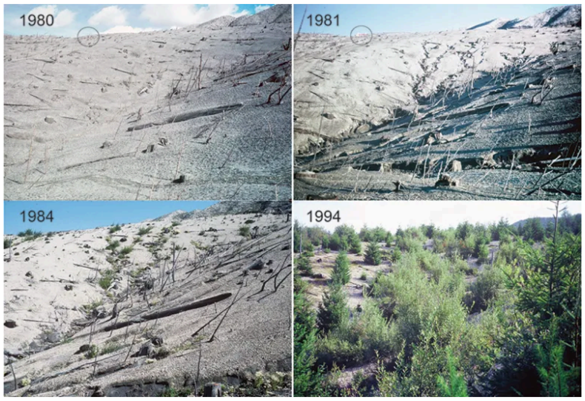

Volcanic eruptions can reshape landscapes, influence biodiversity, and alter ecosystem dynamics via various successions post-event due to pyroclastic and lava flows, ash plumes, and gasses (98% of which are water, carbon dioxide, and sulfur dioxide) [1]. Pyroclastic flows, composed of hot gas and volcanic material, can reach temperatures of 200 to 700 °C (392 to 1,292 °F) and travel at speeds of up to 700 km/h (435 mph), obliterating everything in their path [2]. The intense heat can incinerate flora and fauna, leaving a barren landscape. In the days to weeks following the eruption, ash fallout significantly affects soil properties, leading to initial plant die-off. Volcanic ash, primarily composed of fine-grained minerals such as volcanic glass, feldspar, and various silicates, is rich in essential nutrients like potassium, phosphorus, and silicon dioxide, altering the soil's chemical composition.

Ash and other volcanic deposits are often high in reactive silica and aluminum oxides, iron oxides, magnesium oxides, and traces of zinc and copper, which contribute to soil development and fertility through weathering processes [3]. Though toxic volcanic gasses, such as sulfur dioxide (SO_2), can form sulfuric acid (H_2SO_4) when they react with atmospheric water vapor, resulting in acid rain that significantly lowers soil pH, affecting nutrient availability and impacting surrounding ecosystems.

Toxic compounds released during eruptions can pose challenges for recovering ecosystems. Heavy metals such as arsenic, lead, and mercury can be mobilized during eruptions and deposited in the surrounding environment. These compounds can adversely affect plant growth and soil microbial communities, disrupting nutrient cycling and reducing biodiversity. Certain plant species may exhibit sensitivity to these toxins, inhibiting their ability to establish and thrive, while others may develop adaptations to tolerate elevated metal concentrations.

As months progress, pioneer species—such as mosses, lichens, and certain grasses—begin to colonize the porous and barren ground. These organisms stabilize the soil and initiate primary succession. Mosses and lichens retain moisture and promote the weathering of volcanic materials, facilitating soil development. Over time, primary succession occurs as plant colonizers enable the establishment of more complex plant communities, ie. nitrogen-fixing species like lupines, that enhance soil nitrogen via symbiotic relationships with rhizobia bacteria [4]. Over time there is a gradual re-establishment of plant and animal communities, leading to increased biodiversity as conditions stabilize.

After the 1980 eruption of Mount St. Helens in Washington, scientists observed a remarkable recovery. The eruption devastated the surrounding landscape, but pioneer species like fireweed and lupines rapidly colonized the area, improving soil quality and paving the way for more complex plant communities. The ash from this eruption contained significant amounts of potassium, calcium, and magnesium, contributing to the rapid recovery of flora [5]. Aside from changes in soil composition and habitat destruction, and alterations in water systems due to new formations generally occur like carved out valleys and craters for lakes and rivers created by lava flows. As the land recovers and plants re-establish, carbon sequestration helps stabilize the environment further into a positive feedback loop of development.

1. https://www.usgs.gov/faqs/what-gases-are-emitted-kilauea-and-other-active-volcanoes#:~:text=Ninety%2Dnine%20percent%20of%20the,and%20other%20minor%20gas%20species.
2. https://www.usgs.gov/programs/VHP/pyroclastic-flows-move-fast-and-destroy-everything-their-path
3. https://pmc.ncbi.nlm.nih.gov/articles/PMC10610550/
4. https://pmc.ncbi.nlm.nih.gov/articles/PMC98982/
5. https://www.usda.gov/media/blog/2020/05/18/past-present-and-future-research-mount-st-helens#:~:text=The%20return%20of%20plants%2C%20animals,is%20disabled%20in%20your%20browser.&text=The%20Mount%20St.,at%20www.mshinstitute.org%20.
   Mt St helens pic 1:
   https://eos.org/features/lessons-from-a-post-eruption-landscape
   Mt st helens pic 2:
   https://mountainscenes.com/images/south_cascades/SOU.998.html

Snowpack-Mediated Volcanic Degassing, Earthquakes, and Tree Death at Mammoth Mountain

Becky Williams Ge136a Fall 2024

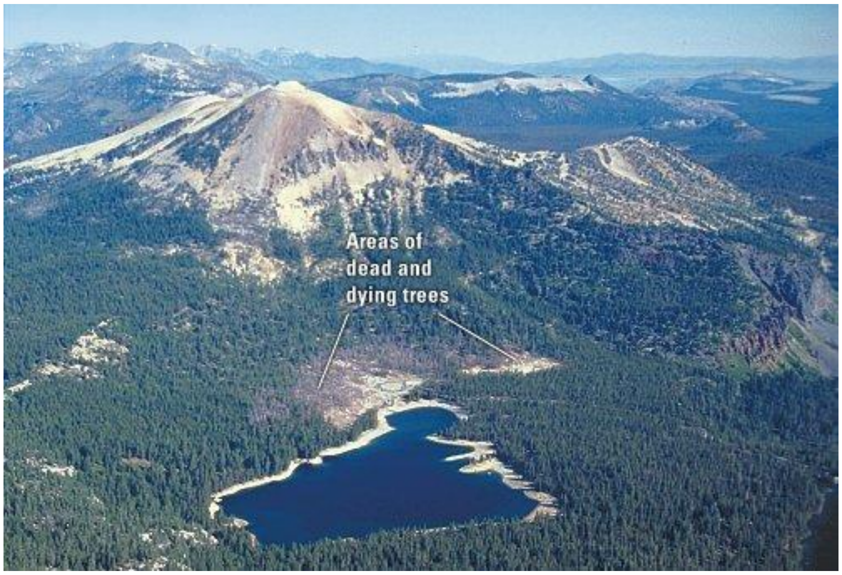

Figure 1: Tree death at Mammoth Mountain (credit: John D. Rogie)

On May 4th, 1989, a small earthquake occurred in the Long Valley Caldera. This earthquake marked the beginning of a series of earthquakes that occurred over the next 6 months. During this time period, as many as 25 M>1.2 events were recorded per day, and the largest magnitude of an earthquake was about 3 (Hill et al. 1990). Soon after this series of earthquakes, large numbers of trees started dying on Mammoth Mountain (Figure 1), a young volcano sitting on the southwest rim of the Long Valley Caldera. Investigations on the cause of these tree deaths showed that high amounts of carbon dioxide were present in the soil (Farrar et al. 1995). Recently, it was shown that the weight of the snowpack on the fault mediates the amount of carbon dioxide released (Hilley et al. 2022).

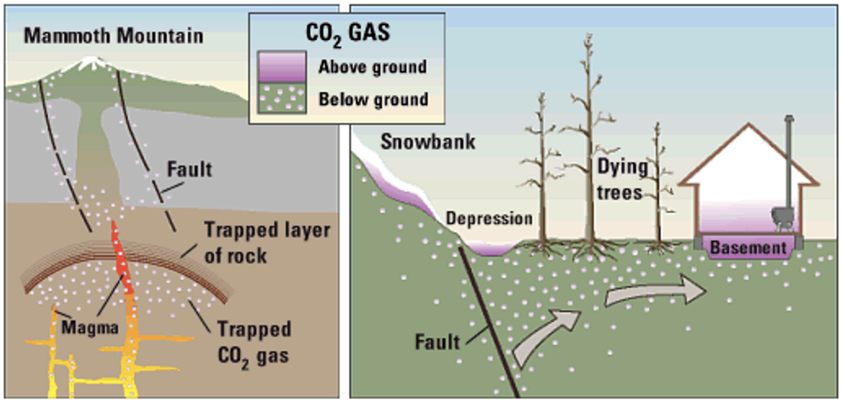

Figure 2: Escape of carbon dioxide at Mammoth Mountain (credit: USGS)

The Long Valley Caldera has been volcanically active for about 4 Myr, with the last eruption occurring about 200 years ago (USGS). During the series of small earthquakes in 1989, it was discovered that magma was rising through a fissure underneath Mammoth Mountain (Figure 2). After several acres of trees began dying, people started to suspect that the volcano might be the cause. Indeed, it was found that the soil contained carbon dioxide concentrations of 20-95%, much higher than the normal carbon dioxide soil levels of 1% or less (USGS). The isotope ratios of the carbon dioxide gas suggested that it originated from magma (Farrar et al. 1995). All trees, regardless of age or species, were affected by these high carbon dioxide levels, and most trees were dead when the carbon dioxide levels exceeded 30%. Likely, the carbon dioxide inhibits the root function of plants, leading to tree death. The dangers of carbon dioxide are not just restricted to the plant life in this area - measurements showed extremely high (even lethal) levels of carbon dioxide in some enclosed spaces, including a cabin (25% CO_2) and a utility vault (89% CO_2), showing that this process can affect human health, as well (Farrar et al. 1995).

Thirty years later, carbon dioxide continues to be released through faults at Mammoth Mountain, though the levels are declining. Close monitoring of carbon dioxide levels since 2014 shows seasonal variations, as well as an overall decline (Lewicki 2021). In 2017, a 20% reduction in carbon dioxide levels was recorded (Figure 3), coinciding with the end of a drought. Hilley et al. 2022 hypothesized that this reduction was somehow related to the snowpack of the area, and explored three hypotheses as to how snowpack could deplete the carbon dioxide levels. Using GNSS data, which records changes in the motion of the ground, they showed that seasonal changes in the compression of the ground can explain the observed decrease in flux. Essentially, the weight of the snowpack compresses the fault, restricting the amount of carbon dioxide escaping through the faults. In years with droughts, the snowpack is less, so the fault does not compress as much, and more carbon dioxide can escape. When Mammoth Mountain emerged from a drought in spring of 2017, the snowpack increased, so the fault was compressed more, and less carbon dioxide was released.

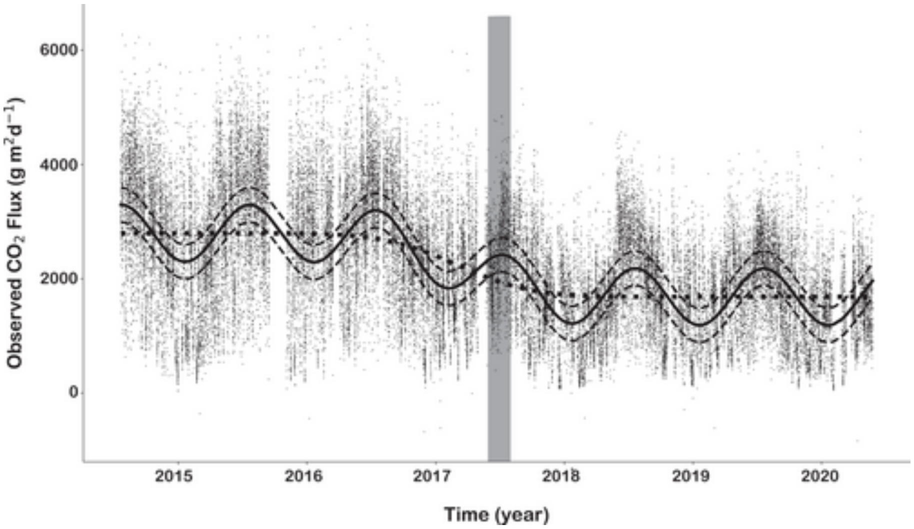

Figure 3: Seasonal and long-term carbon dioxide variations (credit: Hilley et al. 2022)

The case of snowpack-mediated volcanic degassing shows yet another way in which climate change can affect ecosystems and human health. As global temperatures increase, we can expect less snowpack in areas such as Mammoth Mountain. With less snowpack, the faults experience less compression, allowing more carbon dioxide to escape. Trees die, affecting the entire surrounding ecosystem, and carbon dioxide can reach levels dangerous (even deadly) to humans. It seems likely that this process occurs in other parts of the world, as well, in regions near volcanoes and fault lines that experience large amounts of snow pack.

Sources:

Farrar, C. D., et al. (1995). *Nature*, *376*(6542), 675–678. https://doi.org/10.1038/376675a0

Hill, D. P., et al. (1990). *Bulletin of the Seismological Society of America*, *80*(2), 325–339. https://doi.org/10.1785/bssa0800020325

Hill, D., & Diggles, M. (2007, July 9). Invisible CO2 Gas Killing Trees at Mammoth Mountain, California | USGS Volcano Fact Sheet. https://pubs.usgs.gov/fs/fs172-96/

Hilley, G. E., Lewicki, J. L., & Baden, C. W. (2022). *Geophysical Research Letters*, *49*(6). https://doi.org/10.1029/2021gl096595

Lewicki, J. L. (2021). *Journal of Volcanology and Geothermal Research*, *418*, 107347. https://doi.org/10.1016/j.jvolgeores.2021.107347

DON'T EAT THE PINK SNOW or do idc

Chlamydomonas nivalis – the snow algae

Richard Horak

Discovery

In May of 1818, four ships departed England to chart the Arctic coastline of North America and discover the elusive Northwest Passage. Despite failing in their mission, Captain John Ross played an essential role in catalyzing a scientific discovery. Noticing crimson snow, streaking the white cliffs of Baffin Bay, their party landed and collecting this "blood snow" to be brought back to England for analysis. Scientists of the time stated it was meteoric iron deposits. Yet, Robert Brown, a botanist, resisted these claims, suggesting that it was an alga. However, this idea was dismissed for over a century, before scientists in Scotland confirmed that this red snow was caused by the algae Chlamydomonas nivalis.

Astaxanthin structure

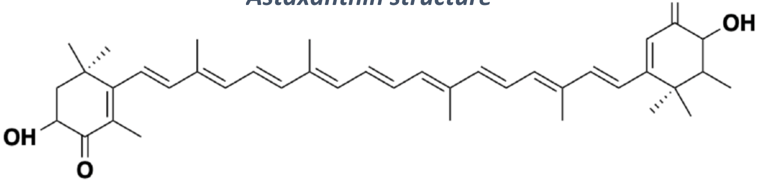

Life cycle

Chlamydomonas nivalis is a freshwater green alga found in cold alpine regions or in the polar coasts and is safe to eat (eyes emoji). Its red color is due to the production of the carotenoid astaxanthin (the same class of molecules that make carrots orange). In the warm summer, C. nivalis lives as a bi-flagellated algae in melted snow, or in the many ponds which dot the Sierra Nevada. As nutrients deplete, this swimming green algae forms zygotes with thick cell walls, becoming a cyst. As the snow covers the algae, it lies dormant as a spore. Finally, as the snows melt, the cysts bloom bright red before diving to begin the cycle anew.

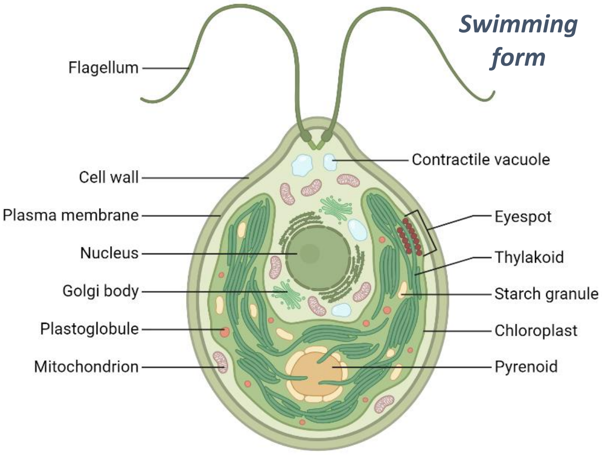

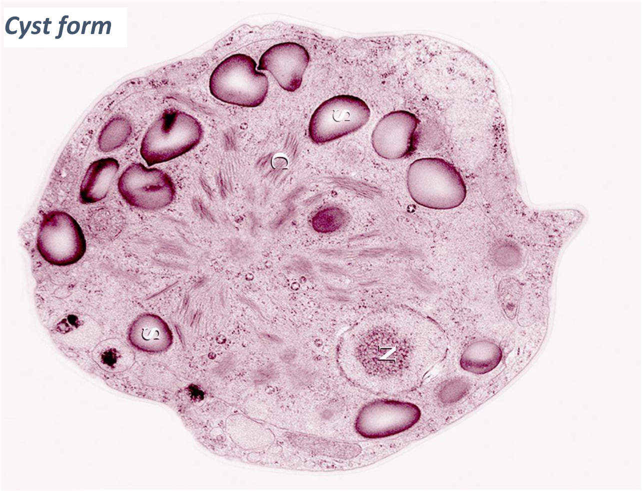

Dealing with stress (looking at you grad students)

A primary issue for many environmental microbes, is starvation. C. nivalis copes by existing as a spore, a highly resilient dormant cell state. However, once nutrients return and the spores awaken, their problems only worsen. Living within alpine zones on/in snow exposes C. nivalis to incredibly high levels of UV as well as cold temperatures. They respond by producing their characteristic red pigment at concentrations 20x that of their chlorophyll pigment, lowering UV absorption and UV-mediated damage. They also produce ice-binding proteins which prevent their cellular membranes from freezing (cool). However, production of astaxanthin or ice-binding proteins requires energy, and a lot of it. As a photosynthetic organism, C. nivalis captures light energy via their chlorophyll pigments, leading to water hydrolysis and excited electrons which then pass between electron acceptors, producing ATP, NADH/NADPH, and O2 in the process, while also driving carbon fixation. NADPH and sugars can be used to build cellular material, while NADH and O2 are used by the mitochondria (powerhouse) to generate ATP.

While this works great on paper, an issue arises when you live in a cold sunny place. Photosynthesis is temperature-independent and light-dependent. However, the rates of biosynthesis and growth are highly dependent on temperature. These leads to what is termed reductive stress, where cells are generating reduced electron carriers (NADH/NADPH) at higher rates than they consume them. Stalled electrons within enzymes and redox-active compounds can react with O2, iron, or cellular macromolecules, producing radical chemical species and lethal cell damage. BUT NEVERTHELESS, C. NIVALIS PERSISTS. C. nivalis, as well as other Chlamydomonas species, have clever ways to deal.

1) Non-photochemical quenching

During photosynthesis, excited electrons from chlorophyll can go one of 3 places, they can be passed to photosystem 2, they can release a photon, or they can release heat. The production of carotenoids by C. nivalis not only helps lower UV absorption, but also provides an "energy trap" by absorbing energy released as heat, which along with their red color, hastens snow melting, and can decrease snow albedo by 13% in artic glaciers!

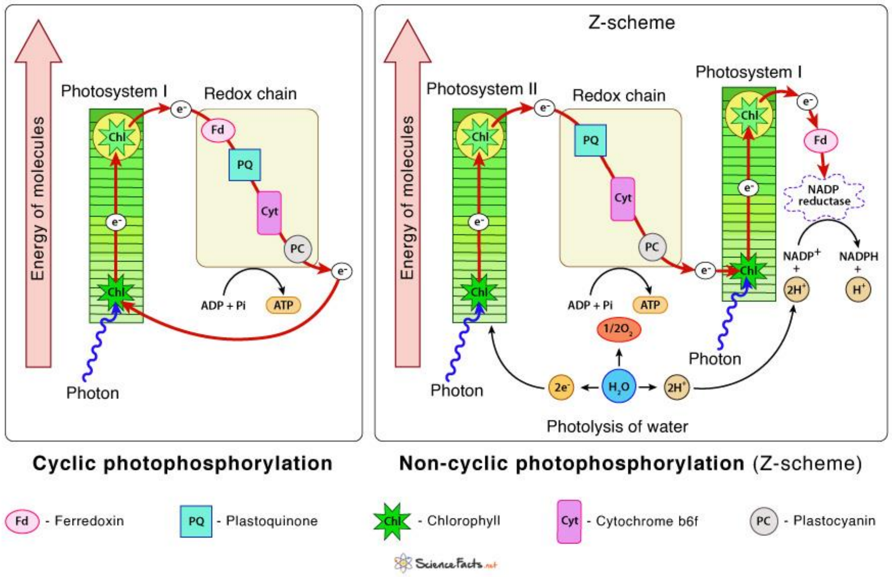
Energy of molecules
Photosystem I
Redox chain
Chl
e⁻
Fd
PQ
Cyt
PC
ADP + Pi
ATP
Photon
Z-scheme
Photosystem II
Photosystem I
NADP reductase
NADP⁺ +
2H⁺
NADPH +
H⁺
1/2O₂
H₂O
2e⁻
2H⁺
Photolysis of water
Cyclic photophosphorylation
Non-cyclic photophosphorylation (Z-scheme)
Fd - Ferredoxin
PQ - Plastoquinone
Chl - Chlorophyll
Cyt - Cytochrome b6f
PC - Plastocyanin
ScienceFacts.net

2) Lowering chlorophyll production

This one is kind of obvious, if you are having a problem where too much photosynthesis is occurring, cells can just lower production of their photosynthetic pigments – chlorophyll.

3) Increasing energy usage

In our analogy of the factory which produces boxes and ships them out, if you have an issue where too many boxes are piling up, a solution is just to ship more boxes out. The cell can do something similar, carrying out nitrogen assimilation or increasing biosynthesis or ribonucleotides, lipid, and proteins.

4) Switching from non-cyclic to cyclic photosynthesis – my favorite

While non-cyclic photosynthesis is the kind that you saw in your biology textbooks, many phototrophs can also carry out cyclic photosynthesis. In non-cyclic photosynthesis, as described above, electrons in chlorophyll are excited and are passed between electron carriers. This catalyzes ATP production and formation of NADH or NADPH for use in energy generation and biosynthesis. However, in cyclic photosynthesis, these electrons generate ATP, but do not go on to generate reducing equivalents such as NADH, instead being passed back to chlorophyll. This is a way for cells to limit the build up of "boxes" while also allowing photosynthesis to continue at similar rates as before, allowing for energy production without causing metabolic stress.

References: 1) Stefanie Lutz et. al., *Nat Comm.,* 2016. 2) Zhao Peng et. al., *Front. Microbiol.* 2021. 3) Yanli Zheng et. al., *Front Microbiol* 2020.

The advent of photosynthesis represents one of the biggest energetic changes in Earth history because it afforded life the ability to use light/water to power metabolisms and release dioxygen into the atmosphere. However, not all forms of photosynthesis produce oxygen, and it remains unclear how life exactly evolved the tools for photosynthesis. One way to probe the history of photosynthesis is to study the phylogeny of Cyanobacteria (the originators of oxygenic photosynthesis) and extant phototrophs, as well as study their present-day environments. The molecular machines that are central to the conversion of light into usable energy for life are the photosynthetic reaction centers. The four categories of photosynthetic reaction centers are reaction center I (RCI), reaction center II (RCII), photosystem I (PSI), and photosystem II (PSII). Different bacteria that conduct anoxygenic photosynthesis use exclusively RCI or RCII, while cyanobacteria and chloroplasts use both PSI and PSII in conjunction for oxygenic photosynthesis. The distribution of photosynthetic reaction center genes among bacteria does not have a canonical evolutionary interpretation and reveals evidence of horizontal gene transfer. (see Figure 1). Models for the origin of photosynthesis disagree about what clades invented the different reaction centers, whether the two photosystems were invented before RCI and RCII, and when certain horizontal gene transfer events occurred. Two popular theories are that RCI and RCII were invented in distinct lineages and the cyanobacteria discovered how to fuse the two molecular machines, vs. cyanobacteria invented phototrophy genes, type one and two centers diverged, and other clades inherited RCI or RCII via horizontal gene transfer (Fischer et al., 2016).

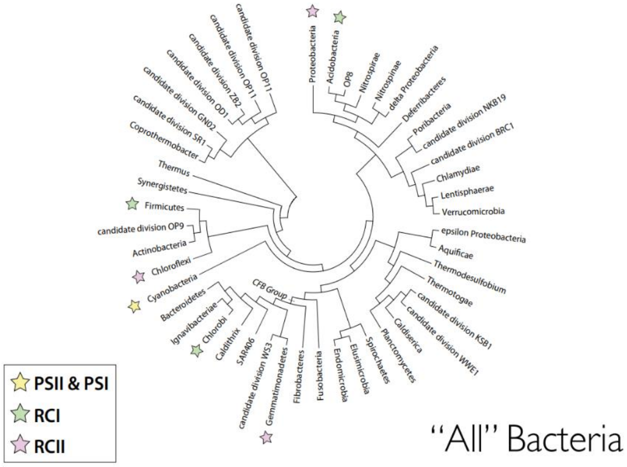
candidate division OP11
candidate division OP11
candidate division ZB2
candidate division OD1
candidate division GN02
candidate division SR1
Coprothermobacter
Thermus
Synergistetes
Firmicutes
candidate division OP9
Actinobacteria
Chloroflexi
Cyanobacteria
Bacteroidetes
Ignavibacteriae
Chlorobi
Caldithrix
SAR406
CFB Group
candidate division WS3
Gemmatimonadetes
Fibrobacteres
Fusobacteria
Endomicrobia
Elusimicrobia
Spirochaetes
Planctomycetes
Caldiserica
candidate division WWE1
candidate division KSB1
Thermotogae
Thermodesulfobium
Aquificae
epsilon Proteobacteria
Verrucomicrobia
Lentisphaerae
Chlamydiae
candidate division BRC1
candidate division NKB19
Poribacteria
Deferribacteres
delta Proteobacteria
Nitrospinae
Nitrospirae
OP8
Acidobacteria
Proteobacteria
PSII & PSI
RCI
RCII
"All" Bacteria

Figure 1. A simplified tree of bacteria phyla, labeled by which phyla carry photosynthetic genes. Note that only cyanobacteria have photosystem I & II. The distribution of photosynthetic genes does not follow a clear pattern, there is no obvious "inventor" of photosynthesis.

Lichens are classically viewed as a symbiotic relationship between algae and fungus. However, as lichen have been increasingly studied, especially with shotgun sequencing, researchers are learning more about other organisms living in lichen that are not typically included in the classical view of lichen. One of the most common rock lichens found in the western US are *Umbilicaria phaea*. *U. phaea* are desiccation tolerant and are commonly found in hot and dry places (even though many are covered by snow for part of year). *U. phaea* are found growing on silicious boulders and their body (called the thallus) can range from 1-6cm in diameter (think 3cm). The thallus can range from a smooth light brown to a darker crunchy brown and has black spots that release spores (looks like a chocolate chip cookie).

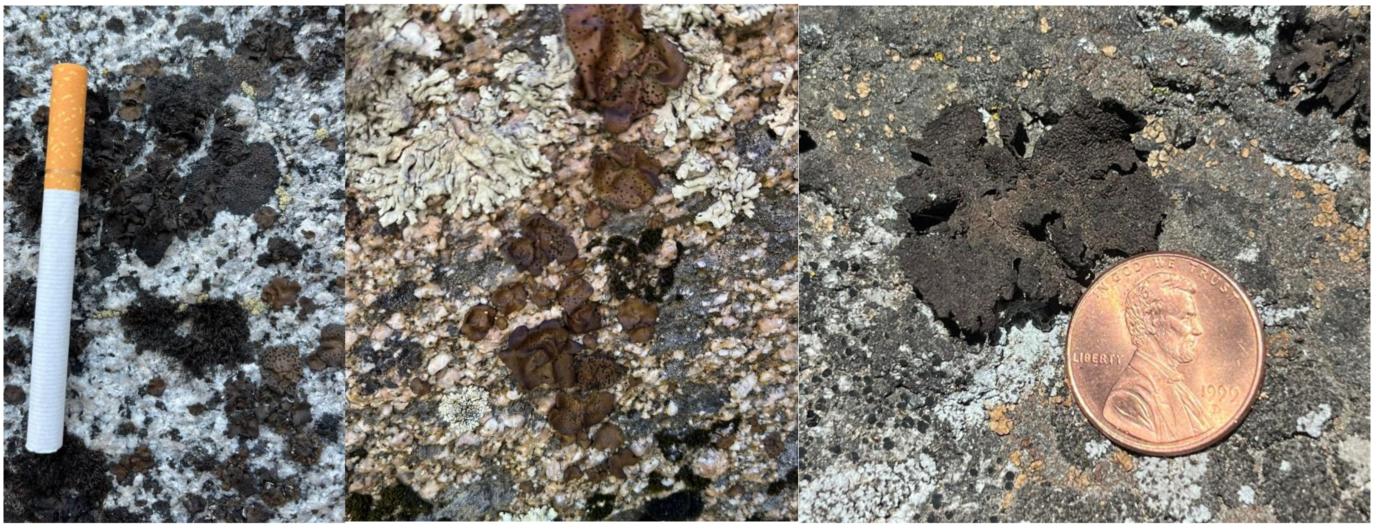

Figure 2. Example photos of *U. phaea*. The photo on the right shows an older specimen that has been more desiccated (it looks darker, dried out, and is larger in diameter). The middle photo shows younger *U. phaea* that are smaller and lighter in color (sorry for no scale). The left photo shows a mix of older and younger lichen. Note that all photos show *U. phaea* living directly around other lichen.

The Fischer group became interested in *U. phaea* because we wanted to determine what possible anoxygenic phototrophs could be living in the lichen. We used shotgun sequencing from both our own collected data and data published by Merges et al. (2021). All *U. phaea* samples were collected in the Sierra Nevada mountains. Short read sequencing data was assembled and annotated for Type I and Type II reaction center genes. The annotated genes of interest were compared using BLAST to the NCBI non-redundant protein sequence database to determine which type of organism they are likely from. The genes where also placed into a phylogenetic tree for comparison. Similarly, long read sequencing data from (Merges et al., 2021) was annotated for Type I and Type II reaction centers and analyzed in the same way. Altogether, our results suggest an unexpected amount of bacterial phototropic diversity in *U. Phaea.* Specifically, we found RCII genes belonging to cyanobacteria, gemmtimonadetes, chloroflexi, and a variety of proteobacteria. These findings suggest that lichen can be a protected environment for extant phototrophs to exist and potentially conduct anoxygenic photosynthesis. Overall, this finding highlights the potential for new investigations into phototrophic bacteria in lichen and explanations for why they thrive in such an environment.

References

Fischer, W. W., Hemp, J., & Johnson, J. E. (2016). Evolution of Oxygenic Photosynthesis. *Annual Review of Earth and Planetary Sciences*, *44*(1), 647–683. https://doi.org/10.1146/annurev-earth-060313-054810

Merges, D., Dal Grande, F., Greve, C., Otte, J., & Schmitt, I. (2021). Virus diversity in metagenomes of a lichen symbiosis (Umbilicaria phaea): Complete viral genomes, putative hosts and elevational distributions. *Environmental Microbiology*, *23*(11), 6637–6650. https://doi.org/10.1111/1462-2920.15802

Amanda L. Bednarick[1]

[1] Division of Geological and Planetary Sciences, California Institute of Technology, Pasadena, CA 91125

Sierran magmatism: Alabama Hills

We are at the junction of two major geologic provinces:

Western Cordillera – this includes the Sierra Nevada Mountains, which are a continental arc that formed when the Farallon Plate subducted beneath the North American Plate

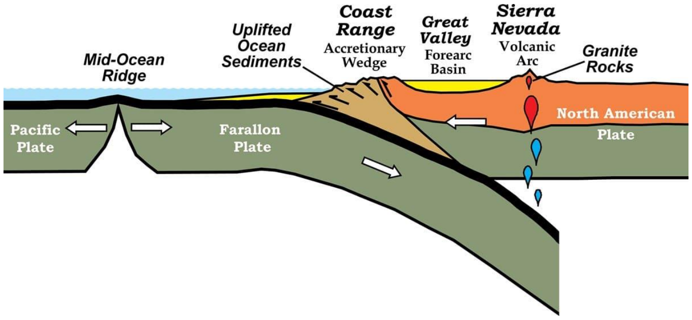
Mid-Ocean Ridge
Uplifted Ocean Sediments
Coast Range
Accretionary Wedge
Great Valley
Forearc Basin
Sierra Nevada
Volcanic Arc
Granite Rocks
Pacific Plate
Farallon Plate
North American Plate

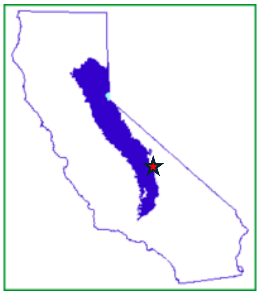

Basin and Range – this includes the Owens Valley, which formed because of extensional forces that are stretching much of western North America. "Basin and range" refers to the alternating valleys and mountains, oriented north-south, that result from the extension between the Pacific Plate in the west and the Colorado Plateau in the east.

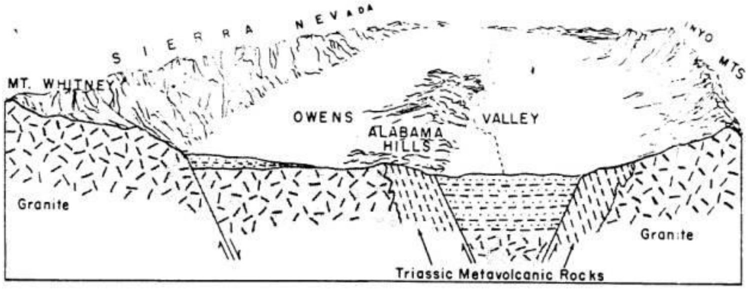
SIERRA NEVADA
MT. WHITNEY
INYO MTS
OWENS VALLEY
ALABAMA HILLS
Granite
Granite
Triassic Metavolcanic Rocks

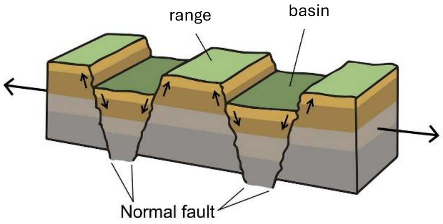
range
basin
Normal fault

The Alabama Hills are geochemically related to the Sierra Nevada Mountains above them. They have been displaced from their original position (~8500 feet vertically down) along the Sierra Nevada frontal fault. They have also probably moved north-south along the Owens Valley.

The granite unit here is ~103 Ma biotite monzogranite (micaceous and relatively low in alkali feldspars).

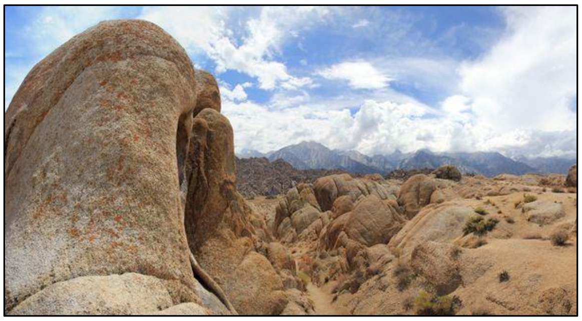

The unit's name is after the CSS Alabama, a confederate warship that was sunk in the high seas by the USS Kearsarge during the Civil War (1864).

Mono-Inyo Volcanic Chain: Obsidian Dome

The extensional forces at work in the basin and range result in the crust being stretched and thinned in the basins or valleys. These low points of thin crust are areas of relatively low pressure, which encourages molten mantle material to ascend toward the surface. This decompression melting forms magma chambers beneath the surface in places like the Owens Valley.

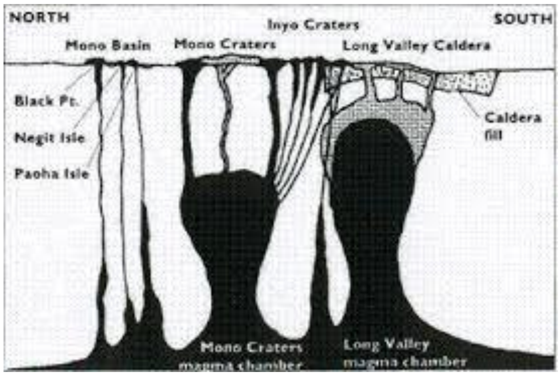
NORTH
SOUTH
Inyo Craters
Mono Basin
Mono Craters
Long Valley Caldera
Black Pt.
Negit Isle
Paoha Isle
Caldera fill
Mono Craters magma chamber
Long Valley magma chamber

The normal faults that bound and cross the valley provide axes along which magma can be brought to the surface. The Mono-Inyo Volcanic Chain is one such fissure system. Explosive eruptions along this 25-mile-long chain began >50,000 years ago (Mono Craters). Obsidian Dome formed only 600 years ago in a silica-rich, volatile-driven phreatic eruption. Obsidian is amorphous silica.

References

Frazer et al., 2022: Insights from the Alabama Hills into Mesozoic Magmatism and Tectonics in Eastern California.
http://www.muststayawake.com/guide12_files/guide12_F06.htm
https://www.usgs.gov/volcanoes/mono-inyo-craters
https://sierra.sitehost.iu.edu/papers/2008/young.html
https://www.monolake.org/learn/aboutmonolake/naturalhistory/geology/

Copper Carbonate Minerals of Cerro Gordo

Azurite and a Little Malachite: © Black Country Museums CC BY-NC-SA 2.0

The Cerro Gordo mines were a group of mines in the Inyo Mountains, east of the Sierra Nevadas. Originally utilized by miners for silver, the mines sit on an area of rich geological intrigue. The geology consists primarily of sedimentary rock cut through by igneous intrusions of mostly felsic rock, causing some of the sedimentary country rock to undergo contact and hydrothermal metamorphism. The native copper and copper ores like cuprite that form in the region can undergo weathering when near the surface and oxidize to form azurite, with the formula $Cu_3(CO_3)_2(OH)_2$. Due to the ease by which azurite can be oxidized from copper minerals, azurite is commonly associated with them and can be found in copper-containing mines like the Cerro Gordo mines. However, azurite is unstable in the air and pseudomorphs into malachite, with the formula $Cu_2CO_3(OH_2)_2$. More specifically, the carbonate in azurite can be replaced by water, leading to changes in the chemical formula, crystal structure, and most notably color, changing from blue to green. This can create dazzling, though rare, mineral specimens of intertwined malachite and azurite on the same sample, called azurmalachite. More commonly, though, the malachite replaces the azurite, creating malachite after azurite, maintaining the same shape as the original malachite specimen but chemically becoming a new substance. The color change is due to the change in the ligands coordinated to the Cu^{2+} metal center. In malachite, the copper ions are coordinated to more hydroxide ions and less carbonate ions than in azurite. As carbonate is a stronger ligand than hydroxide, the d-d transitions in azurite are larger and the energy gap between the t_2g and e_g levels is greater, absorbing at a higher frequency (orange) and appearing blue, while the smaller energy gap in malachite results in absorbances at a lower frequency (red) and appears green. The overall crystal structure, however, stays around the same, maintaining the monoclinic crystal system and many of the physical properties of the mineral. When malachite is formed by itself and not as a pseudomorph of azurite, the process is similar, where typically sulfidic copper ores are weathered and oxidized into malachite. One notable difference though between naturally formed azurite and malachite is the crystal habit of the two minerals. While azurite can often form large tabular or prismatic crystals along with massive habits, malachite does not often form

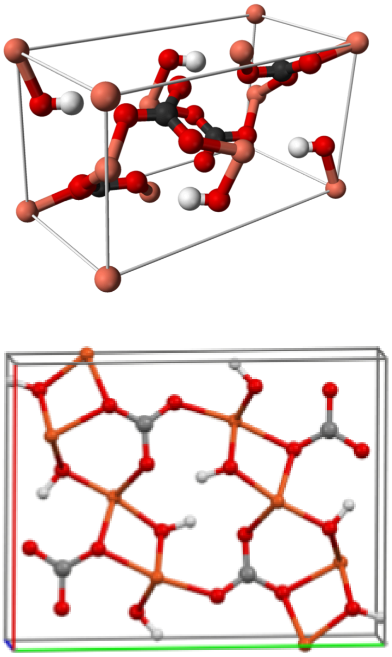

Azurite and Malachite Unit Cells. Source: Wikimedia Commons large crystals; instead, it opts to take botryoidal or stalactitic habits when not massive. This is due to malachite's typically low crystal growth forming tiny acicular crystals that bunch up into these habits.

Botryoidal Malachite: © Rob Lavinsky iRocks.com CC-BY-SA-3.0

Aside from azurite and malachite, the Cerro Gordo Mines area also contains rosasite and aurichalcite, two other copper carbonate minerals with the formulas $(Cu,Zn)_2(CO_3)(OH)_2$ and $(Zn,Cu)_5[(OH)_3|CO_3]_2$. Given the zinc found in the formula, rosasite and aurichalcite do not form in solely copper deposits like azurite and malachite but rather form when copper-zinc deposits undergo supergene weathering. As such, they are less common than azurite and malachite.

Aurichalcite and Rosasite. Source: Wikimedia Commons

Historically, azurite and malachite have found use in pigments, where their brilliant hues provide a wide range of greens and blues for use in paint. Azurite in particular is interesting as a pigment as over time when exposed to air its conversion to malachite gives a greenish tint to works of art pigmented with azurite. Malachite can also be used as an ore of copper, especially in methods involving sulfuric acid where malachite is dissolved to form cupric sulfate, carbon dioxide, and water, a process that bypasses the usual need for smelting ores.

References:

Ata, O. N., and H. Yalap. 'Optimization of Copper Leaching from Ore Containing Malachite'. Canadian Metallurgical Quarterly, vol. 46, no. 2, Informa UK Limited, June 2007, pp. 107–114, https://doi.org/10.1179/cmq.2007.46.2.107.

Braithwaite, R. S. W., and George Ryback. "Rosasite, Aurichalcite, and Associated Minerals from Heights of Abraham, Matlock Bath, Derbyshire, with a Note on Infra-Red Spectra." Mineralogical Magazine and Journal of the Mineralogical Society 33.261 (1963): 441–449. Web.

Dana, James Dwight, Cornelius Searle Hurlbut, and Cornelis Klein. Manual of Mineralogy (after James D. Dana) / Cornelius S. Hurlbut, Jr., Cornelis Klein. 19th ed. New York: Wiley, 1977.

Merriam, Charles Warren. Geology of the Cerro Gordo mining district, Inyo County, California. No. 408. United States Government Printing Office, 1963.

Švarcová, Silvie, et al. "Pigments—copper-based greens and blues." Archaeological and Anthropological Sciences 13 (2021): 1-29.

Vink, B. W. "Stability Relations of Malachite and Azurite." Mineralogical Magazine 50.355 (1986): 41–47. Web.

The Dolomitization of Carbonates

Sophia Westerkamp

The Chemistry and Process of Dolomitization

Carbonates are a class of sedimentary rocks that formed at (or near) Earth's surface via precipitation from solution. The two major types of carbonate rocks are limestone and dolostone, also known as dolomite. Limestone is primarily composed of calcite ($CaCO_3$), while dolomite is primarily composed of the mineral form of dolomite ($CaMg(CO_3)_2$) (Mehmood et al. 2018).

Dolomites are subdivided into two groups based upon their formation process. Primary dolomites precipitate directly from aqueous solution with no $CaCO_3$ dissolution (Mehmood et al. 2018). Secondary dolomites form via the slow replacement of calcite with dolomite (mineral) in limestone. This occurs as calcite dissolves in aqueous solution and is slowly and locally replaced with dolomite around the edges and corners of the calcite crystals. The vast majority of dolomites are formed by this secondary process (Mehmood et al. 2018). Figure 1 shows a scanning electron microscope image of secondary dolomitization, in which dolomite mineral crystals nucleate at the edges of larger calcite crystals (Sibley et al. 1987). A stoichiometric equation for secondary dolomitization is shown below.

$$2CaCO_{3\ (calcite)} + Mg^{+2} \Leftrightarrow CaMg(CO_3)_{2\ (dolomite)} + Ca^{2+}$$

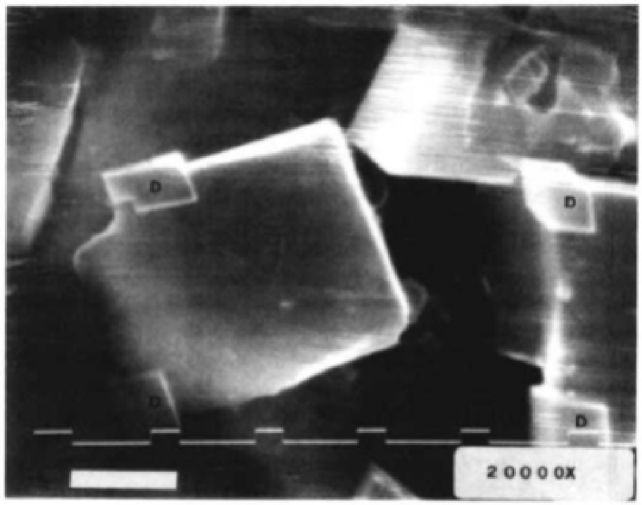

Figure 1 Scanning electron microscope photomicrograph of dolomite rhombs (D) that have nucleated on the corners of calcite. Taken from Sibley et al. 1987.

Dolomites may have different names depending on their ratio of magnesium. 0-32 mol% magnesium dolomites are called high-magnesium calcates, 32 - 45 mol% magnesium dolomites with incomplete segregation of calcium and magnesium into separate layers are called protodolomites, and dolomites with a 50:50 ratio of calcium to magnesium in a near-perfect layering of cationic layers are called stoichiometric dolomites. Figure 2 displays the various crystal structures of each of these three types of dolomite (Mehmood et al. 2018).

Dolomotization requires the presence of a dissolving and precipitating fluid with high concentrations of magnesium. Seawater and subsurface hydrothermal waters have a high enough magnesium content to act as dolomitizing solutions. However, the primary (and most ideal) dolomitizing source is hypersaline waters such as those found at and around Owens lake. Dolomites are unlikely to be formed near aqueous sources such as lakes, rivers, or rainwater that do not contain high amounts of magnesium. A magnesium-rich aqueous solution is required to supply Mg^{+2} and CO_3^{-2} while Ca^{+2} is supplied by the precursor calcite (Mehmood et al. 2018).

The Kinetics of Dolomitization

While the overall process of dolomitization is well understood, the kinetics of dolomitization have remained elusive. Experimental dolomitization has required the application of high-temperatures whereas natural dolomitization is performed under low temperature conditions. Nevertheless, Sibley et al. 1987 were able to perform successful dolomitization experiments to deduce the general kinetics of dolomitization. They found that the transformation of limestone into dolomite has two distinct phases: an induction stage and a nucleation and growth stage. The induction stage tends to be much longer than the nucleation and growth stage. They found that the rate of $CaCO_3$ dolomitization is dependent on the Mg/Ca ratio of the solution, the mineralogy of the reactant, the surface area of the reactant, presence or lack of SO_4^{-2} in solution, and temperature. The results of these experiments were consistent with the occurrence and characteristics of dolomites found in natural settings (Sibley et al. 1987).

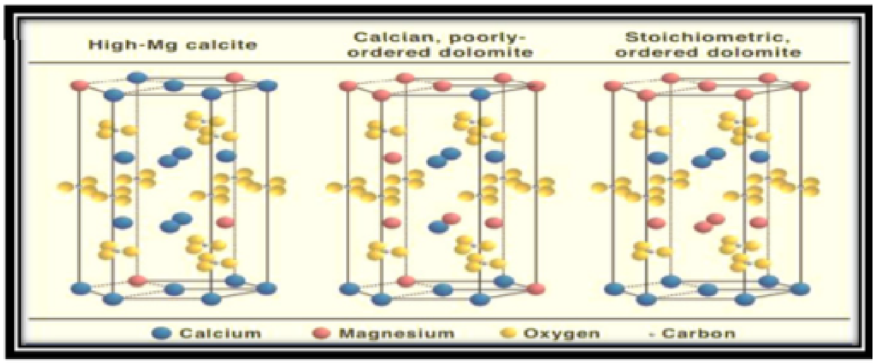
High-Mg calcite
Calcian, poorly-ordered dolomite
Stoichiometric, ordered dolomite
Calcium
Magnesium
Oxygen
Carbon

Figure 2 The different mineralogical structures of dolomite. High-Mg calcite contains less than 32 mol% Mg. Protodolomites contain 32-45 mol% Mg with imperfect Mg-Ca cationic layering. Stoichiometric dolomites have complete segregation of Ca and Mg into cationic layers in a 50:50 ratio. Taken from Mehmood et al. 2018.

Where Can We Find Dolomites?

Dolomites are common around the Owen’s lake and Cerro Gordo regions in California. The following paragraph will focus specifically on Cerro Gordo and Inyo county to describe a series of locations that have dolomite which we may encounter. These locations were taken from a USGS survey authored by Stone et al. 2004.

1) The Hidden Valley Dolomite is a massive saccharoidal dolomite that forms ledgy slopes. Its thickness is between 450 and 580m and can be found between Bonham Canyon and the Holiday Mine.
2) The Ely Springs Dolomite is a thick-bedded dolomite characterized by irregular nodules and lenses of dark-gray chert. It can be found near the Eureka Quartzite in the Holiday Mine area.
3) The Fanglomerate of Bonham Canyon is made up of a thick sequence of gravel deposits forming deeply dissected ridges on the east side of the Inyo mountains. In this region, the gravel consists of ~70% dolomite.
4) Near Cerro Gordo Road a thin-bedded quartzose siltstone and shale can be seen, the upper part of which contains limestone and dolomite.
5) The lower part of the lost Burro Formation east of Gordo peak contains light-medium and dark-gray limestone, dolomite and marble that forms steep slopes and cliffs.
6) The Badger Flat Limestone is a light gray, medium bluish gray and light brown laminated dolomite exposed along the eastern front of the Inyo mountains between Bonham Canyon and Holiday mine.

References:

(1) Mehmood, Mubashir, et al. "Dolomite and dolomitization model-a short review." *International Journal of Hydrology* 2.5 (2018): 549-553.
(2) Sibley, Duncan F., Robert E. Dedoes, and Timothy R. Bartlett. "Kinetics of dolomitization." *Geology* 15.12 (1987): 1112-1114.
(3) Stone, Paul, et al. "Geologic map of the Cerro Gordo Peak 7.5′ quadrangle, Inyo County, California." *US Geological Survey Scientific Investigations Map* 2851.1 (2004): 24-000.